

Durham E-Theses

*New derivatives of strained, redox-active
9,10-bis(1,3-dithiol-2-ylidene)-9,10-dihydroanthracene
systems*

Terry Finn

How to cite:

Finn, Terry (2000) New derivatives of strained, redox-active 9,10-bis(1,3-dithiol-2-ylidene)-9,10-dihydroanthracene systems. Doctoral thesis, Durham University.

Use policy

The full-text may be used and/or reproduced, and given to third parties in any format or medium, without prior permission or charge, for personal research or study, educational, or not-for-profit purposes provided that:

- a full bibliographic reference is made to the original source
- a <https://etheses.durham.ac.uk/id/eprint/4530/> is made to the metadata record in Durham E-Theses
- the full-text is not changed in any way

The full-text must not be sold in any format or medium without the formal permission of the copyright holders.

Please consult the [full Durham E-Theses policy](#) for further details.

New Derivatives of Strained, Redox- Active 9,10-Bis(1,3-dithiol-2-ylidene)- 9,10-dihydroanthracene Systems

The copyright of this thesis rests
with the author. No quotation
from it should be published
without the written consent of the
author and information derived
from it should be acknowledged.

Terry Finn BSc. (Hons.)

Department of Chemistry

University of Durham

**A Thesis submitted for the degree of Doctor of Philosophy
at the University of Durham**

February 2000



18 OCT 2000

Statement Of Copyright

The copyright of this thesis rests with the author. No quotation from it should be published without his written consent and information derived from it should be acknowledged.

Declaration

The work described in this thesis was carried out in the Department of Chemistry at the University of Durham between October 1996 and September 1999. All the work is my own, unless stated to the contrary, and it has not been submitted for a degree at this or any other university.

Acknowledgements

I would like to express my thanks to the following people who have helped, guided and supported me through my time at Durham: My supervisor, Professor Martin Bryce for his insight, discussions and pure enthusiasm towards all matters. Adrian Moore for his advice and problem solving skills. Andrei Batsanov and Judith Howard for performing the X-ray crystallography. Thomas Hansen for his preliminary work on the crown systems. Marta Kamenjicki, Igor Lednev and Sanford Asher for collaboration on the cation binding studies. Ritu Katakya for some of the solution electrochemistry. Derek, for his cheerful and chirpy manner, Richard for extracurricular activities and Christian for his singing and banter. My thanks to the rest of the group, past and present for putting up with me, and my petty quirks. Thanks are also due to the technical staff for all their hard work and patience and the EPSRC, for financial support. Finally, thanks to my family for their unquestionable support.

Abstract

New Derivatives of Strained, Redox-Active 9,10-Bis(1,3-dithiol-2-ylidene)-9,10-dihydroanthracene Systems

Terry Finn B.Sc. (Hons.)

University of Durham (February 2000)

The synthesis of new derivatives of 9,10-bis(1,3-dithiol-2-ylidene)-9,10-dihydroanthracene has been achieved by three general routes. A variety of Horner-Wadsworth-Emmons reagents have been prepared from the corresponding 1,3-dithiolium cations; these have been shown to react in moderate yields to generate novel derivatives of the parent system. Alternative routes have also been developed for the preparation of unsymmetrical compounds, which were unattainable by Horner-Wadsworth-Emmons reagents. This was achieved *via* an addition/elimination reaction and provided a successful route to unsymmetrical derivatives. The use of lithiation chemistry has been extensively developed providing a direct route to a broad range of functionalities. This methodology has paved the way to a new range of crown ethers and sterically strained cyclophanes, some of which have been extensively studied by cyclic voltammetry and X-ray crystallography.

Solution electrochemistry of the 9,10-bis(1,3-dithiol-2-ylidene)-9,10-dihydroanthracene system displayed three redox waves, representing sequential formation of the dication, radical trication and tetracation species in an $E_qE_qE_q$ process. Detailed single crystal X-ray crystal studies have been performed on the neutral compounds and a TCNQ charge transfer complex. The neutral molecule adopts a saddle-like conformation; the bis(1,3-dithiole)benzoquinone system is U-shaped through an 'accumulating bend' comprising the boat conformation of the central (quinonoid) ring and folding of both 1,3-dithiole rings to generate a molecular cavity. Upon oxidation to the dication, the system becomes planar and aromatic with loss of the saddle shaped cavity. The development of this system as a potential sensor for metal cations has also been investigated.

Dedicated to my parents

Table of Contents

Chapter 1: Introduction

1.1 General Introduction	8
1.2 Tetrathiafulvalene	8
1.3 Organic Metals	10
1.4 Modification of the TTF Unit	11
1.5 Organic Superconducting CT Complexes	12
1.6 Extended TTF-Analogues	14
1.6.1 Vinylic Redox Systems	14
1.6.2 Heteroaromatic Spacers	17
1.6.3 Quinonoidal Redox Systems	20
1.7 Quinonoidal Based Redox Systems	23
1.8 Conclusion	31

Chapter 2

2.1 Introduction	32
2.2 Synthesis of 2,6-Dibutoxy-9,10-bis(1,3-dithiol-2-ylidene) -9,10-dihydroanthracene	35 44
2.3 Functionalisation of 2,6-Dihexoxy-9,10-bis(1,3-dithiol- 2-ylidene-4,5-dimethyl)-9,10-dihydroanthracene	38 55
2.4 Electrochemistry of the Bis(1,3-dithiol-2-ylidene) -9,10-dihydroanthracene system	40
2.5 Single Crystal X-ray Crystallography	42
2.6 Conclusion	47

Chapter 3

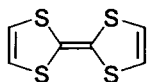
3.1 Introduction	48
3.2 Lithiation of the Dithiole Rings	48

3.3 Functionalisation <i>via</i> Addition/Elimination Reactions	54
3.4 Electrochemistry	60
3.5 Single Crystal X-ray Crystallography	60
3.6 Conclusion	63
<u>Chapter 4</u>	
4.1 Introduction	64
4.2 Synthesis	69
4.3 Cation Binding Studies	72
4.4 Single Crystal X-ray Crystallography	76
4.5 Conclusion	78
<u>Chapter 5</u>	
5.1 Introduction	79
5.2 Synthesis	82
5.3 Synthesis of the First Anthracenediylidene Cyclophanes	85
5.4 Electrochemistry	87
5.5 Single Crystal X-ray Crystallography	87
5.6 Conclusion	92
<u>Chapter 6</u>	
6.1 General Methods	93
6.2 Experimental Procedures For Chapter 2	94
6.3 Experimental Procedures For Chapter 3	97
6.4 Experimental Procedures For Chapter 4	108
6.5 Experimental Procedures For Chapter 5	112
<u>References</u>	118
<u>Appendices</u>	
X-ray Crystallographic data	123
Publications	134
Research Colloquia	136

1.1 General Introduction

Various categories of organic conductors have now been described;^{1,2} these include systems based upon molecular charge-transfer complexes, conjugated polymers, thiaarene systems and stacked organometallic species, where the metal atoms play no active role in conduction. In the quest to develop these systems various other interesting chemical and physical phenomena have come to light. It is on one such divergence that this work is based. The focus of this thesis is the development of a specific bis(1,3-dithiole) system, which undergoes a marked conformational change upon chemical and electrochemical oxidation. A diverse range of new 9,10-bis(1,3-dithiol-2-ylidene)-9,10-dihydroanthracene derivatives have been synthesised and the development of this methodology is described in detail, along with an exploration of the electrochemical and structural properties of these molecules.

1.2 Tetrathiafulvalene



Tetrathiafulvalene (TTF) 1

Tetrathiafulvalene (TTF) 1 first entered the spotlight when Wudl *et al.*, in 1970, reported that TTF could be oxidised sequentially in the presence of chlorine gas to the radical cation, then to the dication, both of which could be isolated.³ The relatively high stabilities of the oxidised species lie in the accompanying gain in aromaticity. The neutral form of TTF consists of two 7π non-aromatic systems. Upon oxidation each dithiole ring donates one electron allowing the formation of two, stable 6π Hückel-type aromatic systems (Figure 1.1). The oxidation is reversible in a range of solvents and can be achieved electrochemically and monitored using cyclic voltammetry (CV), which reveals that the radical cation is formed at $E^{1/2} = +0.34$ V followed by the dication at $E^{1/2} = +0.71$ V vs Ag/AgCl (Figure 1.2).

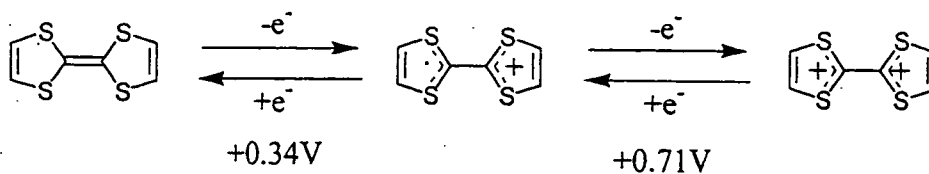


Figure 1.1: Redox behaviour of TTF.

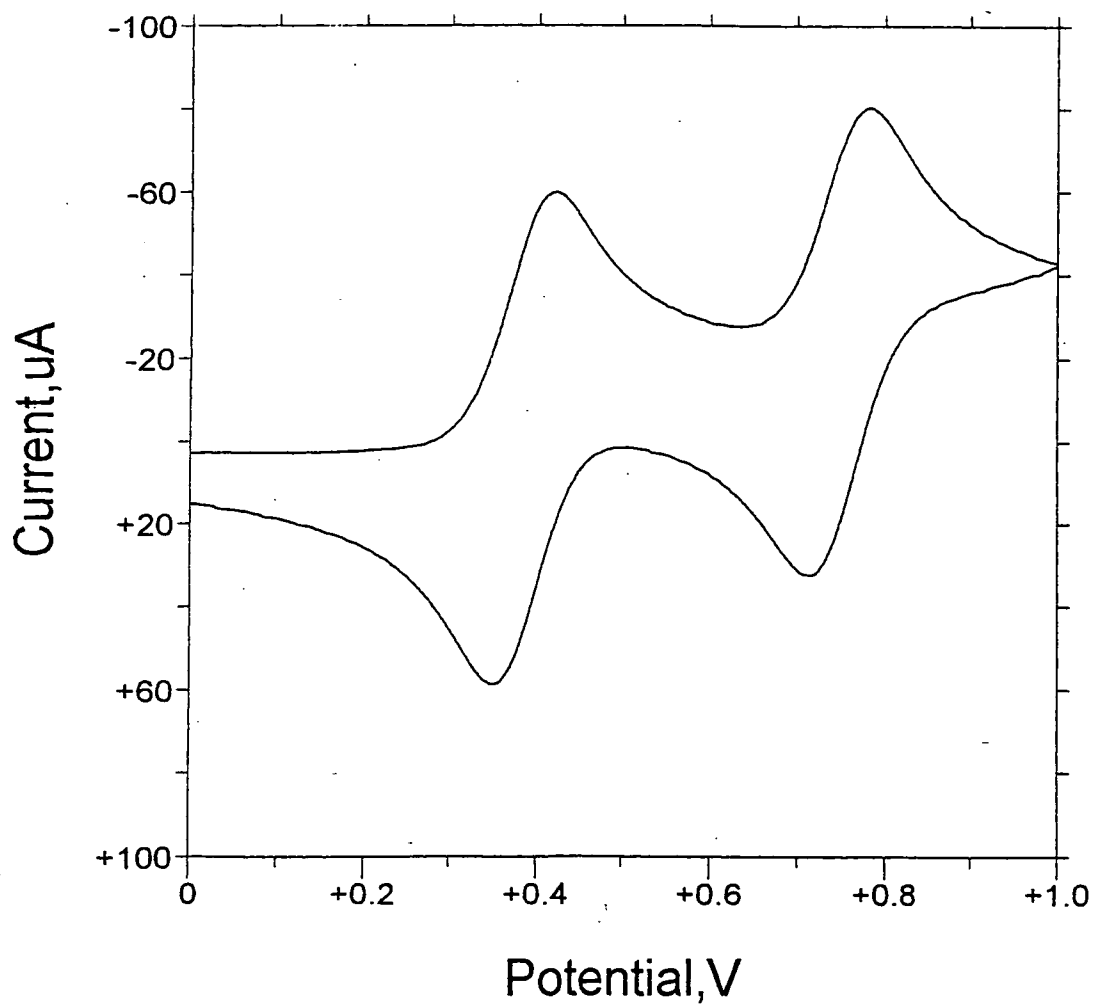
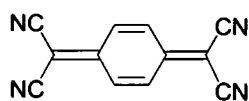


Figure 1.2: Cyclic Voltammogram of Tetrathiafulvalene 1.

1.3 Organic Metals

It is in the development of organic metals that TTF has made the greatest contribution, although TTF derivatives are now emerging as important building blocks in the wider context of supramolecular and materials chemistry. In 1973, it was discovered that TTF formed a 1:1 charge transfer complex with the electron acceptor tetracyano-*p*-quinodimethane (TCNQ) **2**.⁴ Charge transfer (CT) complexes are often highly crystalline materials, prepared by the mixing of an acceptor and donor species in boiling solvents such as acetonitrile.



7,7,8,8-Tetracyano-*p*-quinodimethane (TCNQ) **2**

The crystal structure of TTF-TCNQ illustrated one of the key requirements for conduction in a charge transfer complex, namely, that the crystal lattice consists of segregated stacks of planar TTF and TCNQ molecules.⁵ The geometry of each stack appears tilted relative to the stacking axis with the planes of donor and acceptor molecules lying in opposite directions producing a so-called ‘herringbone structure’ (Figure 1.3). Within each stack, TTF and TCNQ molecules align such that the exocyclic carbon-carbon double bond of one molecule lies directly over the ring of the molecule adjacent to it in the stack. This is referred to as “ring-over-bond” stacking. This arrangement maximises π -overlap within a stack.

A partial electron transfer of 0.59 electrons per molecule occurs between TTF and TCNQ. This has been elucidated using a range of spectroscopic and structural techniques.⁶ The formation of a mixed valence band is a prerequisite for conductivity in CT complexes. In 1:1 complexes, this is achieved by partial charge transfer; in complexes of different stoichiometry, *e.g.* 1:2 or 2:3, this can also be achieved by full charge transfer. In TTF-TCNQ, both donor and acceptor stacks contribute to the overall conductivity. Conductivity measurements showed unusually high electrical conductivity

along the stacking axis ($\sigma_{\text{H}} = 500 \text{ Scm}^{-1}$) with little interaction between the stacks and conduction 10^3 - 10^4 times lower along the other axis. These anisotropic charge transfer complexes have been termed '1-dimensional organic metals'.

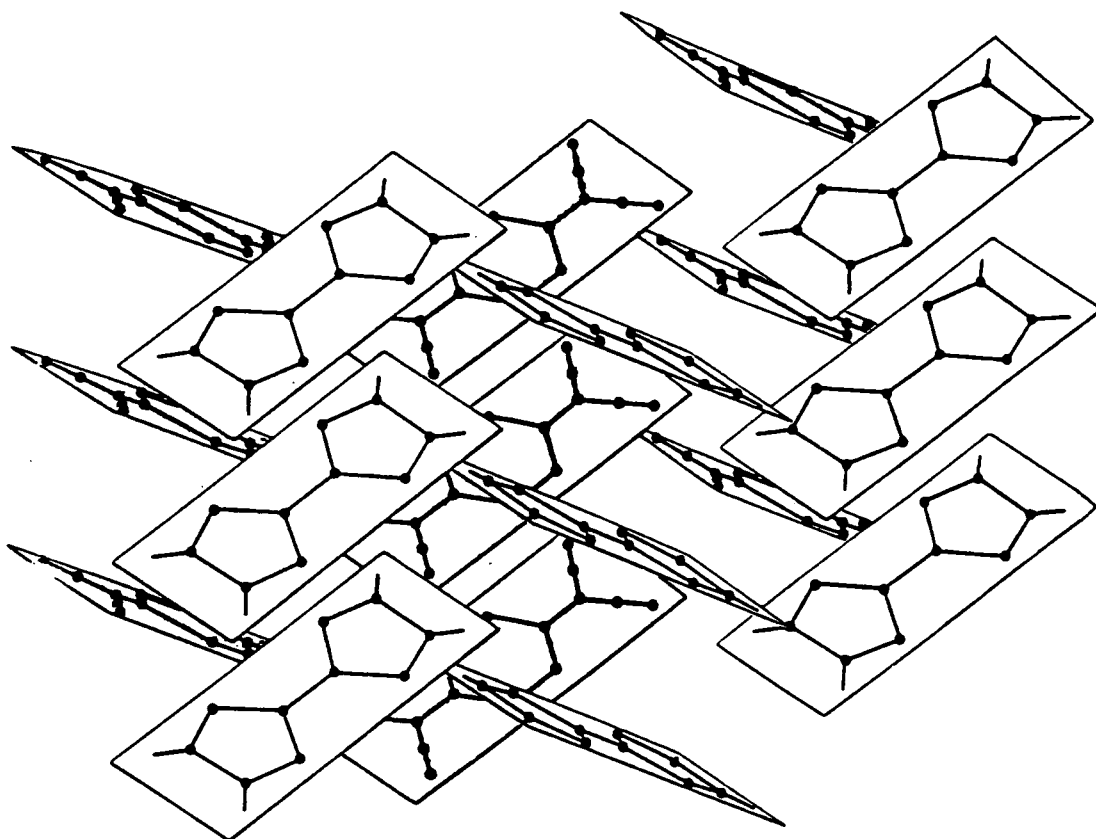


Figure 1.3: Herringbone structure of TTF 1 and TCNQ 2, in the complex TTF-TCNQ.

1.4 Modification of the TTF Unit

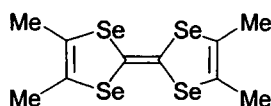
In an effort to improve the conductivity of TTF containing charge transfer complexes various chemical modifications have been implemented and studied. One such modification concerns the exchange of sulfur for more polarisable atoms such as Se and Te. Both tetraselenafulvalene (TSF)⁷ and tetratellurafulvalene (TTeF)⁸ formed charge transfer complexes with TCNQ and exhibited higher conductivity than TTF-TCNQ. The increased conductivity has been attributed to increased intra- and inter- stack interactions.

Other approaches have utilised the sigma-bond framework by the addition of electron releasing groups such as alkyl groups, to lower the oxidation potential of TTF and thereby favour the charge transfer process.⁹

One important discovery not only utilised diffuse atoms and inductive alkyl groups but also inorganic closed-shell anions as the acceptors. These combined modifications paved the way to the first organic superconductors.¹⁰

1.5 Organic Superconducting CT Complexes

The attainment of superconductivity is one of the most competitive areas of materials research. When superconducting materials are cooled below a critical temperature, T_c , their electrical resistance falls to zero; therefore these materials consume no current. Early examples required T_c temperature close to absolute zero, this rendered the materials impractical. Therefore, the search began to understand the processes involved and develop materials capable of superconducting at higher temperatures. The majority of this work became based on synthesised ceramics, which gradually showed improved T_c temperatures. Now materials with T_c temperatures well above the technologically important -196°C (liquid nitrogen) have been prepared. Chemists continue to try and raise the T_c of organic superconductors. To date, no superconducting CT complexes have shown superconductivity at T_c comparable to ceramic superconductors.



Tetramethyltetraselenafulvalene (TMTSF) 3

The first example of a superconducting organic system was prepared by Bechgaard and coworkers in 1979-1980 and consisted of a series of $(\text{TMTSF})_2\text{X}$ salts ($\text{X} = \text{ClO}_4^-$, PF_6^- , AsF_6^- , FSO_3^- and ReO_4^-).¹⁰ These CT salts exhibited metal-insulator transitions between 10 and 200 K. However, under hydrostatic pressure superconductivity was recorded. The first example $(\text{TMTSF})_2^+\text{PF}_6^-$ became

superconducting at 0.9 K, 12 kbar and became a cornerstone in the development of organic superconductors.

The X-ray crystal structure of $(\text{TMTSF})_2^{+}\text{BrO}_4^-$ can be seen in Figure 1.4.¹¹ Similarities can be drawn with one-dimensional metals; the molecules of TMTSF 3 are planar and form defined stacks. The charge compensating anions occupy the cavities created by 'ring-over-bond' stacking and exert negligible influence on the conductivity. The conduction pathway can be attributed to a mixed valence TMTSF stack and has been rationalised by band theory. An important aspect of the donor stacks is the relatively short and similar intrastack and interstack Se---Se contacts, which form an infinite sheet of interactions. It is these interactions which give rise to two-dimensionality, rather than the one-dimensionality of TTF-TCNQ. The formation of a three-dimensional array in $(\text{TMTSF})_2^{+}\text{BrO}_4^-$ is disrupted by the presence of the BrO_4^- counter ions.

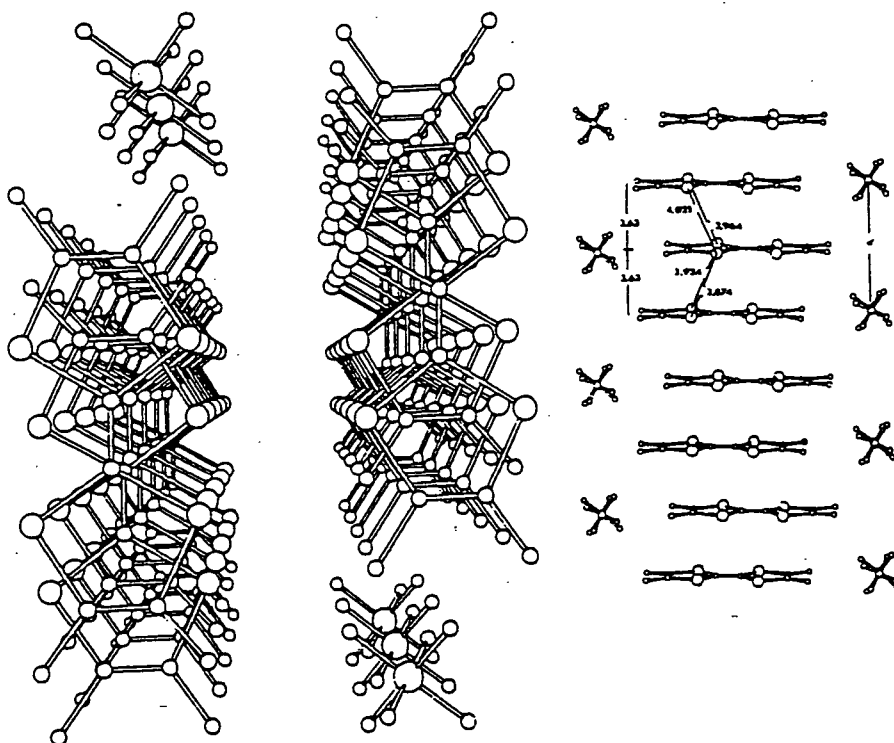


Figure 1.4: X-ray structure of $(\text{TMTSF})_2^{+}\text{BrO}_4^-$, interstack Se—Se distances are shown on the left, whilst the intrastack distances are shown on the right.

1.6 Extended TTF-Analogues

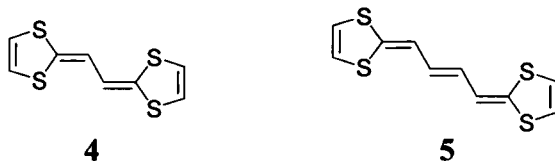
In an effort to break away from the basic tetrachalcogenofulvalene framework and perhaps provide new crystal packing motifs with improved conductivities, a range of extended π -systems have been prepared. One rationale behind the synthesis of extended TTF derivatives is to minimise the effects of coulombic repulsion within the dicationic state. The increased spatial separation of the 1,3-dithiolium cations was expected to lower the energy required for the second oxidation (radical cation to dication). The choice of spacer group is also important. The presence of the vinylic spacer serves to stabilise the intermediate radical cation by delocalisation between the dithiole rings.

In the majority of cases the spacer group can be subdivided into three general categories:

- 1) Those incorporating vinylic spacers ($n = 1, 2, 3$, etc.).
- 2) Those including heteroaromatic groups (furan, thiophene and pyrrole).
- 3) Those based on quinonoidal systems.

1.6.1 Vinylic Redox Systems

The use of conjugated vinylic spacer units between 1,3-dithiole rings was first introduced by Yoshida *et al.* in 1982.¹²



These compounds showed increased stability of the radical cation and dication, relative to TTF **1**, as demonstrated by cyclic voltammetry (Table 1.1).

Compound	$E_1^{1/2}$ (V)	$E_2^{1/2}$ (V)	$E_2^{1/2} - E_1^{1/2}$ (V)
1	0.34	0.71	0.37
4	0.20	0.36	0.16
5	0.22 (2e)	-	-

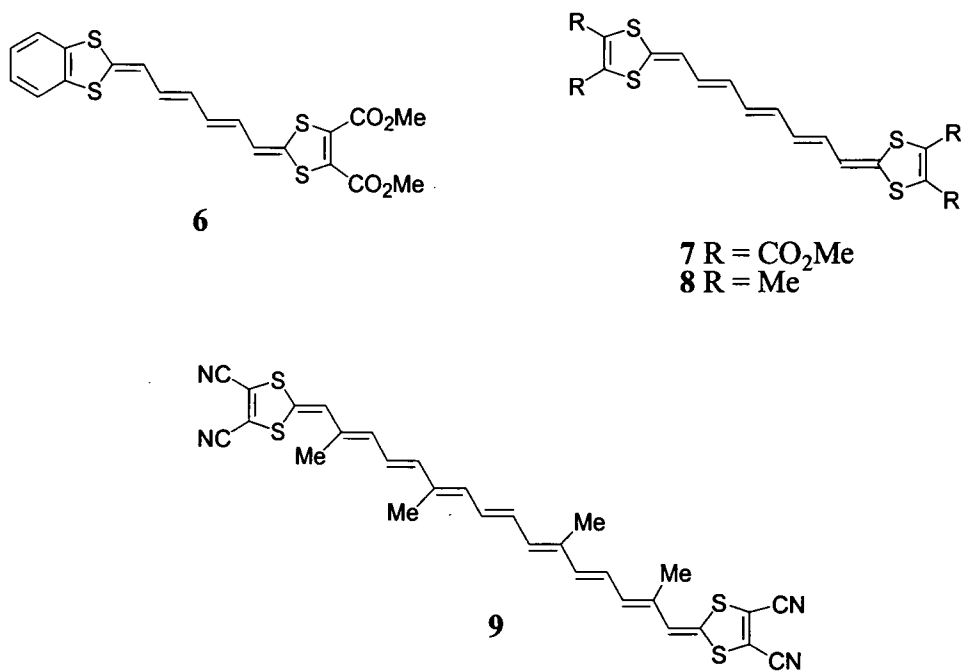
Table 1.1: Cyclic Voltammetric data for TTF 1 and vinylic bridged compounds 4 and 5.

In comparison with TTF 1, donor 4 displayed lower first and second oxidation potentials. This has been rationalised on the basis that increased delocalisation results from the insertion of two sp^2 hybridised carbon atoms and by the reduced through-space effects of increased separation of the dithiole rings. The formation of the radical cation is favoured as a more conjugated carbon skeleton effectively reduces the average charge per atom. The dication is also favoured as the through-space influence of one cation is reduced relative to the other. The difference between the consecutive redox waves ($E_2^{1/2} - E_1^{1/2}$) has been shown to decrease further with the inclusion of two additional vinylic carbon atoms (compound 5); in this example, the two redox waves coalesced into a single, two-electron, oxidation wave. The further incorporation of sp^2 carbon atoms did not, however, lower the first redox potential from that of compound 5. This implies that delocalisation is already maximised with the insertion of one vinylic group. In compound 5, both 1,3-dithiole rings are now acting independently of one another. These studies proved that π -spacers suppress coulombic repulsion and promote the formation of the dication at a lower potential.

Longer polyalkenic spaced compounds have been synthesised by Nguyen *et al.*, compounds 6-8.¹³ While extension of the spacer length does not further change the first oxidation potential, the direct formation of the dication species through a single two-electron transfer was observed for 7. It was reported that the replacement of the ester group by methyl groups 8, leads to a substantial decrease in stability, due to electron donation. This introduces a major limitation that requires extended vinylic systems to be counterbalanced by electron-withdrawing groups on the dithiole units.

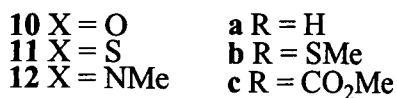
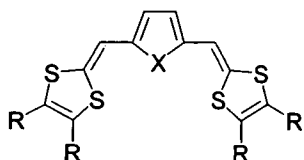
To date, the longest vinylic spaced TTF analogue has been prepared by Markl *et al.*¹⁴ and incorporates 16 sp^2 carbon atoms, compound 9. Again, the compound underwent

a single, two-electron, oxidation. Interestingly, the compound incorporated cyano substituents at the 4 and 5 positions of the 1,3-dithiole rings: again, an example of increased stability arising from the presence of electron-withdrawing groups.



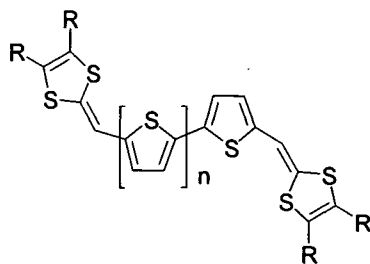
1.6.2 Heteroaromatic Spacers

While polyalkenic spacers showed reduced coulombic repulsion upon oxidation, their major limitations lie in their limited stability and poor solubility. These problems were initially solved by the introduction of a heterocyclic spacer unit. TTF analogues incorporating five-membered heterocyclic spacers such as furan, thiophene and pyrrole have been well documented, **10-12**.¹⁵⁻¹⁸



All these compounds showed two reversible, one-electron oxidations by cyclic voltammetry. The introduction of a heterocyclic spacer reduced the potentials of both the first and second oxidations relative to TTF **1**. Again, this can be understood on the grounds of increased delocalisation and reduced coulombic repulsion. However, contrary to expectations, the first oxidation potential decreased in the order thiophene > furan > pyrrole. Although the aromatic resonance energy of the heterocycle is important, this cannot be the only factor since furan should exhibit the lowest first oxidation potential. The lower oxidation of pyrrole has been attributed to pyrrole's ability to stabilise cationic structures with the positive charge localised on the nitrogen atom. The introduction of the heterocyclic spacer produced in every case a compound with reduced coulombic repulsion providing a small step in the right direction regarding improved conduction.

The next logical step in the development of a heterocyclic spaced donor was to further lower the oxidation potentials by the introduction of multiple spacer units analogous to the multi-vinyl systems previously described. Early examples of this approach were constructed around terthienyl and tetrathienyl cores, compounds **13** and **14**, respectively.¹⁹



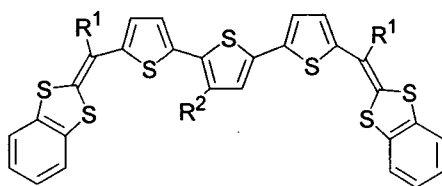
13a-c $n = 1$
14a-c $n = 2$

a $R = \text{CO}_2\text{Me}$
b $R-R = (\text{CH}=\text{CH})_2$
c $R = \text{SMe}$

The stepwise addition of thiophene rings to the spacer unit has provided a valuable insight into the structure-property relationship of heterocyclic systems. Elongation of the thiophene backbone produced unexpected changes in the CV and UV-vis spectroscopic data.

The cyclic voltammery of **13** showed two, consecutive, one-electron oxidations with a lowering of both first and second oxidations of the donor (relative to its vinylic equivalent). As previously described, the insertion of four sp^2 carbon spacer units (compound **5**) produced a single, two-electron oxidation wave. A similar phenomenon was observed for **13**, with the two oxidation waves becoming almost coalesced, ($\Delta E^{1/2} = 90 \text{ mV}$). However, increasing the number of thiophene spacers to three, **14**, lead to an increase in both oxidation potentials. This unexpected behaviour has been rationalised due to an increase in rotational disorder, which distorts the conjugated backbone between the dithiole rings leading to a poorer electron donor. As expected, the replacement of alkyl groups with electron-withdrawing ester groups lead to an increase in both oxidation potentials.

The effects of functionalisation has been studied for a similar thiophene system, compound **15**, which was synthesised in an effort to improve solubility.²⁰ This was achieved by derivatisation of both the vinylic and heterocyclic framework.

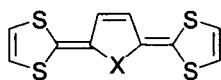


- 15 a** $R^1 = H, R^2 = H$
b $R^1 = H, R^2 = H$
c $R^1 = Me, R^2 = Me$
d $R^1 = H, R^2 = C_8H_{17}$
e $R^1 = H, R^2 = (CH_2CH_2O)_2CH_3$

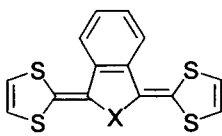
The UV-vis absorption measurements performed on compound **15** showed that the site of functionalisation played a pivotal role in modifying the conjugated pathway of the system. The introduction of solubilising chains on the medial thiophene produced significant red shifts (*i.e.* increased conjugation) of the λ_{max} value in comparison with the unsubstituted terthienyl core. These shifts suggest a change in geometry of the terthienyl core. Whereas substitution of a methyl group on R^1 produced a blue shift (*i.e.* less conjugation) attributed to a loss of planarity due to steric interactions.

A drawback with heterocyclic spacers lie in the steric effect of functionalisation, which contributes to rotational disorder around the core unit, leading to distorted intramolecular π -overlap. Furthermore, the use of additional heterocyclic spacers will probably be ineffective, as these systems seem to adopt an unfavourable twisted conformation. Therefore, more rigid spacer groups have been explored.

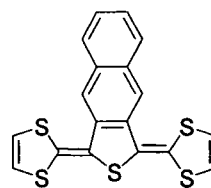
In an attempt to overcome these problems Takahashi *et al.* synthesised a range of heteroquinonoidal extended donors, compounds **16**, **17** and **18**.²¹



- 16 a** $X = S$
b $X = Se$



- 17 a** $X = O$
b $X = S$
c $X = Se$



18

Aryl and naphthyl spacer units have been incorporated into donor molecules to increase ring stability by hindering conformation changes. The extension of the donor π -system also contributed to increased stabilisation of the dication.

The cyclic voltammetry of compounds **16-18** revealed two, well-defined, reversible, one-electron oxidations. The first oxidation potential decreased in the order thiophene > furan > pyrrole, again, this can be rationalised by canonical forms and electronegativities. Table 1.2 shows a comparison of the electrochemistry of thiophene, benzothiophene and naphthothiophene functionalities.

Compound	$E_1^{1/2}$ (V)	$E_2^{1/2}$ (V)	$E_2^{1/2} - E_1^{1/2}$ (V)
16a	0.11	0.34	0.23
17b	0.31	0.55	0.24
18	0.36	0.65	0.29

Table 1.2: Cyclic Voltammetric data for compounds 16a, 17b and 18.

The CV data showed that increased aryl functionality on thiophene increased both the oxidation potentials and the difference between them. The explanation for this lies in the fact that aromaticity is lost in the aryl ring upon oxidation, providing a barrier to oxidation, which increases the oxidation potentials. The barrier to oxidation increases the greater the number of aromatic atoms are incorporated into the spacer unit, hence the oxidative potential is greater for the naphthyl derivative.

1.6.3 Quinonoidal Redox Systems

The use of a quinonoidal spacer group is in some respects similar to those of the heterocyclic systems discussed previously. Again, the 1,3-dithiole rings are separated by a conjugated pathway that increases π -delocalisation and reduces coulombic repulsion. The quinonoidal spacer group is a rigid spacer which fixes the geometry of the two dithiole rings thereby preventing rotational disorder and providing increased stability. However, in quinonoidal systems the spacer group gains aromaticity upon oxidation. This

provides a driving force, which lowers the difference between sequential oxidations (Figure 1.5).

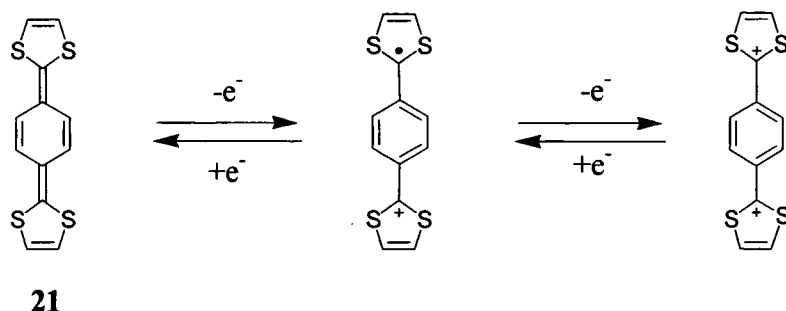
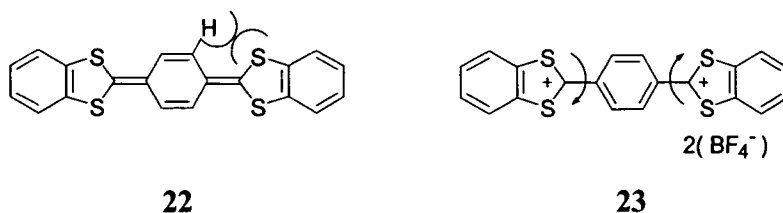


Figure 1.5: The redox behaviour of quinonoidal spacer units.

Due to the gain in aromaticity and relative stability of the charged species, almost all quinonoidal spaced donors exhibit lower oxidations in the cyclic voltammetry than similar vinylic or heteroaromatic spaced moieties. These compounds are, therefore, very good electron donors. However, these redox processes are generally regarded as being quasi-reversible, the gained aromaticity being a barrier to reduction.

The preparation of compound **21** was first claimed, without experimental details, in an early patent by Miles *et al.*²²



This work was later continued by Cava *et al.*, who prepared the bis(benzo-1,3-dithiole) derivative **22** and its dication tetrafluoroborate salt **23**.²³ By using differential pulse polarography the dication **23** could be sequentially reduced back to the monodithiolium radical cation, $E_1^{1/2} = +0.330$ V and the neutral compound, $E_2^{1/2} =$

+0.057 V (no reference stated). The low value for the second reduction illustrates that the effects of coulombic repulsion are negated by the driving force to aromatise.

Yamashita *et al.* repeated the work of Miles *et al.* in 1989,²⁴ believing that quinonoidal spaced systems represented good electron donors, but that they were flawed by poor stability. Yamashita prepared a wide range of quinonoidally spaced systems in an attempt to improve stability. Compound **21** was also prepared using an alternative synthetic approach. CV data showed that compound **21** exhibited two reversible, one-electron oxidations (-0.11 V and -0.04 V vs SCE). A range of other quinonoidal donors incorporating various spacer units and dithiole functionalities were prepared (Figure 1.7).

Detailed investigations revealed that compounds containing either benzo (**21**) or naphthyl (**27**) spacers were air sensitive. These compounds showed two, reversible, one-electron oxidation waves by CV (vs SCE). The use of dibenzo-1,3-dithiole rings instead of 1,3-dithiole rings renders analogues **22**, **24** and **25** stable towards air and these compounds show a reversible, two-electron oxidation wave. The use of a cyclopentadiene adduct of *p*-benzoquinone as a spacer, **23** and **26**, gave compounds which were stable to air and also produced a reversible, two-electron oxidation wave. The exception appeared to be compound **28**; this incorporated an anthraquinone spacer group. This compound showed an irreversible oxidation at +0.25 V. Compounds **21**, **22**, **24** and **27** gave charge transfer complexes with TCNQ **2**.

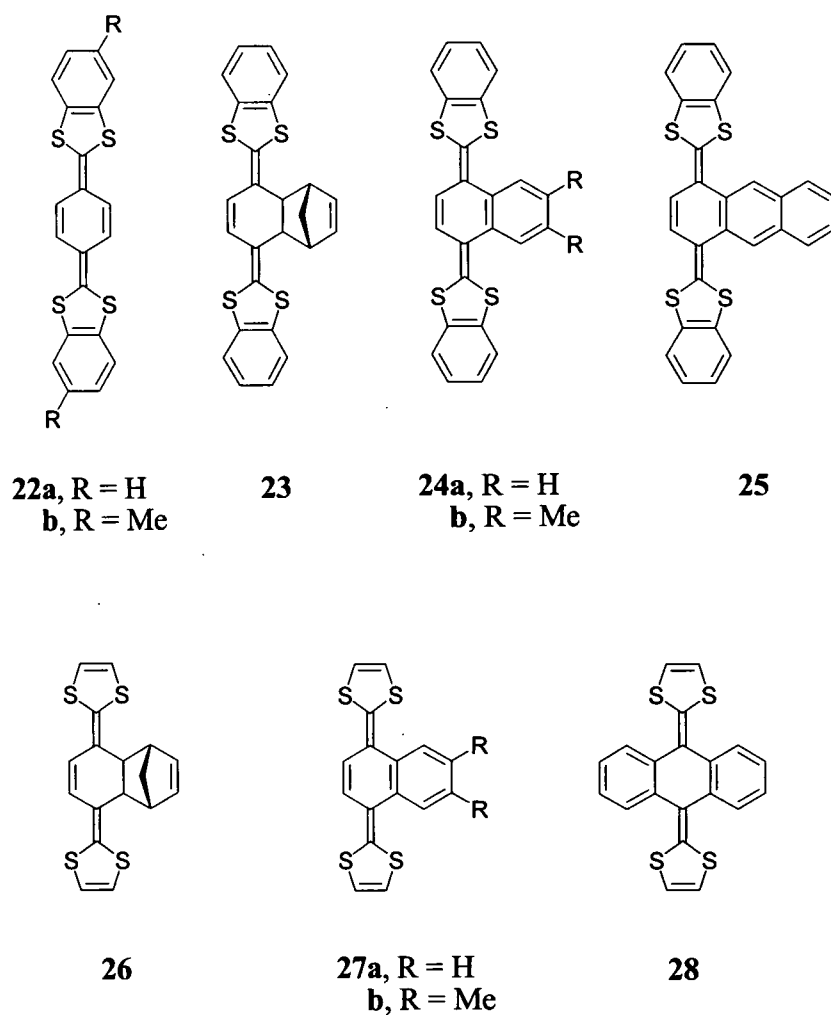
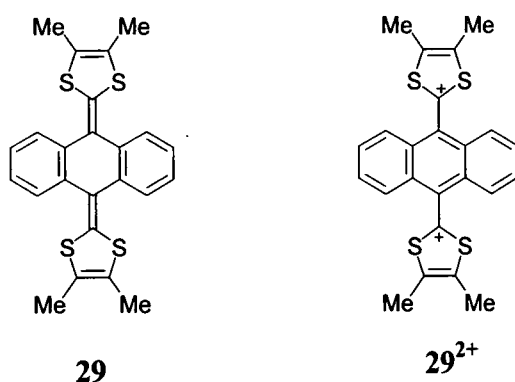


Figure 1.7: Quinoidal donors prepared by Yamashita et al.

1.7 Quinoidal Based Redox Systems

Although first synthesised by Akiba *et al.*,²⁵ many of the properties of anthraquinonoidal spaced systems, including their solid state structure and electrochemistry, have been elucidated by Bryce *et al.*²⁶ Donor **29** was synthesised from anthraquinone.



The crystal structure shows the neutral donor **29** adopts a saddle-shape with the central quinonoid ring severely distorted into a boat conformation. Donor **29** also formed a highly conducting 1:4 charge transfer complex with TCNQ **2**. The crystal structure of the CT salt showed that the central quinonoidal spacer was now a planar anthracene ring, with the attached 1,3-dithiolium rings almost orthogonal to this plane (Figure 1.8). The crystal structure showed that compound **29** formed a 1:4 CT salt with TCNQ **2**. This is an example of a non-stoichiometric CT salt in which the dication plays no direct role in the conduction process: the observed high conductivity ($\sigma_{\pi} = 50 \text{ Scm}^{-1}$) arises from a partially-filled band on the acceptor stacks (two electrons per four TCNQ molecules) as a consequence of the 1:4 stoichiometry.

The distorted structure of neutral donor **29** is attributed to peri-interactions between anthracene bound hydrogens and the large sulfur atoms of the dithiole rings. The cyclic voltammetry shows that on oxidation the system exhibits a quasi-reversible, two-electron oxidation, to the dication species. Again, the explanation for the two-electron oxidation lies in aromatisation of the central anthracene ring. The change in geometry of the donor upon oxidation creates a barrier to reduction of the dication rendering the redox system quasi-reversible.

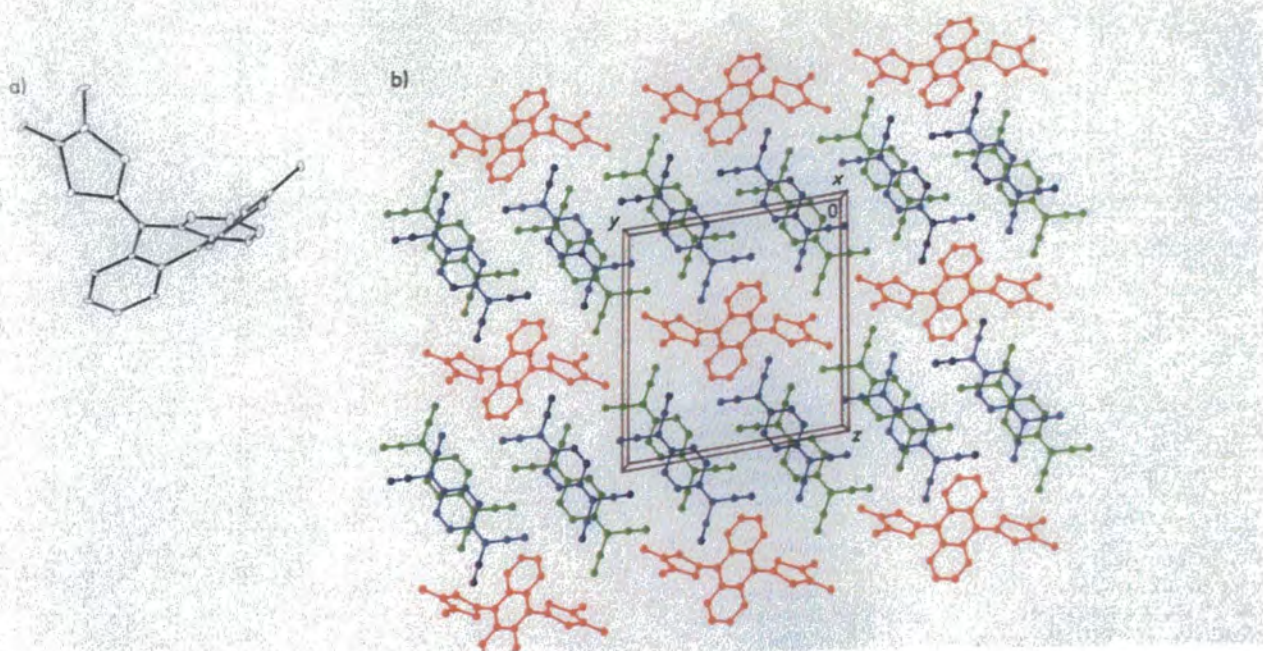
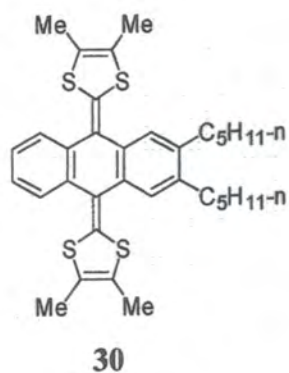


Figure 1.8: The crystal structure of a) neutral donor **29** and b) its 1:4 TCNQ charge transfer salt.

To further elucidate the electrochemistry of these systems Bryce *et al.* synthesised compound **30**, for which the pentyl substituents provided increased solubility for low temperature studies which allowed for the first time, the +3 and possibly the +4 oxidation states to be observed.²⁷ The variable temperature CV data for compound **30** are shown in Figure 1.6.



The first redox wave ($E_{\text{ox}} = +0.28 \text{ V vs Ag/AgCl}$) was a quasi-reversible, two-electron oxidation to yield the dication and is directly analogous to the other quinonoidal systems. Subsequently, there were two further, sequential, one-electron oxidations of the anthracene system. These afforded the trication radical and tetracation species, respectively. The first anthracene oxidation ($E_{\text{ox}} = +1.64 \text{ V}$) is cleanly reversible, whereas the second anthracene oxidation ($E_{\text{ox}} = +2.2 \text{ V}$) was at the limit of the solvent window for dichloromethane and was not cleanly observed. The data also revealed that the first oxidation process at $+0.28 \text{ V}$ was temperature independent; however, the coupled reductive peak of the dication to the neutral compound is shifted progressively to more negative potentials with decreasing temperature. This is undoubtedly due to a stabilisation within the 6π , 1,3-dithiolium rings, at the dication stage. The marked conformational change that must occur on the reduction, accounts for the temperature dependence and the quasi-reversibility of this step.

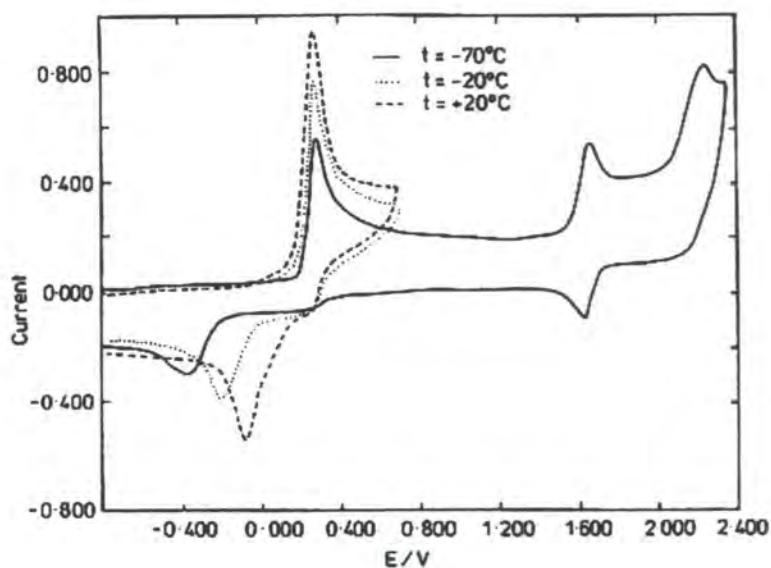
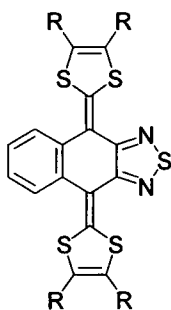


Figure 1.6: The variable temperature cyclic voltammetry of compound 30.

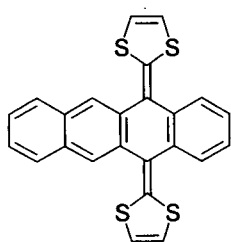
Yamashita *et al.* have also prepared compounds incorporating naphtho[c]-1,2,5-thiadiazole spacers, compound 31.²⁴



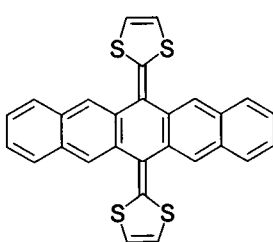
- 31a** R = H
b R = Me
c R-R = SCH₂CH₂S
d R-R = benzo

These compounds contain only two hydrogen-sulfur peri interactions. A crystal structure of the neutral compound 31 revealed the formation of a distorted saddle conformation.

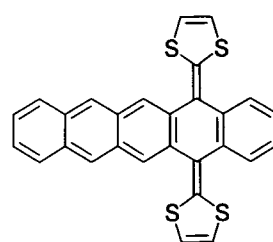
Only a limited number of aryl spaced redox systems have been prepared, some having benzannelated spacers.



32



33



34

Martin *et al.*, synthesised compounds 32- 34 providing a systematic increase in the aryl π -spacer.²⁸ Cyclic voltammetry studies of these compounds allowed a comparison of their oxidation potentials (Table 1.3). Compounds 32-34 showed a quasi-reversible first oxidation wave involving two electrons to form the corresponding

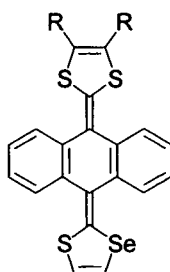
dication. An irreversible, second oxidation to the trication was also observed as a shoulder at 1.1-1.3 V.

Compound	E_{ox} / V
28	0.28 (2e)
32	0.39 (2e)
33	0.50 (2e)
34	0.49 (2e)

Table 1.3: Cyclic Voltammetric data for compounds **28**, **32-34** (vs. SCE).

The cyclic voltammetry data showed that increased π -extension on the central spacer increased the potential of the first oxidation. This is presumably due to difficulties in aromatising the extended system. Therefore, compounds **32-34** represent poorer donors than the anthracene bridged compound **28**.

Investigations into mixed heteroatom quinonoidal systems have also been conducted by Bryce *et al.* 1,3-Selenathiole analogues, *e.g.* **35**, were synthesised and their electrochemistry investigated.²⁹



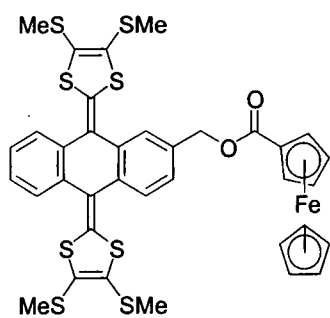
35a R = H
b R = Me

The donor ability of the bis(1,3-dithiol)-9-10-dihydroanthracene system is significantly reduced by the incorporation of one selenium atom into the ring system (**35a** $E_{ox} = 0.45$ V, **35b** $E_{ox} = 0.47$ V). This was consistent with known selenium analogues of TTF derivatives, and is attributed to selenium forming weaker π -bonds with carbon than

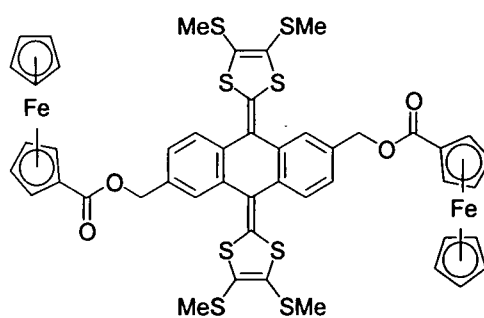
does sulfur. Thus, the selenium cations are less stable than their sulfur counterparts. Selenium atoms are less able to redistribute charge; this raises the overall energy required for ionisation of selenium donors.

Another development of quinonoidal spaced systems is the preparation of multistage redox donors, the rationale being the development of a donor capable of donating more than 4 electrons. Two groups have spearheaded this work, Bryce *et al.* prepared compounds **36-38** and Martin *et al.* prepared the first bis[bis(1,3-dithiole)-9,10-dihydroanthracene] system **39**.³⁰⁻³² The electrochemistry of compounds **36-37** revealed that functionalisation of the anthracene ring increased the oxidation potential for the first two-electron, quasi-reversible oxidation to between 0.50-0.61 V. The oxidation of the ferrocene rings occurred simultaneously to yield a cleanly reversible, one-electron oxidation per ferrocene. Compound **39a** showed the formation of a bis-dication at 0.50 V (**4e**). Again this process was quasi-reversible.

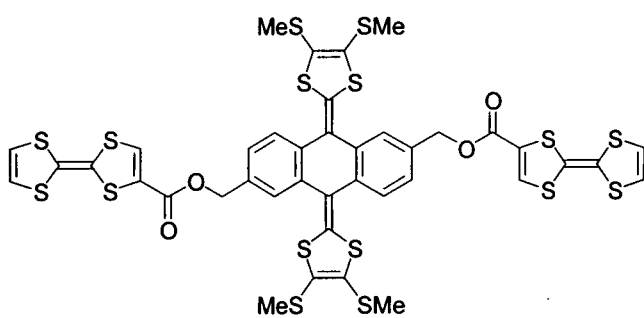
Recently, Martin *et al.* reported the first bis(1,3-dithiol)-9-10-dihydroanthracene C₆₀-based, donor-acceptor system **40**.³³ Redox properties determined by cyclic voltammetry revealed the presence of four cathodically shifted reduction waves, relative to C₆₀, which correspond to the C₆₀ core, and a two-electron single oxidation wave to form a stable dication.



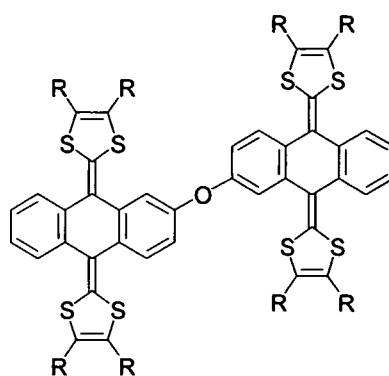
36



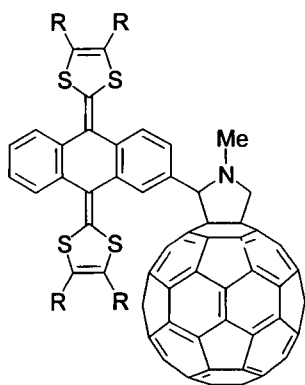
37



38



39a R = H
 b R = SMe
 c R-R = SCH₂CH₂S



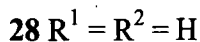
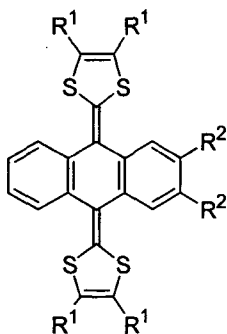
40

1.8 Conclusion

The 9,10-bis(1,3-dithiol-2-ylidene)-9,10-dihydroanthracene molecule represents an interesting electron donor system, which adopts a saddle-shaped conformation created by peri-interactions between sulfur and hydrogen atoms. This conformation creates a cavity between the two 1,3-dithiole units. These compounds readily donate two electrons (the dication is formed at a lower potential than TTF) and are capable of donating up to 4 electrons. On oxidation, a dramatic conformational change occurs which renders the anthracene spacer planar with loss of the cavity. At the outset of this project only a very limited number of derivatives had been synthesised. We recognised it was an interesting challenge to develop these systems with the aim of exploring chemical derivatisation, cavity properties, electrochemistry and structural conformations.

2.1 Introduction

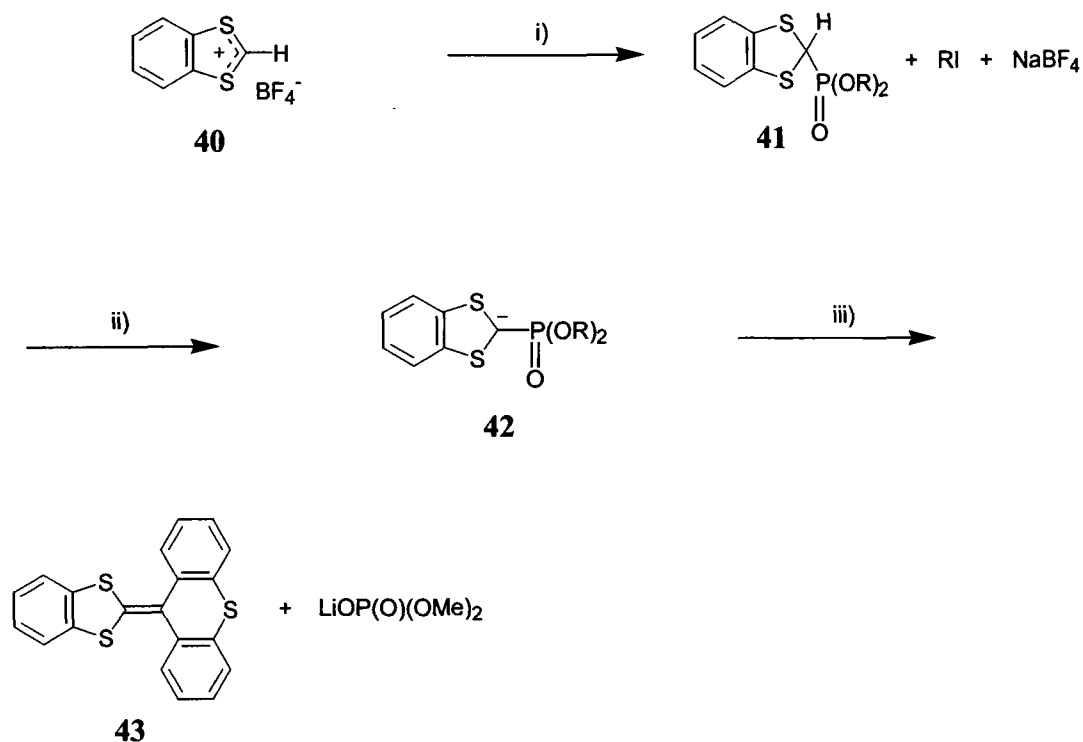
Compound **28**, has been independently studied by the groups of Bryce *et al.*^{26, 34-36} and Yamashita *et al.*²⁴ Studies have shown that compound **28**, undergoes a two-electron oxidation, which was observable by cyclic voltammetry as a single quasi-reversible redox wave. However, the insolubility of the generated dication precluded further investigation into the higher oxidative states of the system.



The oxidation of the more soluble compound **34** was studied by cyclic voltammetry in three different solvents (dichloromethane, acetonitrile and propylene carbonate) under rigorously anhydrous conditions.²⁷ Studies in dichloromethane at reduced temperature (-70°C) revealed three distinct oxidative steps. The first redox wave ($E_{\text{ox}} = +0.28$ V) was a quasi-reversible, two-electron transfer to yield the dication species and was comparable to that of other similar donors at 20°C. The first anthracene oxidation ($E_3^{1/2} = +1.64$ V) was cleanly reversible, a second anthracene oxidation ($E_4^{1/2} = \text{ca. } +2.2$ V) was also observed, but was at the limit of detection due to solvent masking.

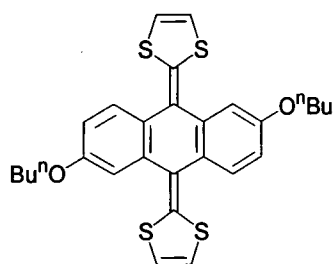
This chapter aims to broaden our understanding of the electrochemistry and charge-transfer properties of the bis(1,3-dithiol-2-ylidene)-9,10-dihydroanthracene system by studying new derivatives with solubilising substituents. Initial experiments on the lithiation of this system are also described. This aspect is developed in detail in Chapter 3.

In general, bis(1,3-dithiol-2-ylidene)-9,10-dihydroanthracene compounds have been prepared *via* Horner-Wadsworth-Emmons reactions onto anthraquinone in moderate yields. The required Horner-Wadsworth-Emmons reagents were first developed by Akiba *et al*, who described the reaction of benzo-1,3-dithiolium tetrafluoroborate salts **40**, with trialkyl phosphites in dry acetonitrile to give the corresponding phosphonate ester **41**, in > 90% yield.²⁵ These phosphonates were then deprotonated with *n*-butyllithium in tetrahydrofuran at -78°C generating the reactive anion, **42**, which proved to be more reactive than the analogous trialkylphosphine ylid. Wittig reagents fail to react with anthraquinone, however, the more reactive phosphonate anion reacted with anthraquinone and a range of heteroatom containing anthrones. In this example, Akiba quenched the anion **42** with 10H-9-thiaanthracen-10-one to give **43** (Scheme 2.1).



Scheme 2.1 Reagents and Conditions: i) NaI , $\text{P}(\text{OR})_3$, MeCN , *rt*. ii) *n*-BuLi, THF, -78°C . iii) 10H-9-thiaanthracen-10-one

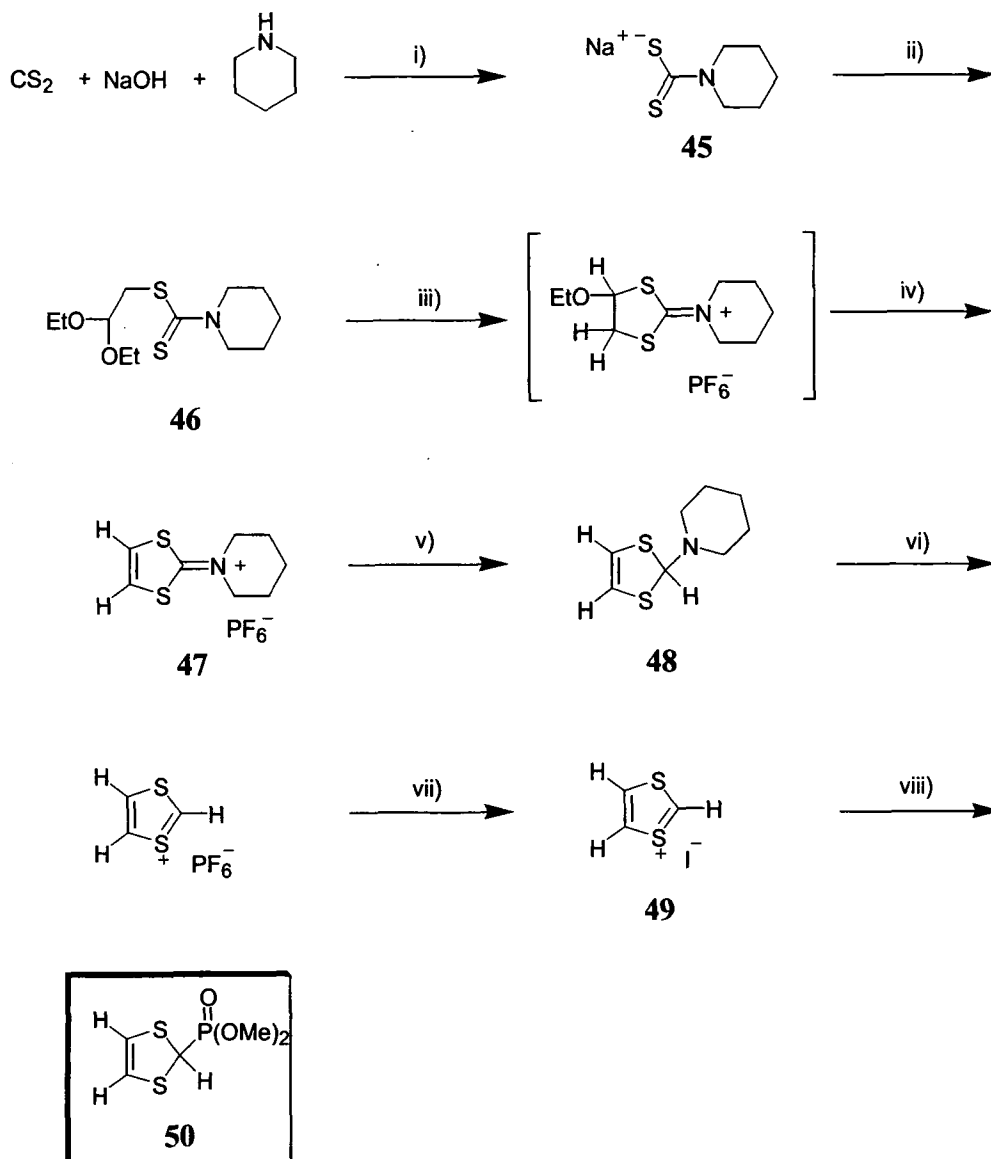
At the outset of this project, the literature contained only a limited range of functionalised bis(1,3-dithiol-2-ylidene)-9,10-dihydroanthracene compounds, utilising either alkyl or aryl groups on the dithiole rings, or with the 2 and 6 positions of the anthracene spacer bearing substituents.³⁰⁻³² We decided to use 2,6-dihydroxyanthraquinone (anthraflavic acid), **51**, as a starting material for new derivatives, *e.g.* **44**.



44

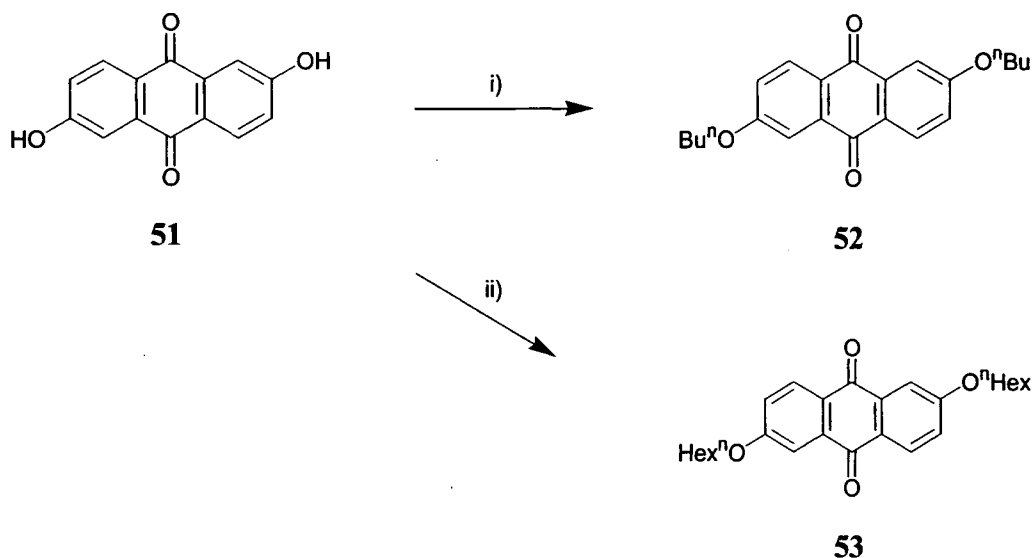
2.2. Synthesis of 2,6-dibutoxy-9,10-bis(1,3-dithiol-2-ylidene)-9,10-dihydroanthracene 44

The required phosphonate reagent **50** was described in the literature and prepared in seven steps, outlined in Scheme 2.2.³⁶



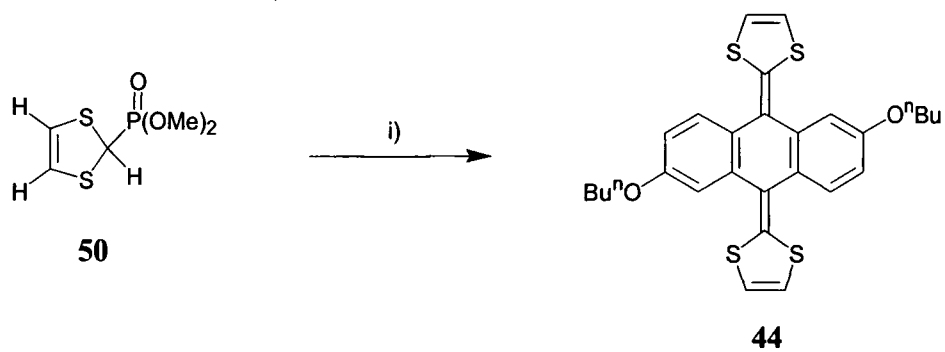
Scheme 2.2 Reagents and Conditions: i) EtOH, rt, 5h. ii) $(\text{EtO})_2\text{CHCH}_2\text{Br}$, EtOH, reflux, 24h. iii) $c.\text{H}_2\text{SO}_4$, 70°C , 4d. iv) HPF_6 , 0°C , 1h. v) NaBH_4 , THF/PrOH, 0°C , 1h. vi) HPF_6 , $\text{Ac}_2\text{O/Et}_2\text{O}$, 0°C , 1h. vii) NaI , Me_2CO , rt, 1h. viii) P(OMe)_3 , MeCN, rt, 1h.

2,6-Dialkoxy-anthraquinones were prepared *via* Williamson ether synthesis from anthraflavic acid **51**, which reacted with iodobutane and iodohexane in the presence of silver (I) oxide to afford derivatives **52** and **53** in 56% and 57% yields, respectively (Scheme 2.3).



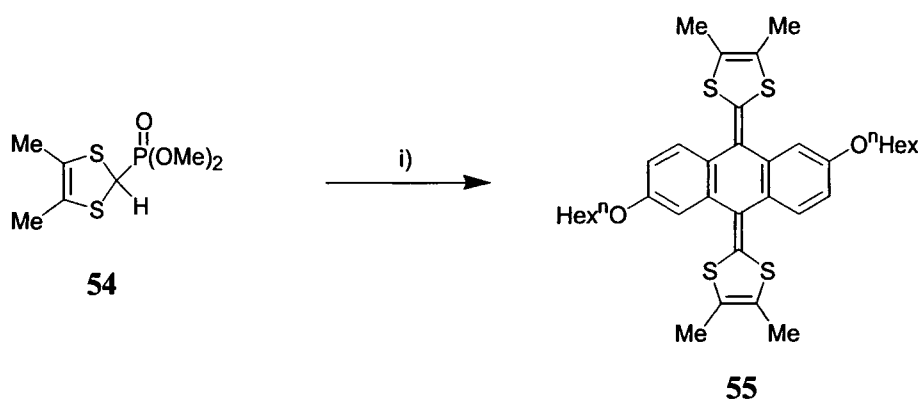
Scheme 2.3 Reagents and Conditions: i) iodobutane, Ag_2O , DMF, rt, 2d. ii) iodohexane, Ag_2O , DMF, rt, 2d

2,6-Dibutoxyanthraquinone **52** underwent Horner-Wadsworth-Emmons reaction with the carbanion generated from phosphonate ester **50**, to yield the anthracenediylidene derivative **44** in 51% yield, which proved to be soluble in a wide range of organic solvents (Scheme 2.4).



Scheme 2.4 Reagents and Conditions: i) LDA, THF, -78°C , 3h. followed by compound 52.

Using a similar procedure we synthesised analogue 55, from the literature dimethyl phosphonate ester 54, in 59% yield (Scheme 2.5).³⁷



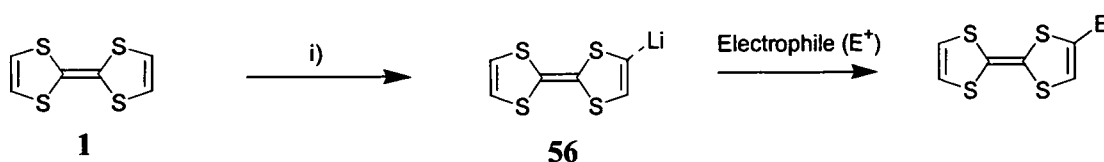
Scheme 2.5 Reagents and Conditions: i) LDA, THF, -78°C , followed by compound 53.

2.3 Functionalisation of 2,6-dibutoxy-9,10-bis(1,3-dithiol-2-ylidene)-9,10-dihydroanthracene 44

Having prepared the highly soluble compounds **44** and **55** we sought to expand the synthetic diversity of the system, *via* lithiation chemistry analogous to that of TTF **1**; the transient anion could then be quenched with a range of electrophiles allowing the attachment of a range of functional groups.

Green first showed that formation of the TTF anion **56** could be accomplished with either *n*-butyl lithium (*n*-BuLi) or lithium diisopropylamide (LDA) at -78°C and that the resulting anion could then be trapped with a wide range of electrophiles, to give mono-substituted derivatives in moderate yields (Scheme 2.6 and Table 2.1).³⁸

Temperature is critical for the success of TTF anion reactions. At temperatures above -78°C , disproportionation of the TTF monoanion occurs to give a range of multi-lithiated species, which lead to multi-substituted products and a substantial drop in reaction yield. These problems are avoided if the temperature is carefully controlled at -78°C .



Scheme 2.6 Reagents and Conditions: *i*) LDA or *n*-BuLi, THF or Et_2O , -78°C .

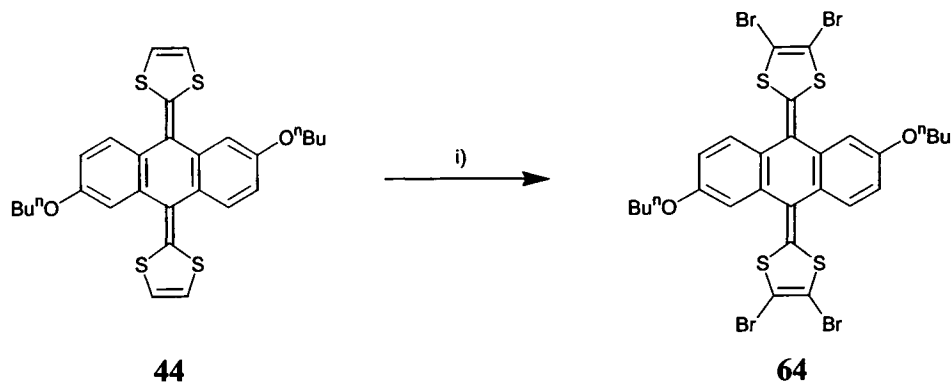
Compound	Electrophile	E
57	Et_3OPF_6	Et
58	DMF, followed by H_2O	CHO
59	ClCO_2Et	CO_2Et
60	CO_2 followed by HCl	COOH

61	MeC(O)Cl	C(O)Me
62	Me ₂ SO ₄	Me
63	HCOH	CH ₂ OH

Table 2.1: Electrophiles used in TTF anion reactions.

Efforts to employ lithiation chemistry on compound **44** proved problematic. Compound **44** was deprotonated at -78°C , using one equivalent of lithium diisopropylamide to generate the mono-anion. The lithium anion was then trapped with an excess of tosyl bromide. However, the reaction produced a range of substituted products, with the majority being the mono-substituted product (TLC evidence).

Attempts to tetra-lithiate the system also proved problematic. Compound **44** was lithiated using 5 equivalents of lithium diisopropylamide to generate the tetra-anion. This was then quenched with excess tosyl bromide to give tetrabromide **64** in low yield (12%, Scheme 2.7).



Scheme 2.7 Reagents and Conditions: i) LDA (5 equivalents), THF, -78°C , 3 h, followed by tosyl bromide.

Due to the formation of multiple products, which were difficult to separate by chromatography, and poor yields, this approach was abandoned and alternative precursors to functionalised derivatives were devised (Chapter 3).

2.4 Electrochemistry of the bis(1,3-dithiol-2-ylidene)-9,10-dihydro anthracene system

The solution electrochemistry of compounds **44** and **55** has been studied by CV and by square wave voltammetry (SQV) in acetonitrile. Both compounds displayed three redox waves at the following potentials: compound **44** E^{ox} 0.320 V, 1.49 V and 1.64 V; compound **55** E^{ox} 0.275 V, 1.47 V and 1.62 V (vs Ag/AgCl). The lower values of these potentials for the latter compound, especially E_1^{ox} , is consistent with the trend observed with compounds **28** and **29**, arising from tetramethyl substitution on the 1,3-dithiole rings.³⁷ Analysis of the data is consistent with an *EqEqEq* process (*Eq* = quasi-reversible). Figure 2.1 shows the SQV and CV for compound **44**. The first wave is a two-electron process (neutral to dication, with aromaticity gain at the dication stage) and the second, reversible, one-electron wave is ascribed to oxidation of the anthracene unit (dication to radical trication) by analogy with previous work.^{27,39-40} Repeated recycling through the first wave resulted in no significant change in the CV, demonstrating that this is a chemically reversible redox process. The effect of the alkoxy substituents is to shift the second oxidation wave to lower potentials by *ca.* 150 mV (*cf.* compound **28** E_2^{ox} 1.64 V, and **29** E_2^{ox} 1.62 V, under the same conditions). The entirely new feature of compounds **44** and **55** is the presence of a third redox wave, which is also a quasi-reversible, one-electron process. This wave has not been unambiguously observed in previous derivatives of the system **28**, (it was very tentatively seen for the 2,3-dipentylanthracene analogue **34** at *ca.* +2.2 V, *i.e.* at the limit of the solvent window)²⁷ and we assign this process to the formation of the tetracation species **44**⁴⁺ and **55**⁴⁺ which could be stabilised by the electron-donating effect of the two alkoxy substituents.⁴¹ This assignment is further supported by comparison with the voltammetric data for 9,10-diphenylanthracene, which undergoes two, single-electron, oxidation waves (E_1^{ox} 1.23 V,

and E_2^{ox} 1.70 V, vs. SCE in MeCN) and these waves (especially E_2^{ox}) are cathodically shifted in 9,10-di(*p*-methoxyphenyl)anthracene (E_1^{ox} 1.15 V, and E_2^{ox} 1.37 V).⁴² This latter separation (ΔE^{ox} 220 mV) approaches the value (ΔE^{ox} 150 mV) which we observe for E_2^{ox} and E_3^{ox} for compounds **44** and **55**. We eliminated the possibility that this third wave for **44** and **55** was derived from a different chemical species (*e.g.* a species in which the alkoxy groups had been cleaved in the electrochemical reaction) as recycling between 1.00V and 1.75 V for 50 cycles resulted in no significant change in the appearance of the CV.

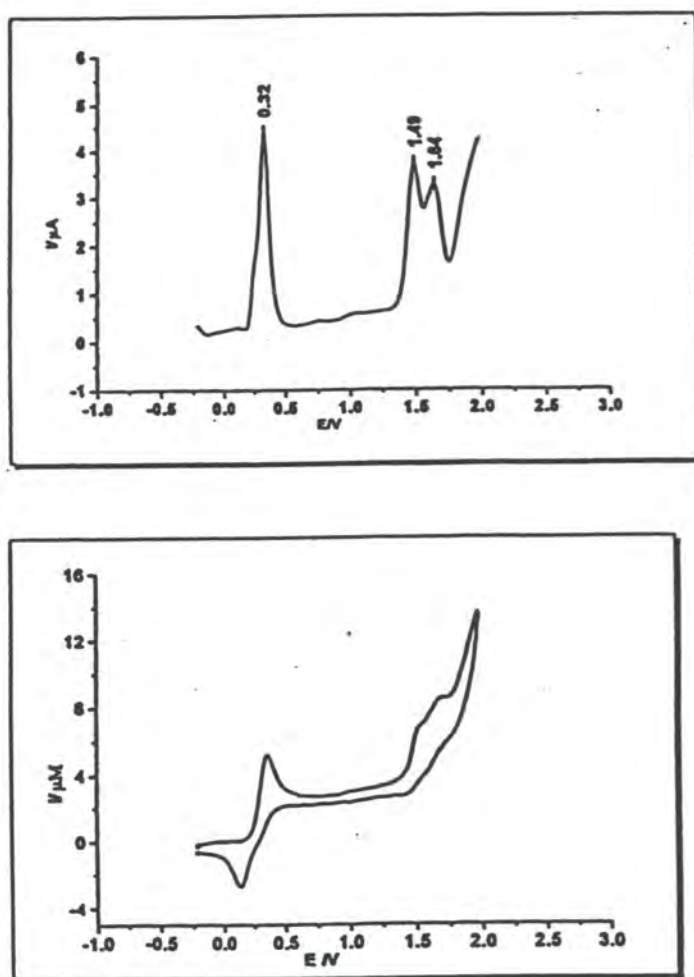


Figure 2.1: The SQV (top) and CV (bottom) for compound 44.

2.5 Single Crystal X-ray Crystallography

The structure of compound **44** has been determined by single crystal X-ray analysis (Figure 2.2). Neutral molecule **44** adopts a saddle shaped conformation, in a similar manner to previously reported analogues.^{26,43} The anthracene system is folded along the C(7)...C(21) vector by 34.6°. The fold angle is slightly smaller than in previous systems, which vary from 38-45°, and the system actually comprises two isolated benzene π -systems, linked to C(7) and C(21) by single bonds. The bis(dithiol)benzoquinone system displays the usual 'accumulating bend' inward, with the dihedral angle of 91.5° between the S(1)...C(9)...C(10)...S(2) and S(3)...C(23)...C(24)...S(4) planes (literature 76-87°).^{26,43} Both dithiole rings are folded along the S(1)...S(2) and S(3)...S(4) vectors, by 6.6° and 10.0°, respectively. The crystal packing motif is a dimer, wherein the cavities of the bis(dithiol)benzoquinone systems engulf each other.

The molecular structure of **55** (Figure 2.3) is similar to that of **44**. Folding of the anthracene moiety in **55** [44.8° along the C(7)...C(25) vector] is stronger, but folding of the dithiole rings [5.9° and 12.2° along the S(1)...S(2) and S(3)...S(4) vectors, respectively] means that the overall dihedral angle between the S(1)...C(9)...C(10)...S(2) and S(3)...C(27)...C(28)...S(4) moieties (90.0°) of the system are practically the same. From comparison with previous structures,^{26,43} and those described in Chapter 3, it is evident that a non-planar molecular conformation is, in principle, necessary to distance sulfur atoms from *peri* hydrogens of the anthracene moiety. However, non-planarity is achieved by a number of modes of distortion, which shows no obvious correlation with each other and with electronic properties of the substituents. Thus the actual degree of bending is rather flexible and can adjust to the demands of the crystal packing.

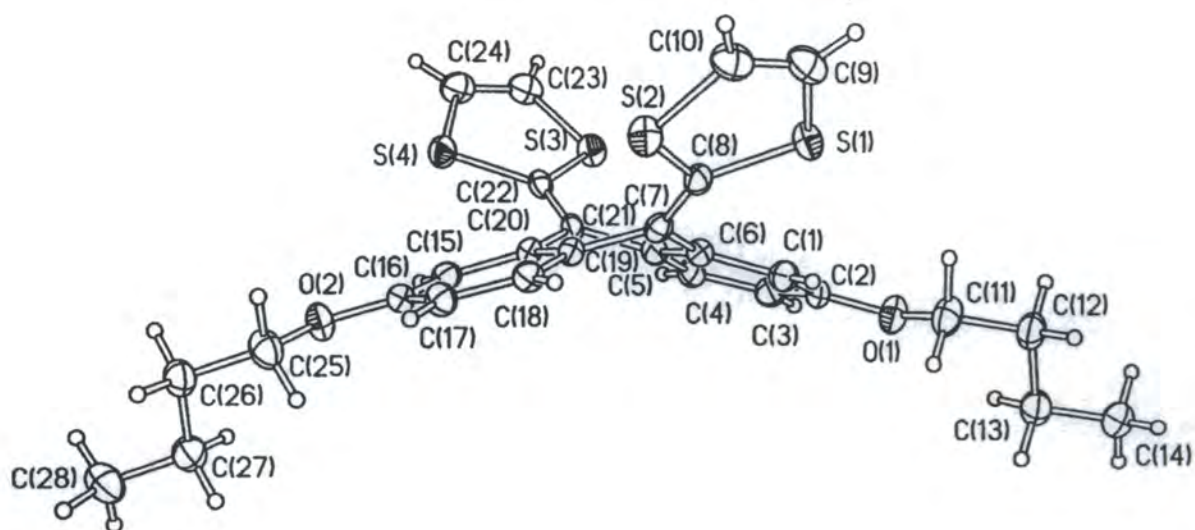


Figure 2.2: Single crystal X-ray structure of compound 44.

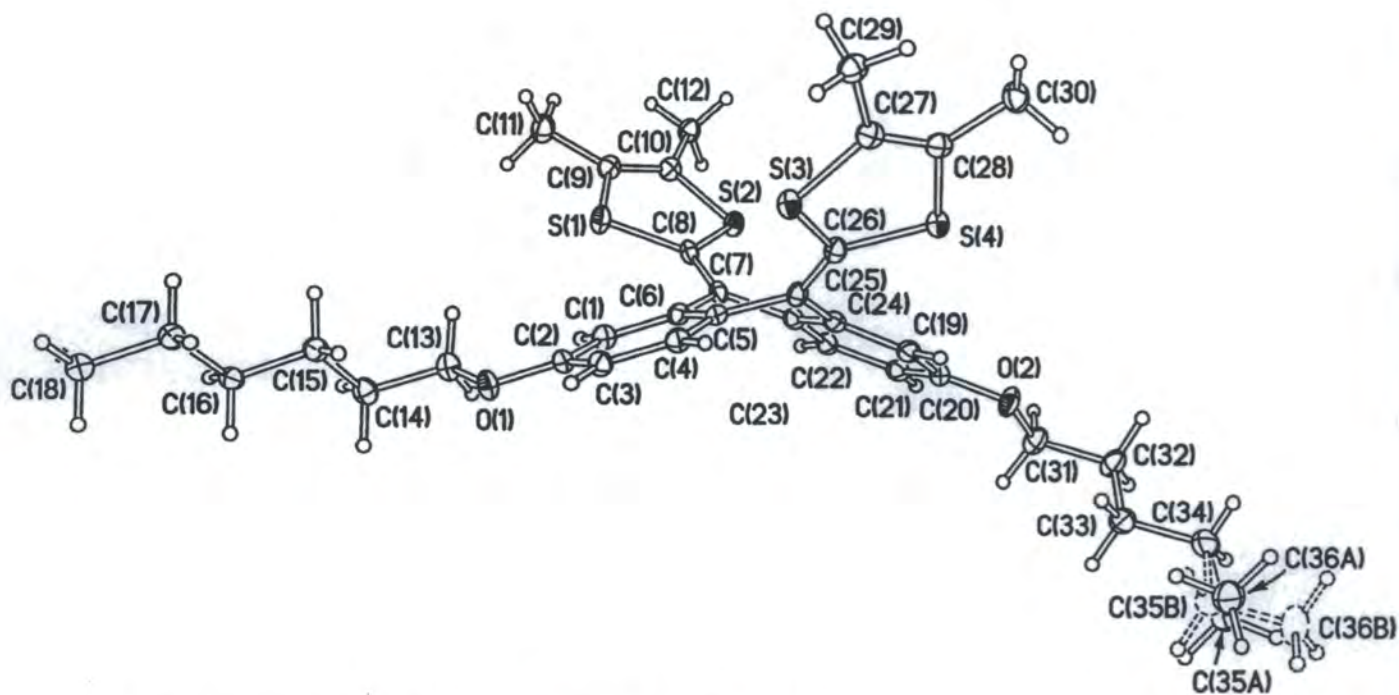


Figure 2.3: Single crystal X-ray structure of compound 55.

A charge transfer salt of compound **44** was prepared with TCNQ (Figure 2.4). The charge transfer salt comprised a 1:2 stoichiometry of donor: TCNQ and included two molecules of solvent acetonitrile. The asymmetric unit comprised a TCNQ anion radical and an acetonitrile molecule in general positions, and half of a dication 44^{2+} located at a crystallographic inversion centre (Figure 2.5). The dication has a structure similar to the literature examples incorporating methyl and thiomethyl substituted bis(1,3-dithiol-2-ylidene)-9,10-dihydroanthracenes.^{26,44} The anthracene system is planar and aromatic, bond distances therein are essentially the same as in the neutral anthracene.⁴⁵ The dithiolium rings are also planar, their geometry is close to that of (TMTTF)(ClO₄)₂ and consistent with a charge of +1, or thereabouts, on each ring.⁴⁶ The dithiolium and anthracene planes form a dihedral angle of 78°; the intervening C(7)...C(8) bond is essentially single. It is well known that charge transfer onto a TCNQ molecule results in lengthening of the carbon-carbon double bonds⁴⁷ p and r and shortening of the single bonds q and s , so that $q \approx r \approx s$ for the charge of -1 (Figure 2.5). In the charge transfer salt the average distances are $p = 1.371(2)$, $q = 1.425(2)$, $r = 1.423(2)$ and $s = 1.423(2)$ Å which clearly indicate TCNQ to be mono-anion. Crystallographically parallel anions form a stack of dimers (Figure 2.6). The dication forms a stair-like stack, but perpendicular orientation of the dithiolium rings enforces a large interplanar separation of 3.97 Å. A notable feature of the structure is that both sulfur atoms of the dithiolium ring participate in short contacts with nitrogen atoms of the TCNQ: S(1)...N(1'')(- x , 1- y , - z) 2.959 (3) and S(2)...N(3) 2.865 (3) Å, *cf.* the standard van der Waals contact of 3.42 Å. In either case, the contacting nitrogen atom is nearly co-planar with the dithiolium ring and opposite to the C(8)-S bond, *viz.* the angles C(8)S(1)N(1) 173.1(2)° and C(8)S(2)N(3) 178.5(2)°. Short contacts of this kind are rather common in charge transfer complexes comprising TCNQ and TTF or their derivatives and could be expected, since the N and S atoms are the main centres of negative and positive charges, respectively. The single crystal conductivity of 44^{2+} (TCNQ⁻)₂ 2MeCN, measured using a two-probe technique is low ($\sigma_{\pi} = 10^{-8}$ Scm⁻¹), consistent with a fully anionic TCNQ stack. The C≡N stretching frequencies in the IR spectrum (2172 and 2155 cm⁻¹) are consistent with a fully anionic TCNQ.⁶

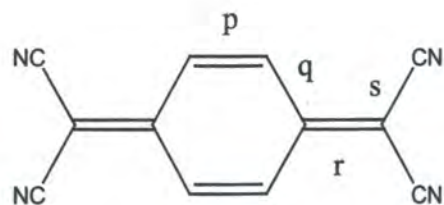


Figure 2.5: Identification of bonds for crystallographic analysis of TCNQ.

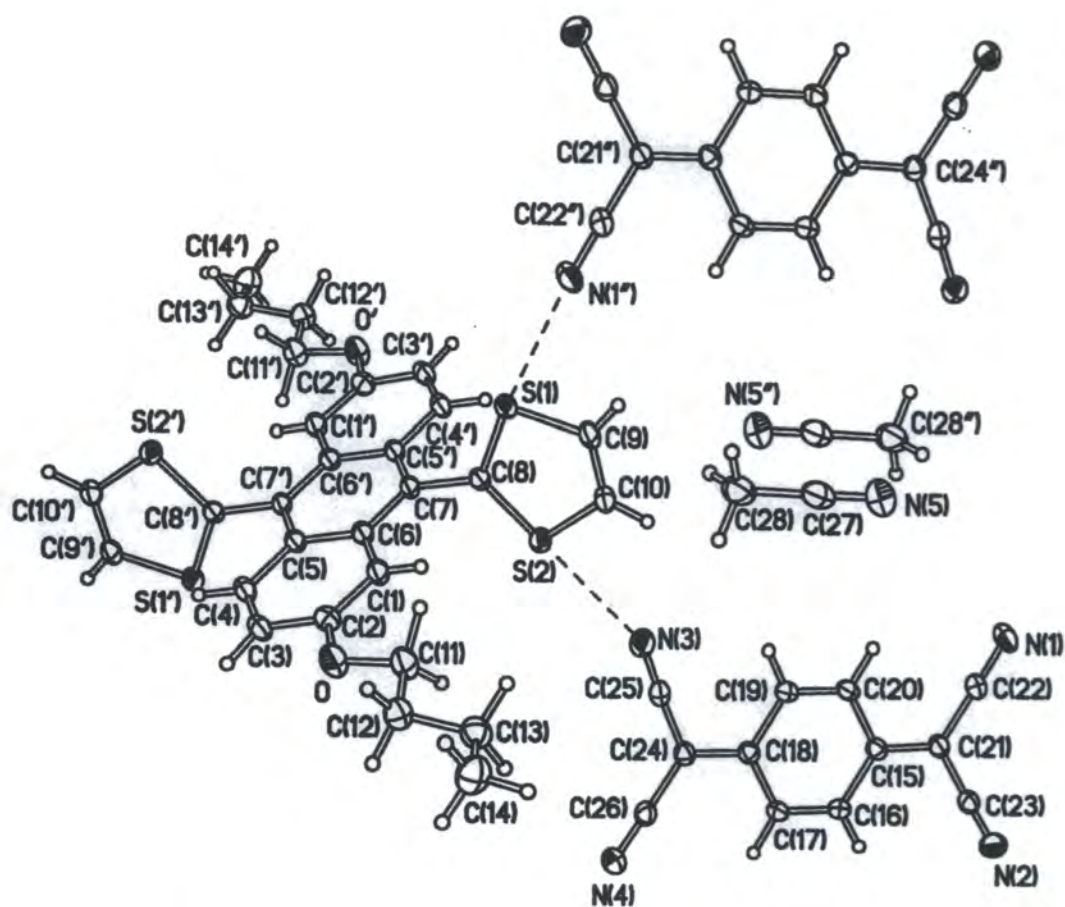


Figure 2.4: Single crystal X-ray structure of a charge transfer salt of 44^{2+} $(TCNQ^{-})_2 \cdot 2MeCN$.

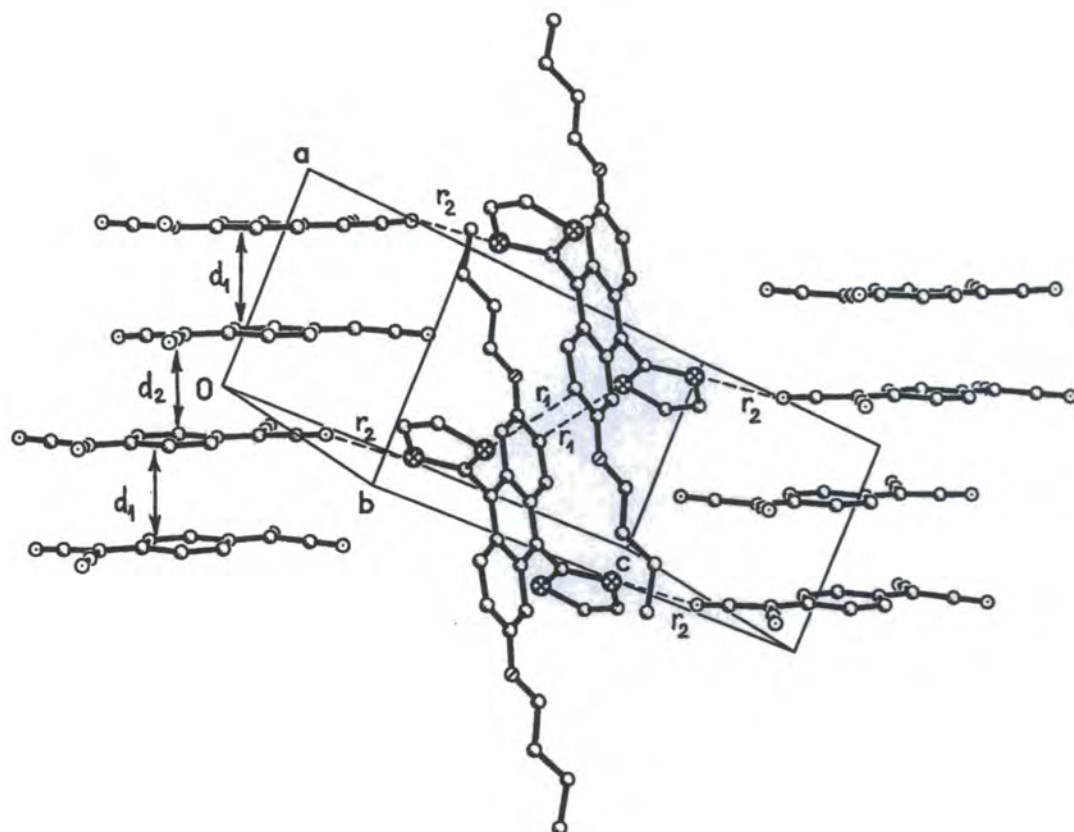


Figure 2.6: A packing diagram of the charge transfer salt $44^{2+} (\text{TCNQ}^-)_2 2\text{MeCN}$ (solvent molecules omitted for clarity). Interplanar separations $d_1 = 3.15 \text{ \AA}$, $d_2 = 3.50 \text{ \AA}$, C...S contacts $r_1 = 3.289(2) \text{ \AA}$, N...S contacts $r_2 = 2.865(3) \text{ \AA}$.

2.6 Conclusion

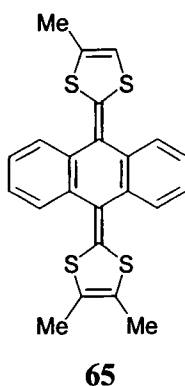
We have synthesised new derivatives of 9,10-bis(1,3-dithiol-2-ylidene)-9,10-dihydroanthracene possessing flexible dialkoxy substituents. CV data establish increased π -donor strength with the detection of the tetracation oxidation state. X-ray crystal structures reveal the dramatic conformational change, which accompanies oxidation of the neutral molecule **44** to the dication. $\mathbf{44}^{2+} (\text{TCNQ}^-)_2 \cdot 2\text{MeCN}$ is the third TCNQ complex of a 9,10-bis(1,3-dithiol-2-ylidene)-9,10-dihydroanthracene donor to be characterised crystallographically. Its stoichiometry is different from that of its two predecessors; a notable feature of the structure is that both sulfur atoms of the dithiolium ring participate in short intermolecular contacts with nitrogen atoms of a TCNQ moiety. This study further demonstrates that 9,10-bis(1,3-dithiol-2-ylidene)-9,10-dihydroanthracene is a very interesting π -electron rich system with unusual redox and structural properties.

3.1 Introduction

The design and synthesis of new anthracene bridged π -electron donor molecules is central to this thesis. In Chapter 2, we showed that functionalisation could be achieved *via* ether linkages to the central anthracene spacer. However, our attempts to functionalise the dithiole rings proved problematic. In this chapter, we reinvestigate the lithiation chemistry of the dithiole rings. We intended to synthesis a range of functional derivatives, which could later be utilised in target driven synthesis. We chose to functionalise the dithiole rings as substituents placed here were essentially unexplored and should afford reactive ‘handles’ for further transformations. It was also of interest to investigate how substituents affected the structural and electrochemical properties of the system.

3.2 Lithiation of the Dithiole Rings

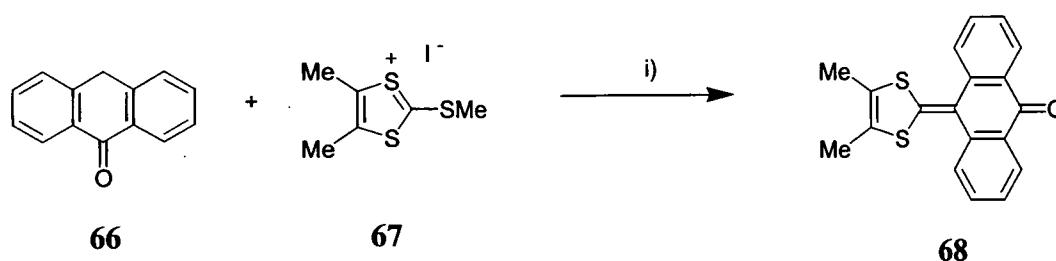
Given the problems encountered with the lithiation of compound **44** (Chapter 2) we chose to prepare compound **65**, which would possess only one acidic hydrogen. We anticipated that the methyl substituents would provide sufficient solubility (and indeed this proved to be the case).



One possible route to compound **65** was *via* two sequential, Horner-Wadsworth-Emmons reactions onto anthraquinone. However, initial investigations showed that the reactions of one equivalent of both anthraquinone and Horner-Wadsworth-Emmons

reagent **54** gave a mixture of mono- and di- substituted products, with the disubstituted product **29** predominating. It was decided that this methodology was impractical for the first stage of a multi-step synthetic route.

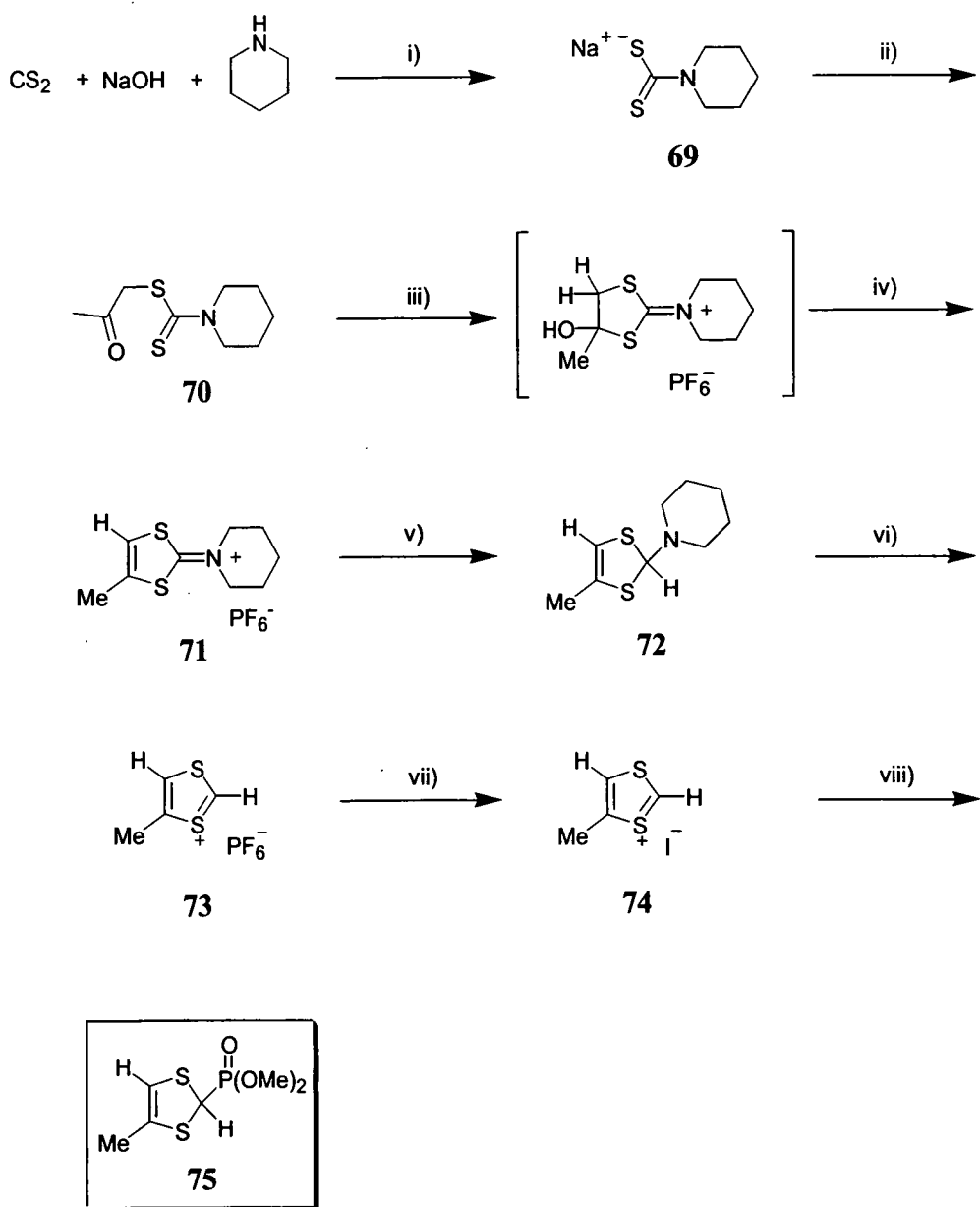
Our efforts then focused on the methodology of Gompper and Kutter who described the reaction of a benzo-1,3-dithiolium salt with anthrone **66**, in an addition reaction followed by elimination of methylthiol under mildly basic conditions.⁴⁸ Further investigation of this reaction in our laboratory had previously afforded compound **68** which provided a readily available starting material (Scheme 3.1).³⁷



Scheme 3.1 Reagents and Conditions: i) Pyridine/acetic acid 3:1 v/v, 50-60°C.

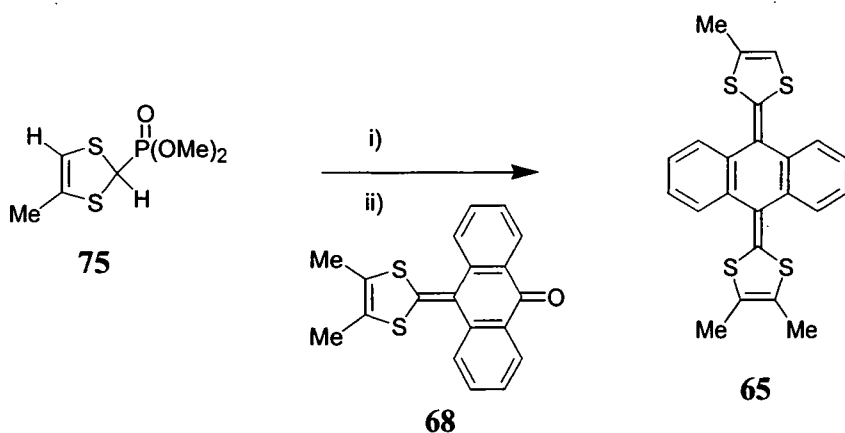
The ketone **68** could then undergo a Horner-Wadsworth-Emmons reaction using the novel phosphonate ester reagent **75** to yield target **65**. Compound **68** was synthesised as reported in the literature.³⁷

The new mono methyl Horner-Wadsworth-Emmons reagent **75** was prepared as shown in Scheme 3.2. Treatment of carbon disulfide with piperidine under basic conditions yields sodium piperidine-1-carbodithioate **69**. Further reaction with 1-bromopropan-2-one in refluxing ethanol affords 2-oxopropylpiperidine-1-carbodithiolate **70**. Sulfuric acid-induced cyclisation of **70** affords the desired imminium salt **71**, which is isolated as the hexafluorophosphate salt. Reduction of the imminium salt **71** occurs with sodium borohydride to afford amine **72**. The subsequent conversion of compound **72** was achieved by slow addition to anhydrous hexafluorophosphoric acid forming a white solid. Purification of salt **73** was most easily achieved by conversion to its iodide salt **74**, reaction of which with trimethyl phosphite affords the phosphonate ester **75**.



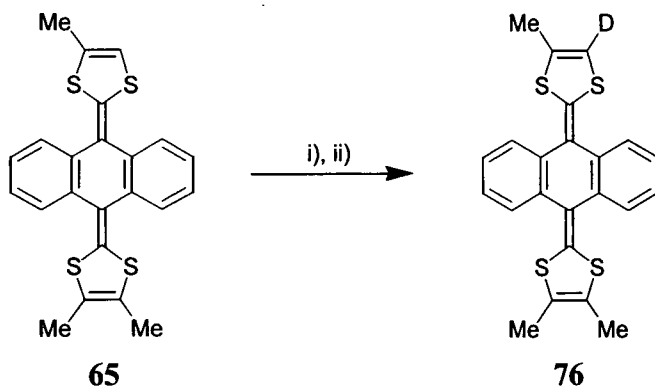
Scheme 3.2 Reagents and Conditions: i) EtOH, rt, 5h. ii) $\text{CH}_3\text{COCH}_2\text{Br}$, EtOH, reflux, 24h. iii) c. H_2SO_4 , 70°C , 4d. iv) HPF_6 , 0°C , 1h. v) NaBH_4 , THF/PrOH, 0°C , 1h. vi) HPF_6 , $\text{Ac}_2\text{O}/\text{Et}_2\text{O}$, 0°C , 1h. vii) NaI , Me_2CO , rt, 1h. viii) $\text{P}(\text{OMe})_3$, MeCN, rt, 1h.

The reaction of compound **68** with the phosphonate anion obtained by deprotonation of reagent **75** using lithium diisopropylamide (LDA) in THF at -78°C afforded compound **65** in 55% yield (Scheme 3.3).



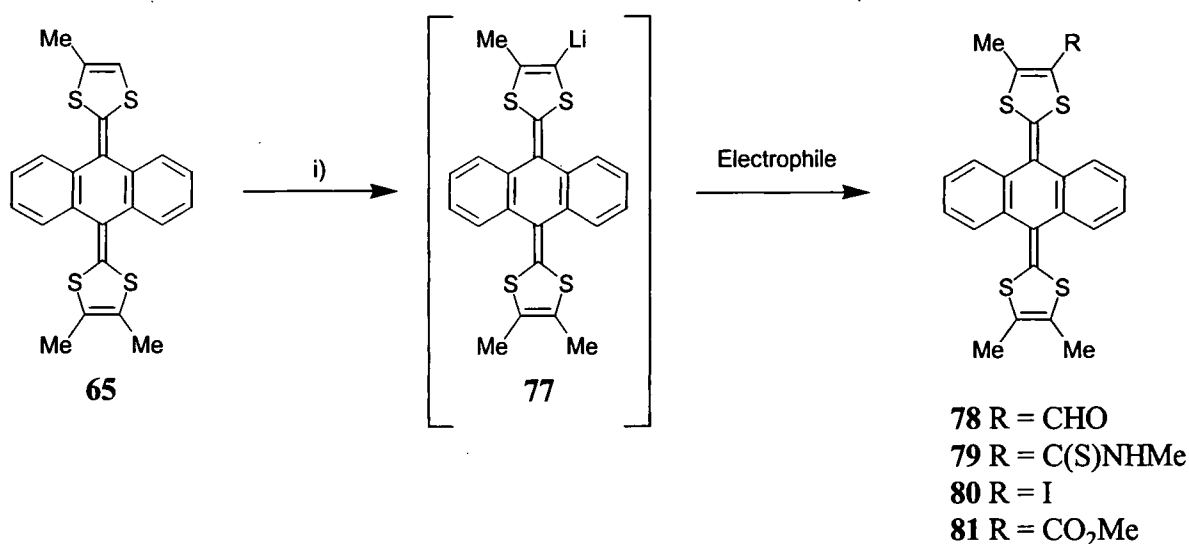
Scheme 3.3 Reagents and Conditions: i) LDA, THF, -78°C , 3h.

Our initial reaction to assess the lithiation of **65** was to perform a deuterium exchange, which was monitored by proton NMR spectroscopy (Scheme 3.4).



Scheme 3.4 Reagents and Conditions: i) LDA, THF, -78°C , 3h. ii) D_2O .

Deprotonation of **65** using LDA in THF at -78°C followed by quenching with an excess of deuterium oxide gave a quantitative yield of the mono-deuterio derivative **76** (^1H NMR evidence) thus confirming the very efficient generation of the lithiated species. The results of the trapping of the metallated species **77** with a selection of electrophiles are shown in Table 3.1 (Scheme 3.5).



Scheme 3.5 Reagents and Conditions: i) LDA, THF, -78 °C, 3h.

Electrophilic Reagent	Reaction Product	Yield (%)
DMF	78	13%
N-Methyl formanilide	78	0%
N-Methyl isothiocyanate	79	17%
Perfluorohexyl iodide	80	55%
Methyl chloroformate	81	83%

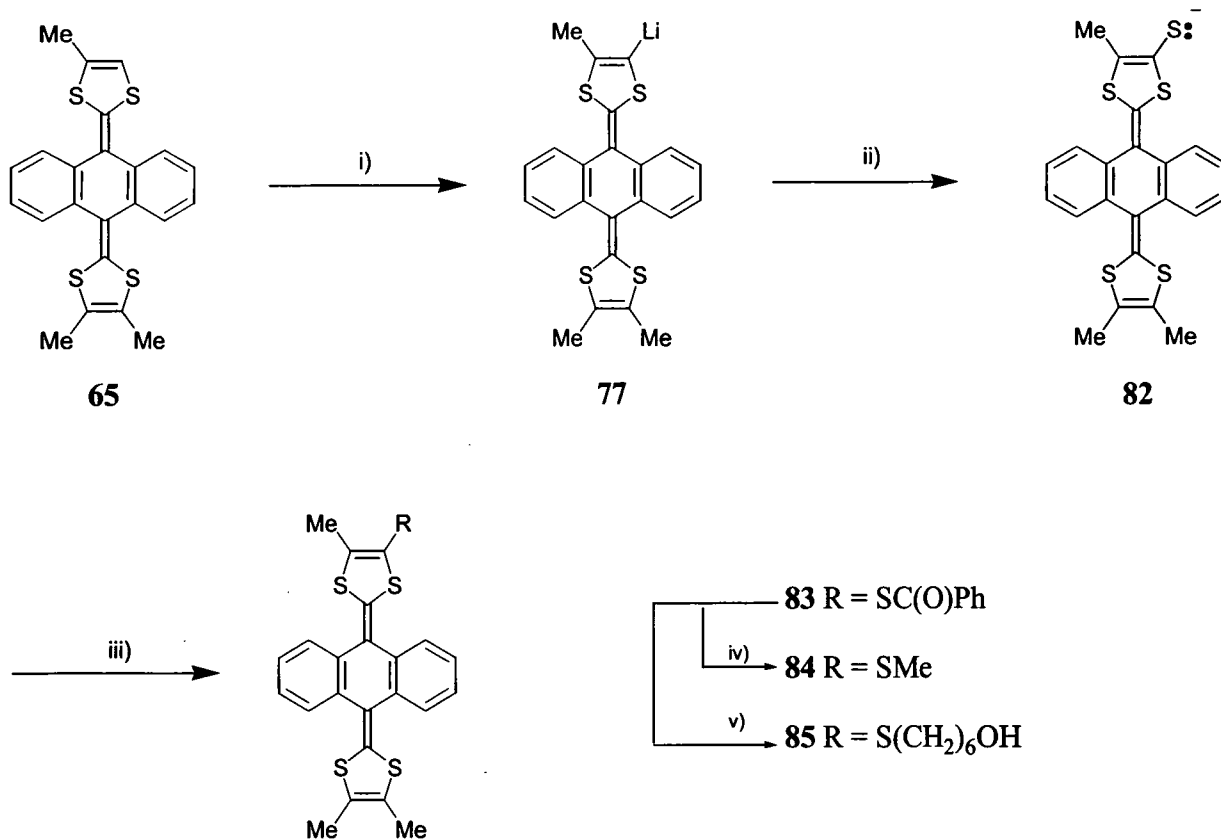
Table 3.1: Trapping of the lithium salt of compound **77** with various electrophiles.

The yields of the substituted products, **78** and **79**, were consistently lower than those for the analogous trimethyl-TTF derivatives⁴⁹: with the majority of unreacted compound **65** being easily recovered. The aldehyde and thioamide derivatives **78** and **79** were repeatably obtained in only 13% and 17% yields, respectively, with N,N-dimethylformamide and N-methylisothiocyanate as the electrophiles. For the synthesis of **78**, N,N-dimethylformamide was preferable to N-methylformanilide as the formylating reagent, in direct contrast to the analogous reaction with TTF **1**⁵⁰ or trimethyl-TTF.⁴⁹ A

considerably more efficient trapping of the lithiated species **77** occurred with methyl chloroformate, to yield the ester derivative **81** (83% yield).

Sulfur insertion into the lithiated species **77**, followed by reaction of the transient thiolate anion with benzoyl chloride gave the thioester derivative **83** (53% yield). Compound **83** is a convenient shelf-stable precursor of mono-functionalised derivatives of **65**. Saponification of **83** was readily achieved (sodium methoxide, room temperature) with the transient thiolate anion being regenerated and efficiently trapped with iodomethane and 6-bromohexan-1-ol to yield **84** and **85**, respectively (80-93% yields, Scheme 3.6).

We established, therefore, that this lithiation approach provided a valuable route to some derivatives. The introduction of a methyl ester group should provide access to the alcohol allowing the formation of ester and ethers linkages, with the iodide derivative **80**, providing a route to organometallic couplings. The development of a shelf stable protected thiolate, **83**, increases the nucleophilicity of the anion and allows reactions to be performed at room temperature.



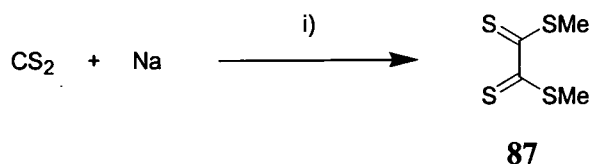
Scheme 3.6. Reagents and Conditions: i) LDA, THF, -78 °C, 1h. ii) S₈ iii) PhC(O)Cl iv) NaOMe/MeOH, THF, rt, 1h followed by MeI v) NaOMe/MeOH, THF, rt, 1h followed by 6-bromohexan-1-ol.

3.3 Functionalisation via Addition/Elimination Reactions

Having developed approaches for direct dithiole modification (Section 3.2) we now addressed other routes to different functionality. Here we describe a complimentary approach for the addition of functional groups directly to anthrone.

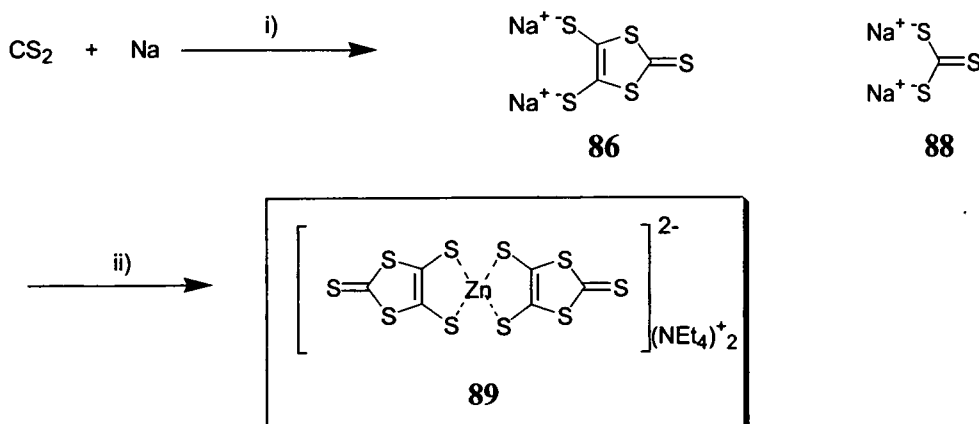
The starting point for our synthesis was 4,5-dithiolate-1,3-dithiole-2-thione **86**, which was prepared *via* the chemical reduction of carbon disulfide in the presence of sodium.⁵¹ The mechanism of the reaction has been the focus of much debate since it was first reported by Fetkenhauser *et al.*⁵² The major product, trapped by the addition of chloromethane, was initially assigned as dimethyl tetrathioxalate **87**, which is analogous

to the chemical reduction of carbon dioxide to oxalic acid performed by Kolbe in 1868 (Scheme 3.7).⁵³



Scheme 3.7 Reagent and Conditions: i) DMF, 0 °C followed by MeI.

This proposal was later disproved as the reaction produces 4,5-dithiolate-1,3-dithiole-2-thione **86**, and 1,3-dithiolate-2-thione **88**.⁵¹ The desired compound **86** can be separated from compound **88** by the addition of zinc chloride which selectively complexes with **86**, precipitating **89** as a red solid (Scheme 3.8). Recently an improved procedure has been developed and a new mechanism for the formation of **86** proposed in our laboratory.⁵⁴

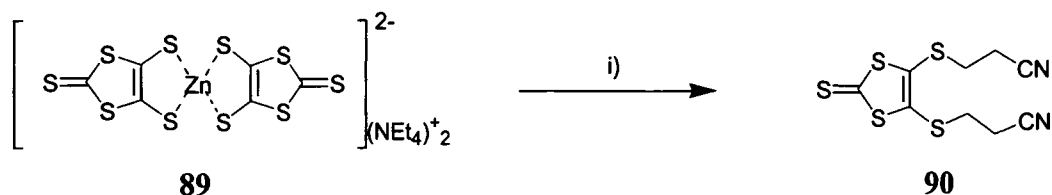


Scheme 3.8 Reagents and Conditions: i) DMF, 0 °C. ii) ZnCl₂, Et₄NBr.

It has been shown from TTF chemistry that sulfur insertion reactions can lead to products in higher yield than their lithium analogues.³⁸ The use of zincate salt **89** provides an analogous dithiolate.

The literature contains a variety of protecting groups for thiolates ranging from thioesters to silyl reagents.⁵⁵⁻⁵⁸ Ideally, the protecting group should be stable towards strong bases which would allow conversion to the thiolate protected Horner-Wadsworth-Emmons reagent.

The problems experienced with various protecting groups were that they did not withstand the varied conditions of subsequent reactions. If a Horner-Wadsworth-Emmons approach was to be utilised then the protecting group would have to be stable against strong bases such as LDA and fluorine rich environments *e.g.* triflate salts, but also powerful electrophiles such as methyl triflate. The propionitrile group provided stability against the electrophilic methyl triflate but not strong bases. Therefore, a Horner-Wadsworth-Emmons type approach would fail, as strong bases would deprotect the thiolate. To overcome this problem we decided to introduce the protected thiolate *via* an addition-elimination type reaction. After experimentation we settled on the propionitrile-protecting group. The protecting group was applied directly to compound **89** affording **90** in a single step with an 85% overall yield, following the literature (Scheme 3.9).⁵⁹

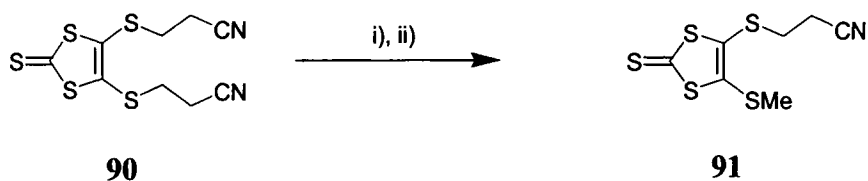


Scheme 3.9 Reagents and Conditions: i) 3-bromopropionitrile, toluene, reflux, 6h.

This protecting group is stable to acid and weak bases but is easily removed by strong base.⁶⁰ The system could then be deprotected and functionalised before performing a Horner-Wadsworth-Emmons reaction.

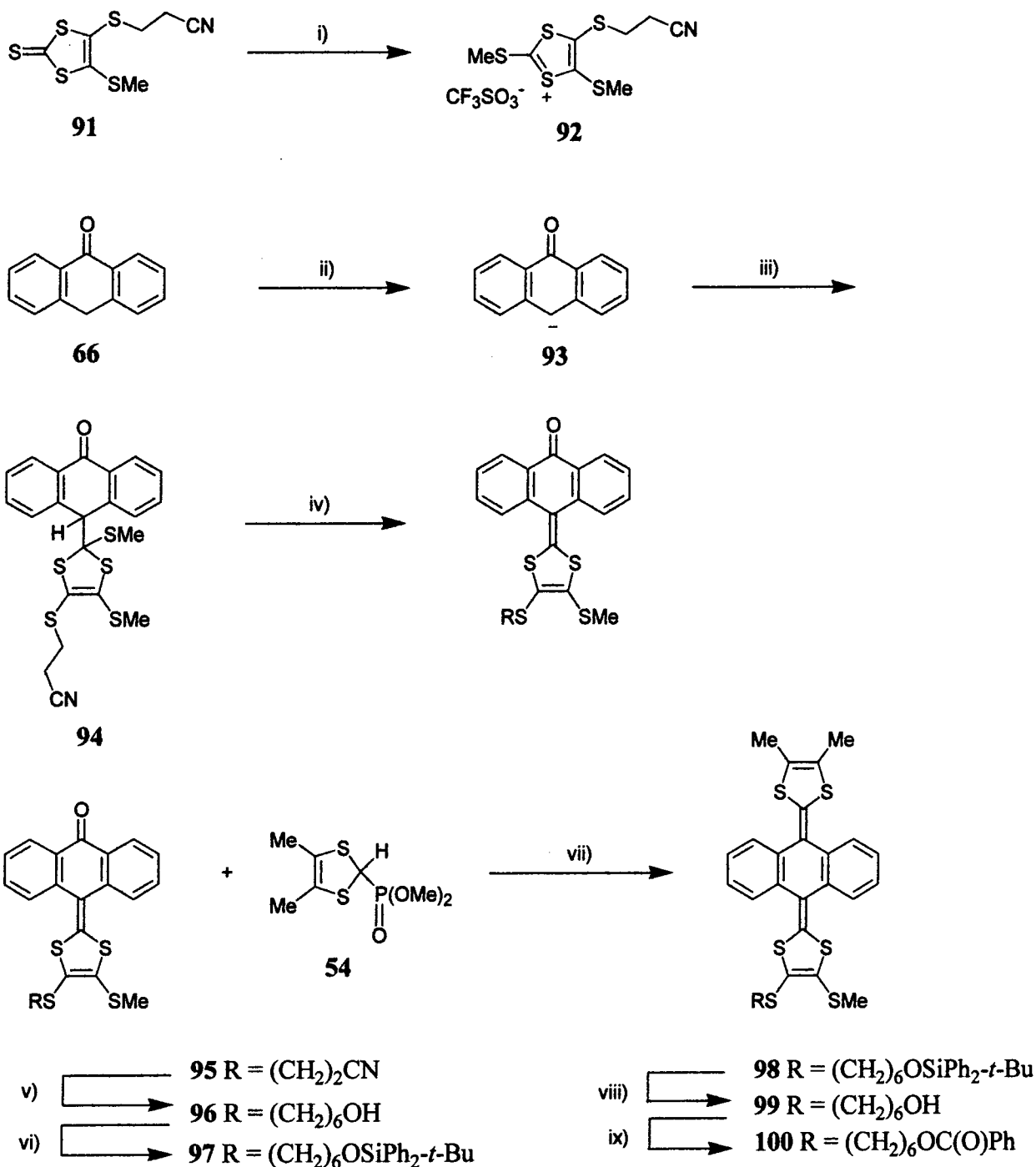
One of the advantages of the bis protected reagent **90** is that it may be mono-deprotected under certain conditions.⁶¹ If more basic conditions are imposed then the dithiolate is generated. In order to simplify our system we chose to selectively mono-deprotect at this stage, as this would reduce the number of potential products, simplifying

reaction monitoring. A methyl group was chosen as the blocking group for simplicity (Scheme 3.10).⁶²



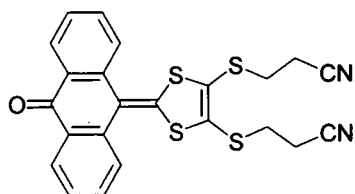
Scheme 3.10 Reagents and Conditions: i) $\text{CsOH} \cdot \text{H}_2\text{O}$, MeOH/THF , rt, 3h. ii) MeI

The methylation of thione **91** with methyl triflate gave the cation salt **92**, which was reacted, without purification, with the anion of anthrone, **93** (generated using LDA at room temperature), to afford initially compound **94**, which was converted into the desired compound **95** by treatment with *p*-toluene sulfonic acid (18% yield, based on thione **91**). The low yield occurred due to the competing deprotection of the cyanoethylthio group of **95** under these basic conditions. The thiolate anion derived from **95** was cleanly liberated using Becher's conditions (caesium hydroxide at room temperature) and trapped *in situ* with 6-bromohexan-1-ol to afford the alcohol derivative **96** in 89% yield. Conversion of **96** into *t*-butyldiphenylsilyl ether derivative **97** (90% yield) and subsequent Horner-Wadsworth-Emmons reaction with the anion derived from reagent **54**, gave compound **98** (70% yield) desilylation of which (tetrabutylammonium fluoride) gave alcohol derivative **99** (79% yield). The suitability of compound **99** for further elaboration was established by reaction with benzoyl chloride in the presence of triethylamine, which gave the benzoyl ester derivative **100** in 50% yield (Scheme 3.11).



Scheme 3.11 Reagents and Conditions: i) MeSO₃CF₃, DCM, 1h, rt. ii) LDA, ⁱPrOH, rt, 20min. iii) Compound **92** iv) *p*-TSA, PhMe, reflux. v) CsOH.H₂O, THF, 20°C, then Br(CH₂)₆OH vi) *t*-BuPh₂SiCl, imidazole, DMF, 20°C. vii) LDA, THF, -78°C. viii) TBAF, THF, 20°C ix) PhC(O)Cl, NEt₃, CH₂Cl₂, 20°C.

To capitalise on the protecting group's ability to be selectively removed, we constructed compound **101** in a similar manner to that of ketone **95**. Compound **101**, represents the first building block for di-substituted systems and was prepared from compound **90** in 3 steps with an overall yield of 19%. We have not pursued reactions of **101** but it should prove to be a useful intermediate for other reactions.



101

3.4 Electrochemistry

Solution electrochemical and UV-vis spectroscopic data for the new derivatives of the parent system **30** are entirely in accordance with their structures. Cyclic voltammetric data obtained in acetonitrile established that the redox properties are only slightly modified by the presence of the substituents: a predictable trend⁴⁹ is that the two-electron oxidation wave is anodically shifted by an electron-withdrawing substituent on the 1,3-dithiole ring: *cf.* E^{OX} values for compound **65** (0.320 V), compound **78** (0.450 V) and compound **81** (0.425 V). The lowest energy absorption in the UV-vis spectra is observed at λ_{max} 420-430 nm, and is essentially unaffected by the substituents. Comparable data for the parent system **30** and benzoannulated analogues have been discussed recently by Martín *et al.* on the basis of theoretical calculations.⁶³

3.5 Single Crystal X-ray Structures of compounds **81** and **84**.

Molecule **81** adopted a saddle-like conformation, relieving steric repulsion between sulfur atoms and hydrogen atoms in *peri* positions of the anthracene moiety (Figure 3.1) and incorporated one CDCl₃ molecule of crystallisation. The former being folded along the C(9)...C(10) axis by a dihedral angle (ϕ) of 40.5°. The bis(1,3-dithiol)benzoquinone system is U-shaped through an 'accumulating bend' comprising the boat conformation of the central (quinonoid) ring, folding of both 1,3-dithiole rings along S...S vectors, and out-of-plane tilting of the exocyclic carbon-carbon double bonds, all in the same (inward) direction. Thus, the S(1)C(16)C(17)S(2) and S(3)C(22)C(23)S(4) moieties form an acute dihedral angle (θ) of 75.6°. The C-S bonds in the methoxycarbonyl-substituted dithiole ring of **81** are asymmetrical, S(1)...C(16) shortened to 1.743(11) Å and S(1)...C(15) lengthened to 1.785(11) Å [*cf.* S(2)...C(15) 1.757(10) and S(2)...C(17) 1.756(10) Å]. The crystal structure of thiocarbamoyl-TTF and thiocarbamoyl-Me₃TTF similarly reveals mesomeric effects (*i.e.* a contribution from canonical forms, Figure 3.2).⁶⁴ In the other (dimethyl substituted) dithiole ring of **81**, the

C(21)...S(3) and C(21)...S(4) bonds are equivalent (1.767(9) Å) as are the S(3)...C(22) and S(4)...C(23) bonds (1.749 (10) Å).

At this point it was also worth considering the questions of geometric isomers. Anthracene containing bis-dithiole compounds show a saddle shape in the solid state, if this geometry holds true for compound **65** in the solution state then two possible geometric isomers exist. These can be easily visualised as a saddle with the handle on either the left or right. These isomers were never separated and all reactions were performed on the mixture of geometric isomers.

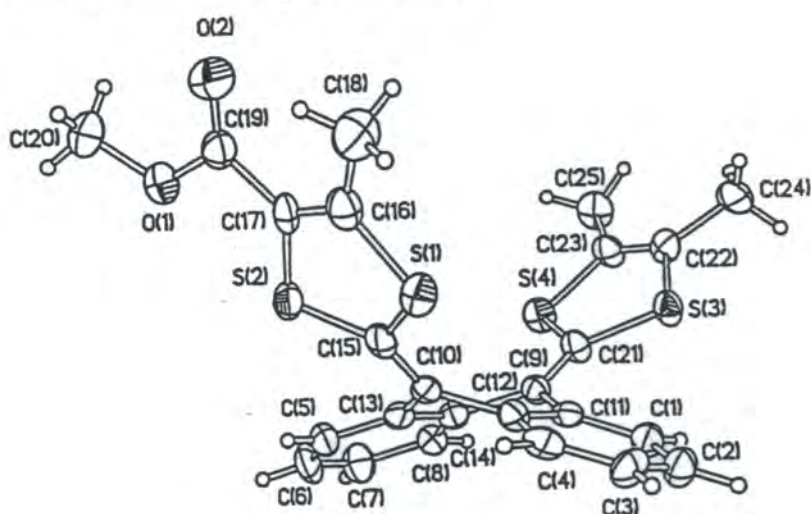


Figure 3.1: Single crystal X-ray structure of compound **81**.

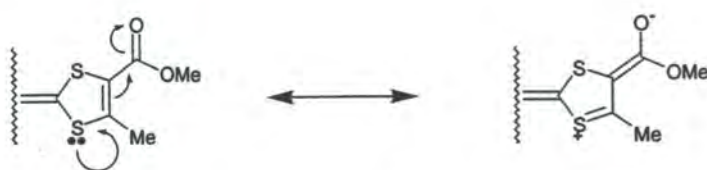


Figure 3.2: The internal mesomeric CT of compound **81**.

Crystal packing of **81** (Figure 3.3) showed the motif reported earlier for the tetra(thiomethyl) analogue,⁴³ with pairs of inverted molecules engulfing each other's dimethyl substituted dithiole moiety. These moieties contact face to face, but the interplanar separation of *ca.* 3.7 Å is rather long. CDCl₃ molecules occupy cavities between these pairs and are disordered.

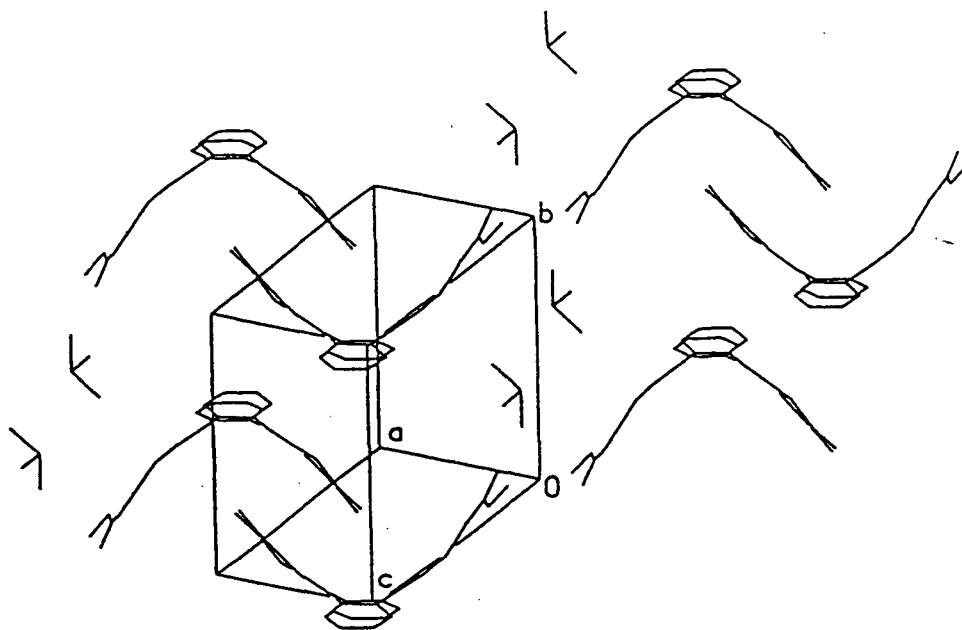


Figure 3.3: Single crystal X-ray packing motif of compound **81**.

Compound **84** exhibits a wider θ angle (86.9°) due to the more planar dithiole rings, and in spite of more pronounced folding of the anthracene moiety ($\phi = 45.1^\circ$). It has the same packing motif as **81**, but without any solvent of crystallisation. The thiomethyl group is disordered over three positions, at C(16), C(17) and C(21), with occupancies of 80%, 15% and 5%, respectively. For the former two, the nearly overlapping positions of the sulfur and the methyl carbon atoms, S(5) and C(19), could not be resolved and were refined as a single atom; for the latter, the methyl group bound to sulfur was not located, the major position is shown in Figure 3.4.

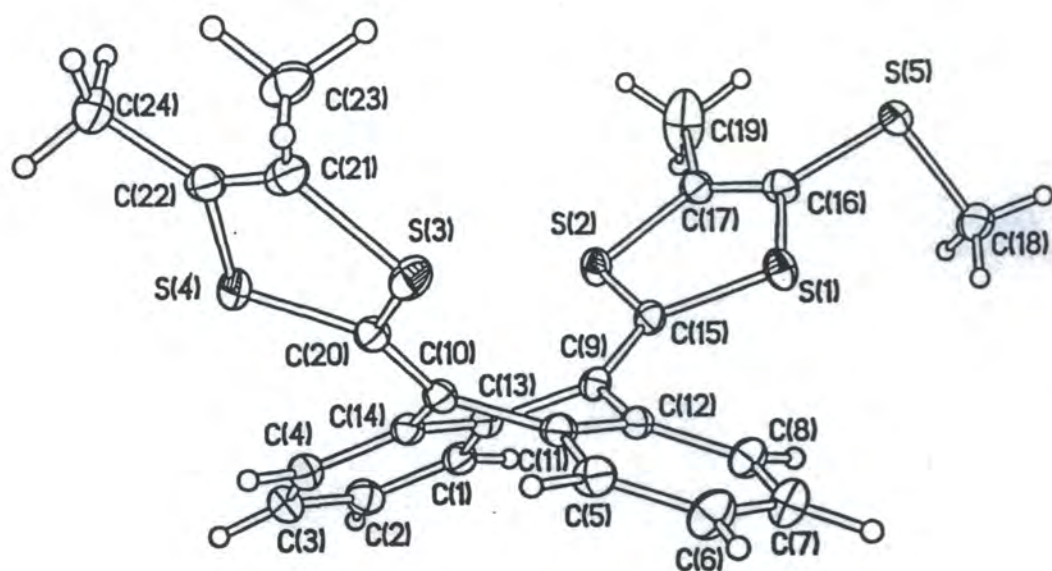


Figure 3.4: Single crystal X-ray structure of compound 84.

3.6 Conclusion

Two routes have now been developed to gain access to unsymmetrical derivatives of the 9,10-bis(1,3-dithiol-2-ylidene)-9,10-dihydroanthracene system which contain a 'reactive handle' suitable for further chemical elaboration. We have also shown from electrochemical and UV-vis studies that functionalisation on the dithiole ring has little influence over the redox behaviour of the system. The single crystal X-ray studies confirm the presence of the cavity after functionalisation. The availability of these new derivatives in synthetically useful quantities paves the way for the development of this very interesting, strained ring system as a redox-active building block in supramolecular chemistry.

4.1 Introduction

Chapters 2 and 3 describe the synthesis and electrochemical properties of new 9,10-bis(1,3-dithiol-2-ylidene)-9,10-dihydroanthracene derivatives, with little emphasis on potential applications. In this chapter, we address molecular sensors based on the 9,10-bis(1,3-dithiol-2-ylidene)-9,10-dihydroanthracene system by virtue of annulated crown ether substituents.

Much of the groundwork on molecular sensors owes its origin to biological processes. Nature has long been using molecular sensors for catalysis, recognition, regulation and transport; it is from such well-developed systems that much can be learned. A molecular sensor is a system for which the physiochemical properties change upon interaction with a chemical species in such a way as to produce a detectable signal, *e.g.* binding of a guest analyte ion or molecule to a receptor (the host) is transduced to the signalling unit which responds by changing its electronic state, which is monitored spectroscopically or electrochemically. Interactions between host and guest range in complexity, and utilise a variety of interactions, such as hydrogen-bonding, ion-dipole, hydrophobic, π - π , or a combination of these;⁶⁵⁻⁶⁸ such interactions are important as they determine the specificity of the sensor for the guest molecule. Specificity is defined as the degree of selectivity of the guest molecule when compared to other similar competitive guests. Many host molecules possess cavities or cyclic structures, which provide the site of interaction analogous to an 'antenna' (Figure 4.1).

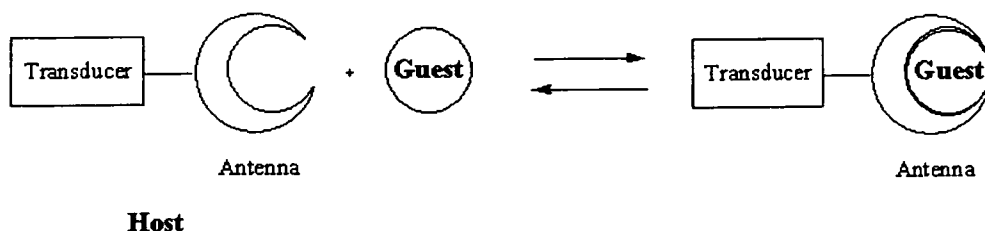
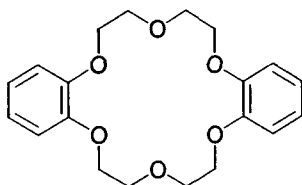


Figure 4.1: Components of a molecular sensor

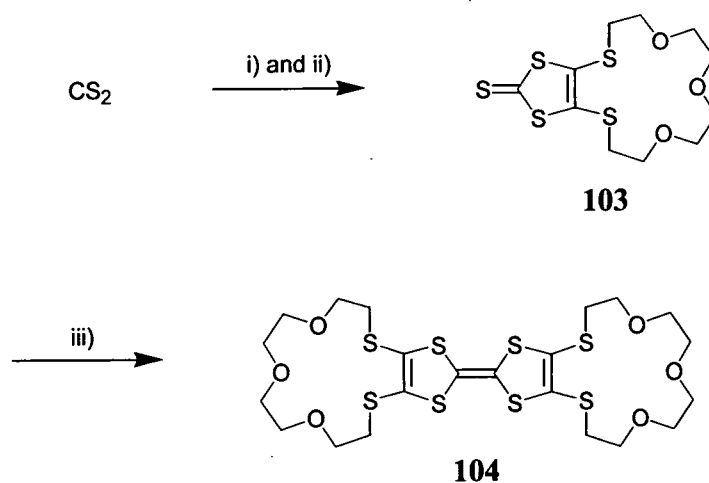
Crown ethers were first prepared by C. J. Pedersen in 1967, for which he later received the Noble prize along with Cram and Lehn. Pedersen synthesised dibenzo-18-crown-6, **102** and showed it selectively bound sodium ions in the presence of methanol.⁶⁹



102

Crown ethers represent a simple antenna, and are well known for their ability to complex alkali metal ions. Further alkali ion selectivity can be achieved by varying the size of the crown, as larger crowns better accommodate larger ions. Measurements on the stability of these complexations show crowns prefer an optimum guest, that is a cation with a diameter closely fitting that of the cavity. The stability of complexation of alkali metals is also influenced by the choice of heteroatom. The complexation of “hard” alkali metal ions being preferential with “hard” oxygen crowns, due to similar orbital overlap. The ease of synthesis and well-understood principals of cation recognition using crown ethers made them a logical choice for our sensor system.

Several examples of macrocyclic systems based on crown ethers incorporating redox centres are contained in the literature.⁷⁰⁻⁷⁴ One example was prepared by Otsubo *et al.*, who described the synthesis of TTF crown ether **104** (Scheme 4.1).⁷⁵



Scheme 4.2 Reagents and Conditions: i) Na, DMF. ii) $\text{Ts}(\text{OCH}_2\text{CH}_2)_3\text{OTs}$ iii) $\text{P}(\text{OEt})_3$

Compound **103** was prepared by direct alkylation *via* reaction of a tosylated crown ether with a crude mixture of 4,5-dithiolate-1,3-dithiole-2-thione **86**, and 1,3-dithiolate-2-thione **88**. The resulting thione **103** was then phosphite coupled to yield compound **104** in low yields.

Other sensors incorporating various crown ethers annulated to TTF have been prepared by Becher *et al.*⁷⁶ who prepared compound **104** using an alternative synthetic route in good yields and went on to show that compound **104** showed a marked response to 250 equivalents of sodium in the cyclic voltammetry (Figure 4.2). The cyclic voltammetry of compound **104** exhibited a marked shift in the first oxidation potential (E_1^{ox}) in the presence of Na^+ , with little change in the second oxidation potential (E_2^{ox}). The electrochemistry can be explained, as the sensors will bind metal ions in the neutral state by ion-dipole interactions. The first oxidation of the TTF will be hindered by the presence of the metal ion due to coulombic repulsion, increasing the first oxidation potential relative to the uncomplexed crown system.

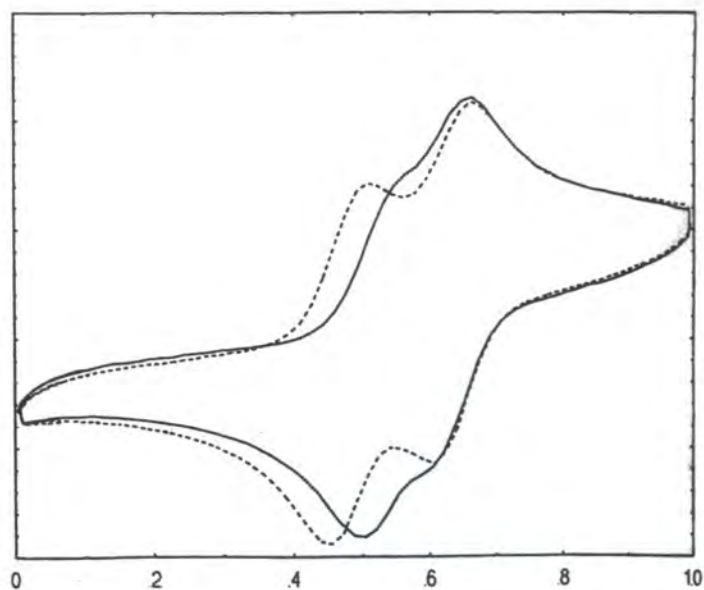


Figure 4.2: CV of compound **104** with 250 eq. NaPF_6 (solid line) and without sodium (dashed line). Recorded versus a SCE electrode in MeCN at a scan rate of 100 mV s^{-1} with $0.2 \text{ M Bu}_4\text{NClO}_4$.⁷⁸

Upon oxidation, repellent ion-ion interactions overpower the weaker ion-dipole interactions resulting in the ejection of the metal ion. The cavity is now empty in the radical cation state and is then oxidised to the dication without metal ion interference (Figure 4.3).

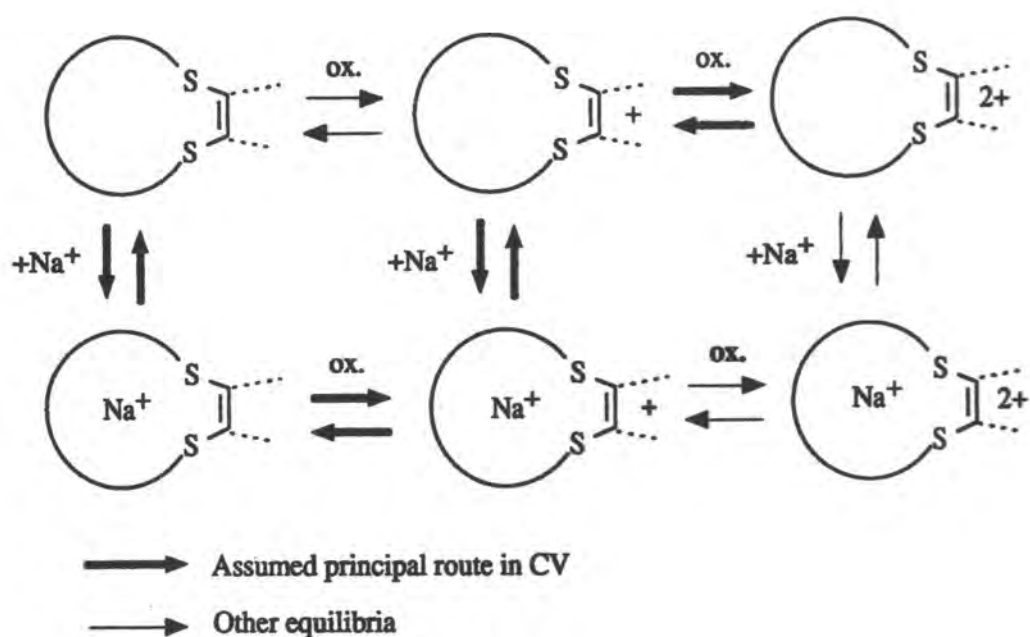
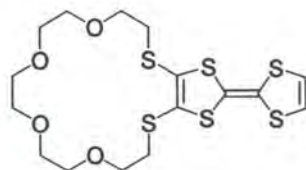


Figure 4.3: Possible mechanism for crown ether complexation within a Cyclic Voltammetric cycle.

More recently, Bryce *et al.* have prepared a range of unsymmetrical TTF-S₂O₄ crowns, *e.g.* compound **105**, and studied their cation binding properties by UV/vis spectroscopy and cyclic voltammetry.⁷⁷

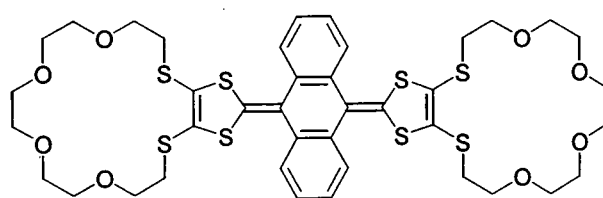


105

The effects of complexation with sodium, barium and silver were studied: mono-crown **105** formed a 1:1 complex with sodium resulting in an anodic shift of 25-35 mV in the CV. Complexation with silver and barium produced the greatest shift in oxidation potential with an anodic shift 70-75 mV for silver. These results are consistent with silver binding primarily at the sulfur sites, inducing a large perturbation in the electronic

structure of the TTF moiety. The stability constant for these systems was estimated to be $\log K = 2.26$ by electrochemical and spectroscopic measurements.

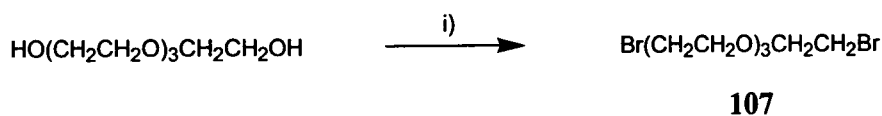
These examples led us to suggest that anthracene spaced bis-dithiole system **106** could be a potential sensor. Due to the high percentage of diffuse (soft) sulfur orbitals present in our system we decided to tailor the sensor toward silver, which possesses equally diffuse orbitals. Silver is a larger cation than sodium and requires a slightly larger crown. We set the goal of preparing and studying target compound **106**.



106

4.2 Synthesis

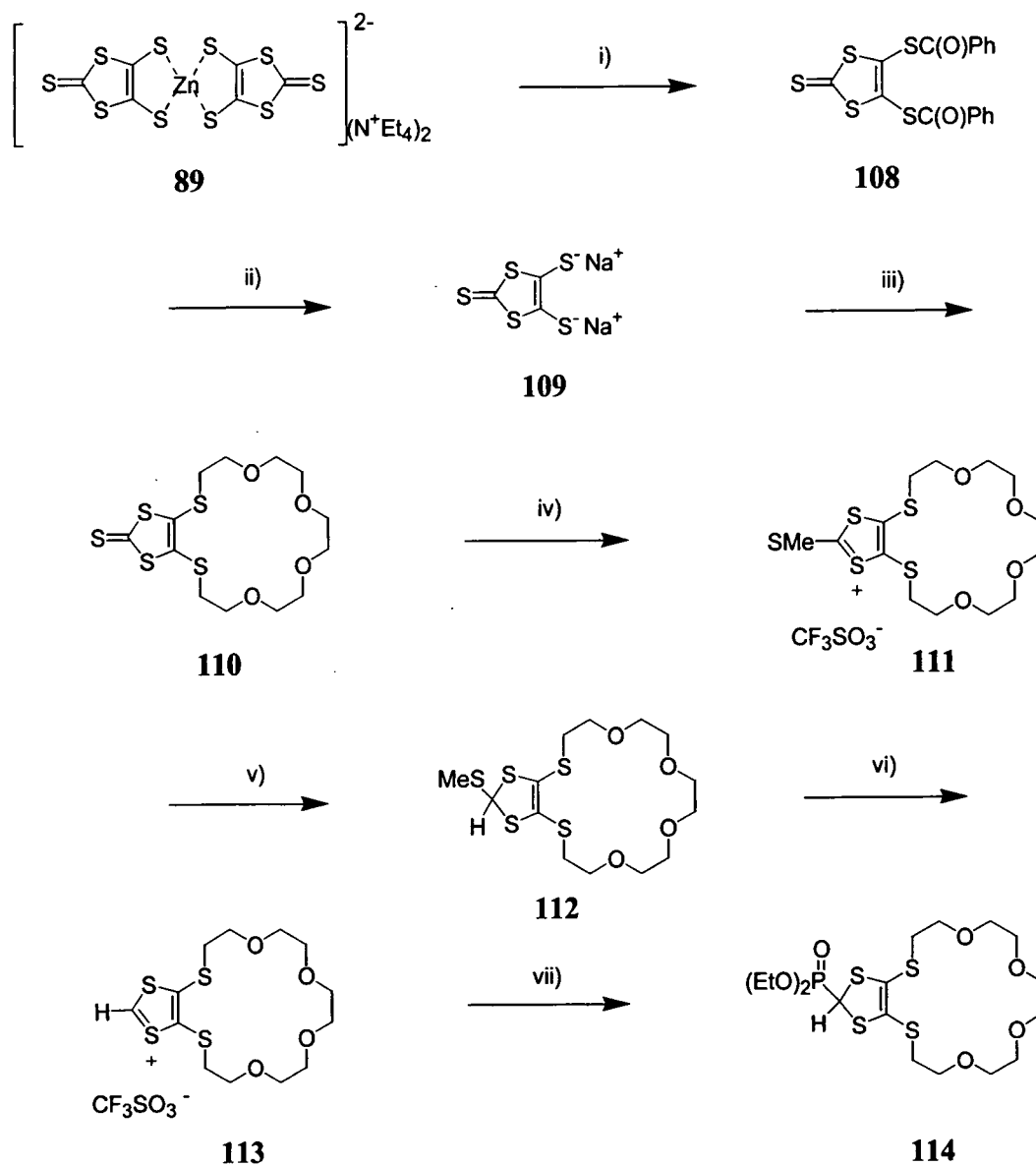
Pentaethylene glycol was utilised as the starting reagent for the crown functionality and was treated with two equivalents of phosphorus tribromide to generate the dibromo intermediate **107**, in 51% yield (Scheme 4.2), which was used without further purification.⁷⁸



Scheme 4.2 Reagents and conditions: i) PBr₃, py, 0 °C.

Saponification of compound **108** with sodium ethoxide generated the dithiolate **109**, which precipitated from solution and was collected by Schlenk filtration. Alkylation with glycol **107** generated thione **110** in 79% yield. The thione was then methylated using methyl triflate to afford compound **111** in 84% yield. Reduction was achieved with sodium cyanoborohydride to give compound **112**, as an off-white solid.

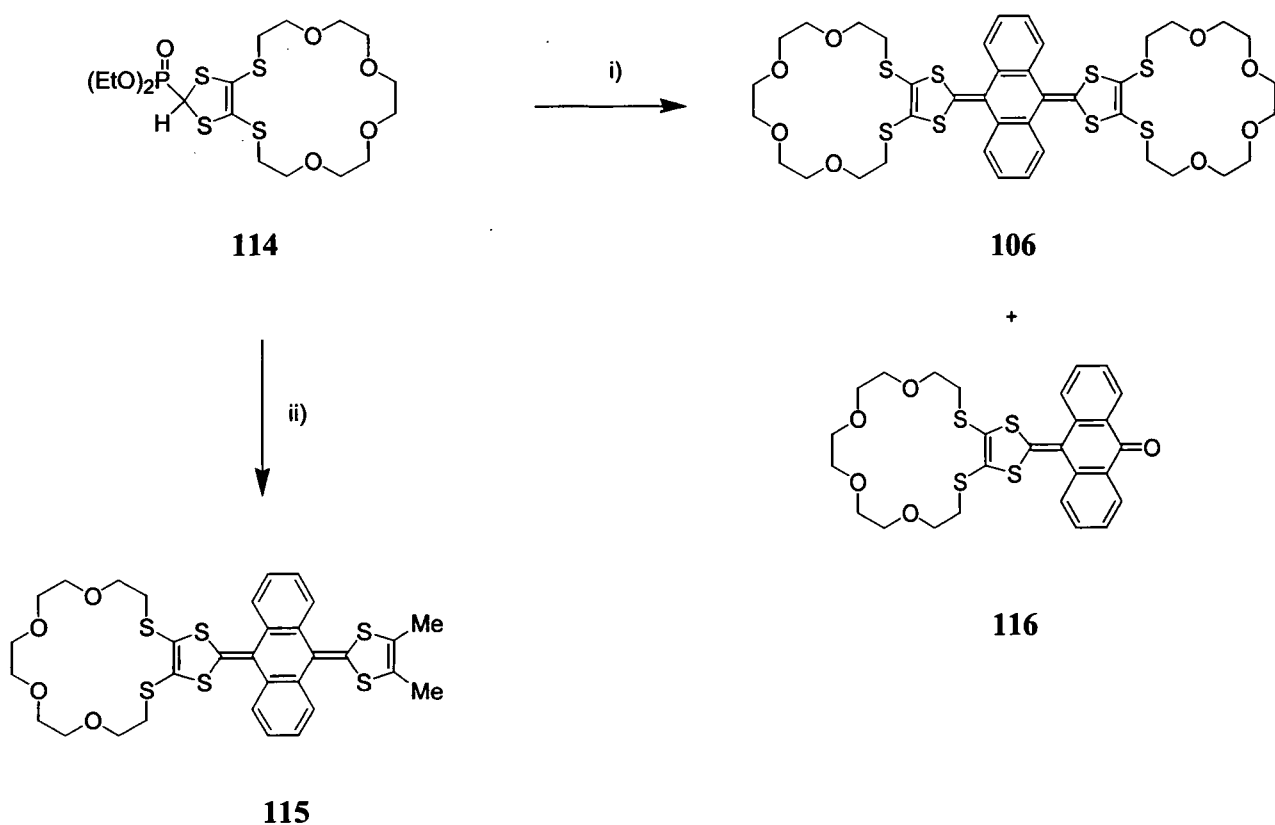
Conversion to the Horner-Wadsworth-Emmons reagent **114** was achieved *via* the triflate salt **113** (Scheme 4.3).



Scheme 4.3 Reagents and Conditions: i) $PhC(O)Cl$, Me_2O , 6 h, rt. ii) $NaOEt/EtOH$, 20 min, rt. iii) Compound **99** iv) $MeSO_3CF_3$, DCM , 1 h, rt. v) $NaBH_3CN$, $EtOH$, 1h, $0^\circ C$. vi) CF_3SO_3H , $MeCN$, 10 min, rt. vii) $P(OEt)_3$, NaI , $MeCN$, 30 min, rt.

Phosphonate ester **114** was stirred in dry THF at -78°C and treated with one equivalent of lithium diisopropylamide to give a white opaque solution containing the reactive anion. Half an equivalent of anthraquinone was then added and the reaction allowed to warm to 20°C , to yield the highly soluble bis-crown compound **106** in 67% yield.

In a similar procedure, compound **114** was stirred in dry THF at -78°C and treated with one equivalent of lithium diisopropylamide to generate the reactive anion. This was then quenched with one equivalent of compound **68** to yield the mono-crown compound **115** in 53% yield (Scheme 4.4).



Scheme 4.4 Reagents and Conditions i) LDA, THF, -78°C , 1h followed by anthraquinone. ii) LDA, THF, -78°C , 1h followed by compound **68**.

Unlike the previous Horner-Wadsworth-Emmons reaction detailed, the reaction of crown reagent **114**, with anthraquinone allowed the isolation of the ketone **116** as a red oil, that solidified on standing.

4.3 Cation Binding Studies.

The cation binding properties of **106** and **115** were initially assessed by ^1H NMR titration studies in CDCl_3 . In the presence of Na^+ and Ag^+ the resonances due to the $-\text{SCH}_2\text{CH}_2\text{O}-$ protons of the crown [(SCH₂) δ 3.020; (OCH₂) δ 3.650] shifted downfield (maximum shift *ca.* 0.07 ppm in the presence of 10 equiv. of Ag^+) while the anthracenediylidene resonances were essentially unaffected, confirming that cation binding occurs at the crown site. In contrast to this, Li^+ and K^+ cations had essentially no effect on the ^1H NMR spectrum.

UV-vis absorption spectroscopic studies were performed on compounds **106** and **115**. These spectra are very similar and show only ~ 2 nm differences in the wavelength of the main absorption peaks. These results indicate that although the sulfur atoms within the crown ether groups are conjugated into the chromophore part of the molecule, the perturbation of the chromophore electronic system due to the crown ether presence is relatively weak.

Investigations into complex formation with soft and hard metal cations in acetonitrile with compound **115** failed due to precipitation. Compound **106** showed normal chromionophore behaviour, the absorption spectra in acetonitrile in the presence of sodium perchlorate and silver perchlorate are shown in Figures 4.5 and 4.6 respectively.

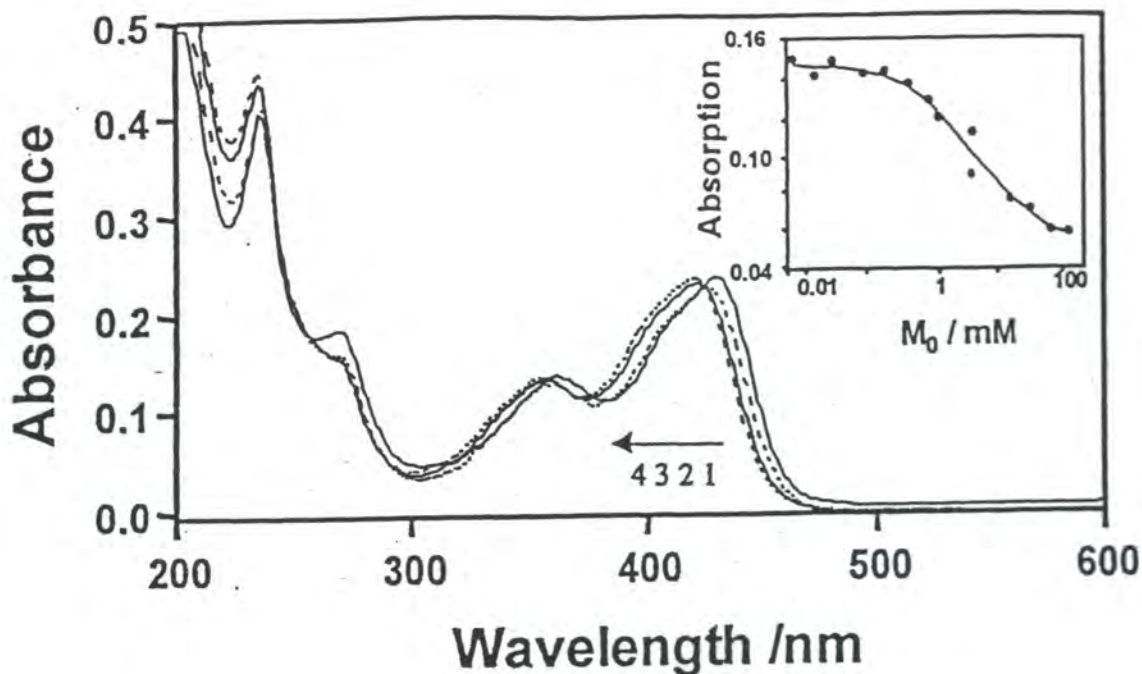


Figure 4.4: The absorption spectra attributed to the formation of the LM^+ complex.

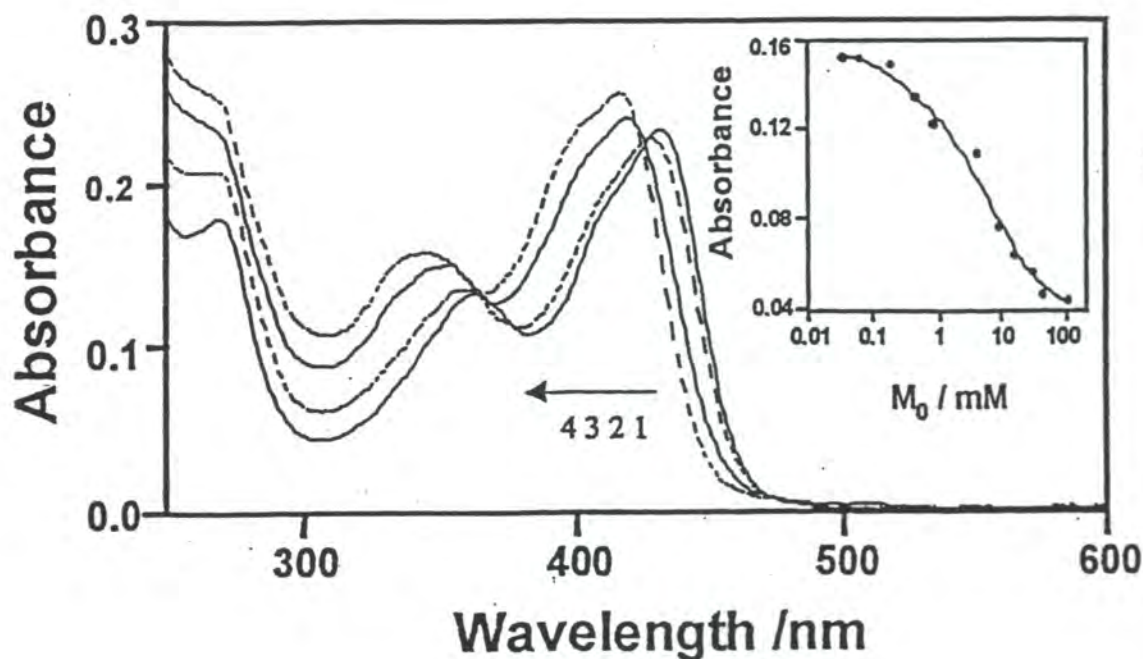


Figure 4.5: The absorption spectra attributed to the formation of the $L(M^+)_2$ complex.

In both cases, no isosbestic points were found, indicating that, most probably, more than one species are formed due to the complexation reaction and the absorption spectra of these species are different. Such behaviour is typical for bis(crown)

chromoionophores and may be attributed to the formation of 1:1 (LM^+) and 1:2 [$L(M^+)_2$] ligand:metal cation complexes. It was evident from absorption spectra (Figures 4.4 and Figures 4.5) that the formation of both LM^+ and $L(M^+)_2$ complexes occur for similar metal cation concentrations. Alternatively, one would expect the presence of isosbetic points for certain concentrations regions, where the formation of one type of complex dominates.

In agreement with reaction Scheme 4.5 the absorbance A of chromoionophore solution at any wavelength λ depends on metal cation concentration M_0 as described by Equation 4.1, where A_0 , A_1 , and A_∞ are the absorbances of the free ligand L and the complexes LM^+ and $L(M^+)_2$, respectively; K_1 and K_2 are the equilibrium constants for complex formation.

$$A = A_0 + \frac{K_1 * M_0 (A_1 - A_0)}{1 + K_1 * M_0 + K_2 * M_0^2} + \frac{K_2 * M_0^2 (A_\infty - A_0)}{1 + K_1 * M_0 + K_2 * M_0^2}$$

Equation 4.1:

The equation was found to fit compound **106** well ($R^2 > 0.98$). The estimated values for the equilibrium constants K_1 and K_2 are presented in Table 4.1. Although the fitting presented in Figure 4.4 is good, the equilibrium constants K_1 and K_2 cannot be accurately determined because of absorption overlap; additional measurements clearly distinguishing the formation of the LM^+ and $L(M^+)_2$ complexes would be required for a more accurate estimation.

	$\log K_{obs}$	Simultaneous Complexation	1:1 and 1:2 Complexes	R^2
Na^+	2.5 ± 0.2	$\log K_1$	~ 2.6	0.982
		$\log K_2$	~ 4.3	
Ag^+	2.4 ± 0.2	$\log K_1$	~ 3.4	0.992
		$\log K_2$	~ 5.5	

Table 4.1: Stability constants for **106** with Na^+ and Ag^+ cations in acetonitrile.

The observed stability constant, K_{obs} , may be wavelength dependent because of the different relative absorptivity of compound **106** and its complexes at different wavelengths. The fitting of the absorbance data taken at a fixed wavelength gave estimated K_{obs} values of 2.5 ± 0.2 and 2.4 ± 0.2 , for sodium and silver cations, respectively. For comparison, the $\log K_{obs}$ for compound **106**, Na^+ is very close to that reported for TTF-bis(crown), Na^+ complexation in acetonitrile.⁷⁷

Cyclic voltammetry and square wave voltammetry (SQV) showed that, as expected, both compounds display a two-electron oxidation wave: $E_1^{ox} +0.405$ V (compound **106**) and $E_1^{ox} +0.345$ V (compound **115**); the lower oxidation potential of the latter compound being consistent with the electron donating effect of the methyl substituents. As observed for previous derivatives, a second reversible one-electron wave, ascribed to oxidation of the anthracene system⁷⁸ (*i.e.* radical trication formation) was seen at $E_2^{ox} +1.62$ V for both compounds [CV data was recorded vs Ag/AgCl, electrolyte $Bu_4N^+ClO_4^-$ (0.1 M), acetonitrile, room temperature, scan rate 100 mV s^{-1}]. The reproducibility between different samples was ± 2 mV. The progressive addition of aliquots of metal triflate salts resulted in a positive shift of E_1^{ox} , while E_2^{ox} remained unchanged, thereby acting as a convenient internal reference. This is consistent with expulsion of the metal cation from the ionophore prior to the second oxidation wave. The maximum positive shifts (ΔE_1^{ox}) are as follows: Li^+ (15-20 mV), Na^+ (100 mV), K^+ (15-20mV) and Ag^+ (115 mV). The value of ΔE_1^{ox} is essentially the same for the mono- and bis-crown systems **115** and **106**, respectively, whereas in the TTF series, *e.g.* compound

104, a larger shift is observed for bis-crowns. This could be a consequence of intramolecular steric interactions between the crown rings of **115**, and/or sandwich complexation between two crowns, favoured by the rigid saddle conformation. A comparison with related S₂O₄-crowned TTF systems shows two important advantages of system **106** and **115**. (1) The positive shifts for Na⁺ and K⁺ are significantly larger, and (2) the system is significantly more sensitive, with saturation being achieved with <10 equivalents of cation (*cf.* 200 equivalents for **104**).⁷⁸

We suggest that these results are a consequence of the unique combination of structural and redox properties of the 9,10-bis(1,3-dithiol-2-ylidene)-9,10-dihydroanthracene transducer unit. The saddle-shape folding of the anthracenediylidene system places the crown ring(s) of **106** and **115** in relatively close proximity to the redox-responsive moiety, and we believe, more significantly, the E₁ redox process which is monitored is a two-electron oxidation (*cf.* the one-electron wave of TTF, ferrocene *etc.*) thereby enhancing the electrostatic repulsion with the adjacent bound metal cation(s) leading to an increase in ΔE_1^{ox} .

4.4 Single Crystal X-ray Crystallography of compounds 115 and 116

An X-ray crystallographic study of compound **115** (Figure 4.6), showed the same structural motif as previous derivatives; the molecules are saddle-shaped with each molecule engulfing each other's dimethyldithiole ends. The anthracenediylidene moiety is folded along the C(9)---C(10) vector, the two benzene rings forming a dihedral angle of 39° (*cf.* 21° in **116**, Figure 4.7). The dithiole rings are folded along the S(1)---S(2) and S(3)---S(4) vectors by 15.5° and 8.7°, the S(1)C(16)C(17)S(2) and S(3)C(19)C(20)S(4) planes form an acute dihedral angle of 81°. No solvent molecules are within the macrocyclic or saddle cavity (Figure 4.6).

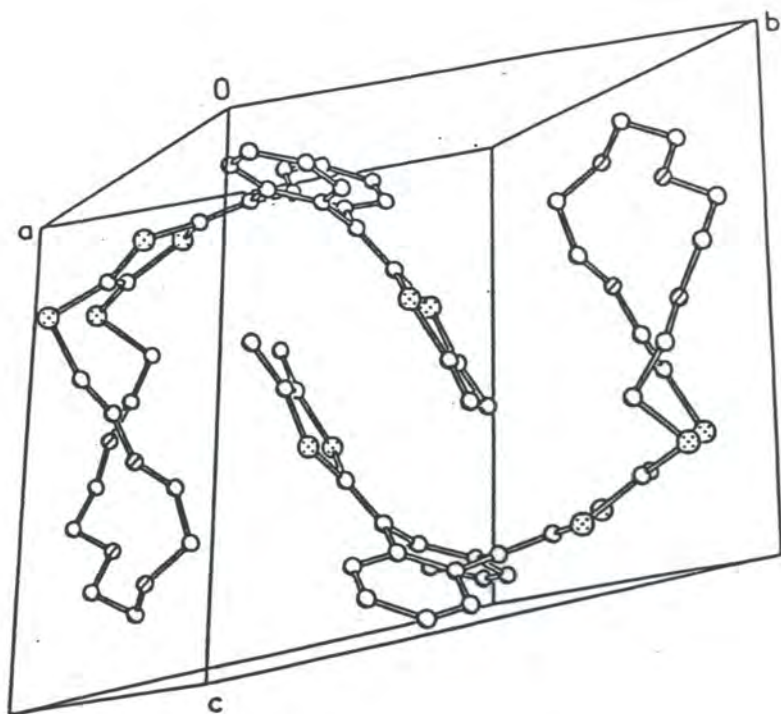


Figure 4.6: Single crystal X-ray structure of compound 115.

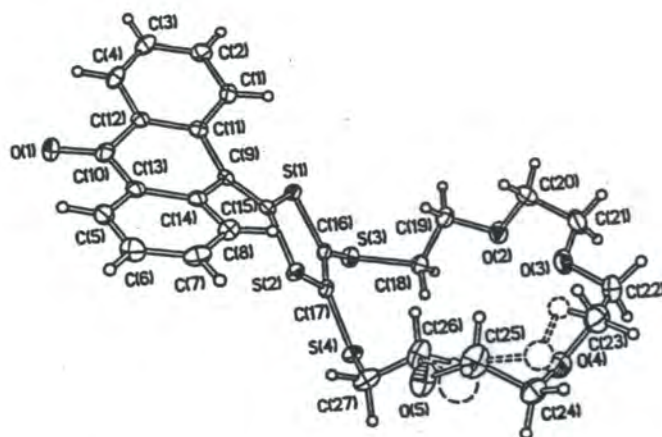


Figure 4.7: Single crystal X-ray structure of compound 116.

4.5 Conclusion

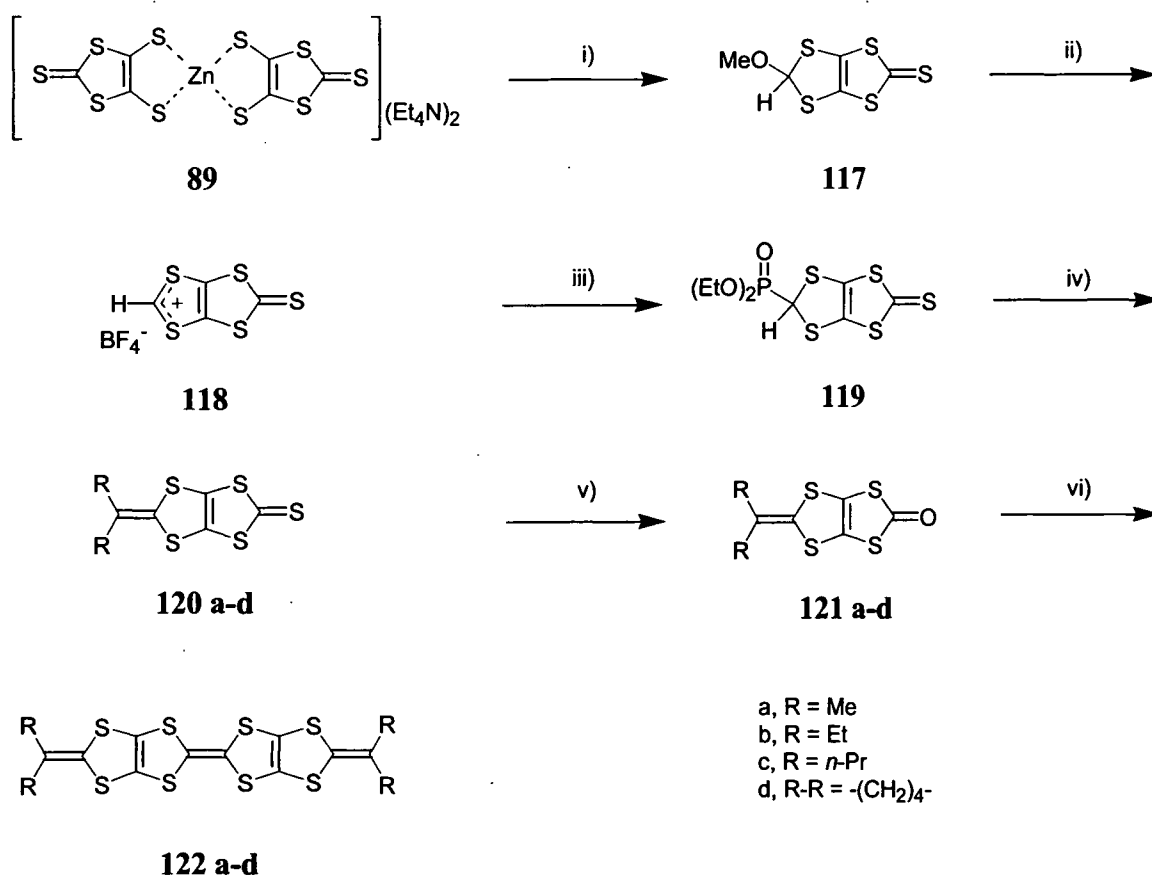
In summary, using prototype ligands **106** and **115** we have exploited for the first time the redox properties of the 9,10-bis(1,3-dithiol-2-ylidene)-9,10-dihydroanthracene transducer system to provide efficient and controllable cation recognition within appended crown ether units. These studies pave the way for the spectroscopic and electrochemical monitoring of supramolecular interactions in new derivatives of this system.

5.1 Introduction

Chapters 2-4 have described the 9,10-bis(1,3-dithiol-2-ylidene)-9,10-dihydroanthracene system in some detail and established through crystallographic studies that intramolecular steric interactions enforce a folding of the central anthracenediylidene ring of the system into a boat conformation, which forces the molecule to adopt a saddle shape.²⁶

The focus of this chapter is the development of a new range of related electron donor molecules, incorporating a cyclic structure. These systems differ from those of the crown ethers (Chapter 4) in that the chain bridges the two dithiole rings, increasing strain to the system. The rationale was to observe the effects of increased strain on the cavity in solution and in the solid state using cyclic voltammetry and single crystal X-ray crystallography.

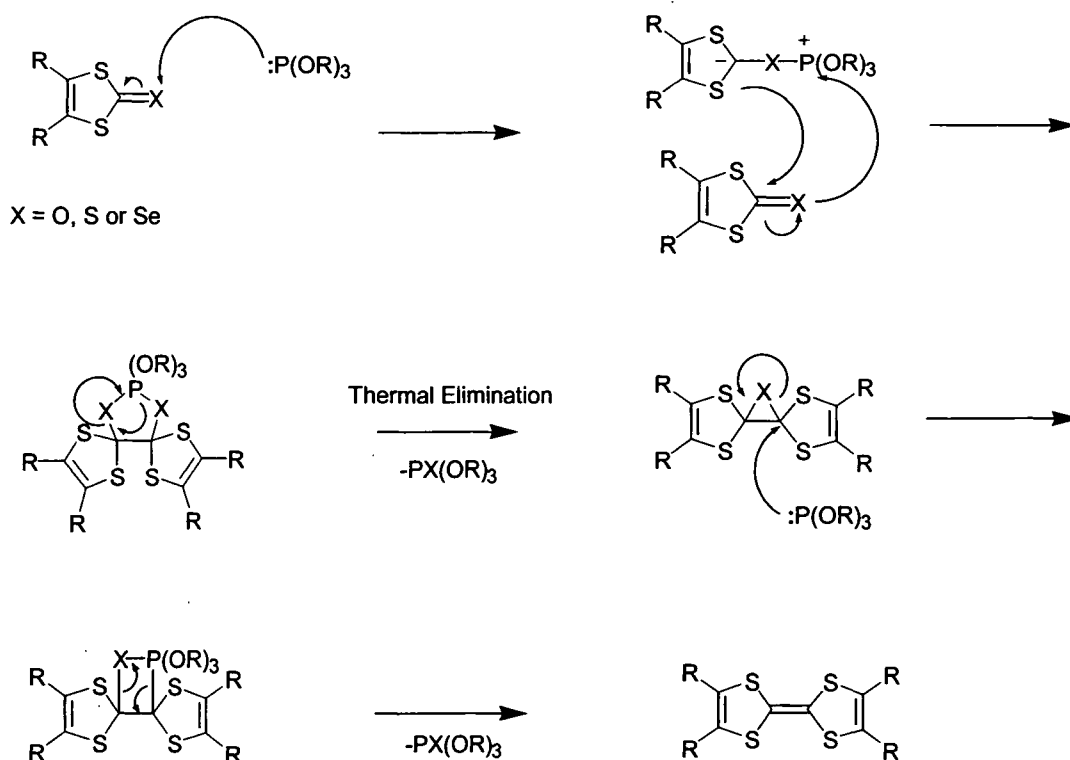
In 1992 Misaki *et al.* succeeded in the preparation of bis(2-methylidene-1,3-dithiole[4,5])tetrathiafulvalene (BDT-TTF), compound **122** (Scheme 5.1).⁷⁹ The zinc complex **89** was reacted with α,α' -dichloromethyl methyl ether in acetone to afford **117** in 73% yield. Treatment of compound **117** with aqueous 42% hydrofluoroboric acid in dichloromethane/acetic anhydride (5:1, v/v) at 0°C gave the corresponding 1,3-dithiolium salt **118**, which was converted to the phosphonate ester **119** with triethyl phosphite and sodium iodide in 88% yield. Treatment of **119** with various ketones and equimolar amounts of lithium diisopropylamide (LDA) in tetrahydrofuran (THF) at -78°C, gave the corresponding 2-methylidene-1,3-dithiole(4,5)1,3-dithiole-2-thione **120a-d** (47-99% yields), which were converted to the corresponding ketones **121a-d**, by reaction with mercury (II) acetate in chloroform/acetic acid (1:1, v/v) in 79-97% yields. The target BDT-TTF derivatives, **122a-d**, were obtained by phosphite induced coupling at 100-110°C in moderate yields.



Scheme 5.1 Reagents and conditions: i) Cl₂CHOMe, Me₂CO. ii) HBF₄, CH₂Cl₂/Ac₂O. iii) P(OEt)₃, NaI, Me₂CO. iv) LDA, THF, RCOR, -78 °C. v) Hg(OAc)₂, CHCl₃/AcOH. vi) P(OEt)₃

The phosphonate ester **119**, represented an extremely interesting compound which could undergo two independent reactions. Misaki *et al.*⁷⁹ demonstrated the ability of compound **119** to undergo a Horner-Wadsworth-Emmons type coupling to various ketones, and it was plausible that this reactivity could be extended to anthraquinones. The system also exhibited the ability to self-couple *via* the 2-oxo-1,3-dithiole functionality.

The use of phosphite induced couplings has provided one of the fundamental reactions in the preparation of TTF derivatives and was originally discovered by Corey, Corey and Winters. The mechanism of this reaction is still debated but is thought to proceed *via* a Wittig type mechanism as outlined in Scheme 5.2.^{80,81}



Scheme 5.2

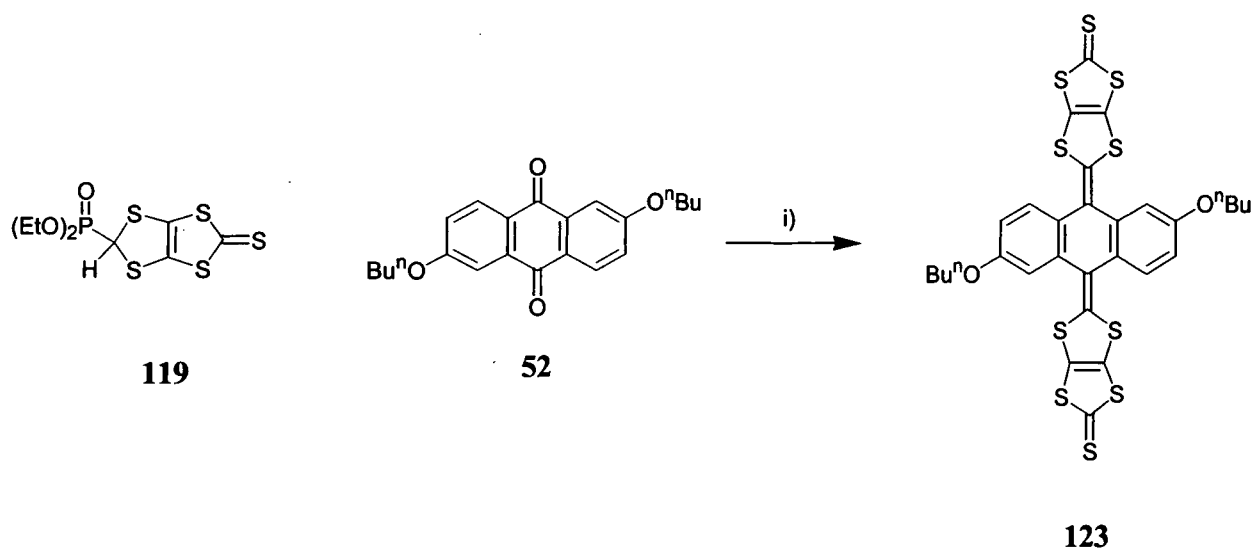
Initial attack of one molecule of trialkylphosphite on the chalcogen of the C=X group polarises the bond making the carbon nucleophilic, allowing attack of a second equivalent containing C=X, forming a five membered ring. At high temperatures the cyclic structure collapses, eliminating one equivalent of trialkylphosphate and forming an epoxide. The epoxide is then ring opened by a second equivalent of trialkylphosphite, which proceeds through a four membered transition state, analogous to that of a Wittig reaction. Further elimination results in the formation of the double bond with elimination of another equivalent of trialkylphosphate. The reaction is thermodynamically driven by the formation of the P=X bond.

In Mizaki's example, the thione **120a-d** was converted to the ketone **121a-d** prior to phosphite induced coupling. There are no clear guidelines governing the outcome of cross coupling reactions; the decision to use the ketone, as opposed to the thione, may have been based on improved yields or ease of separation of the products.

Summation of this information led us to propose the synthesis of compound **123** (with butoxy chains to ensure solubility).

5.2 Synthesis

Reaction of compound **52** with the anion generated from the phosphonate ester **119** gave the expected product **123** in 43% yield (Scheme 5.3).

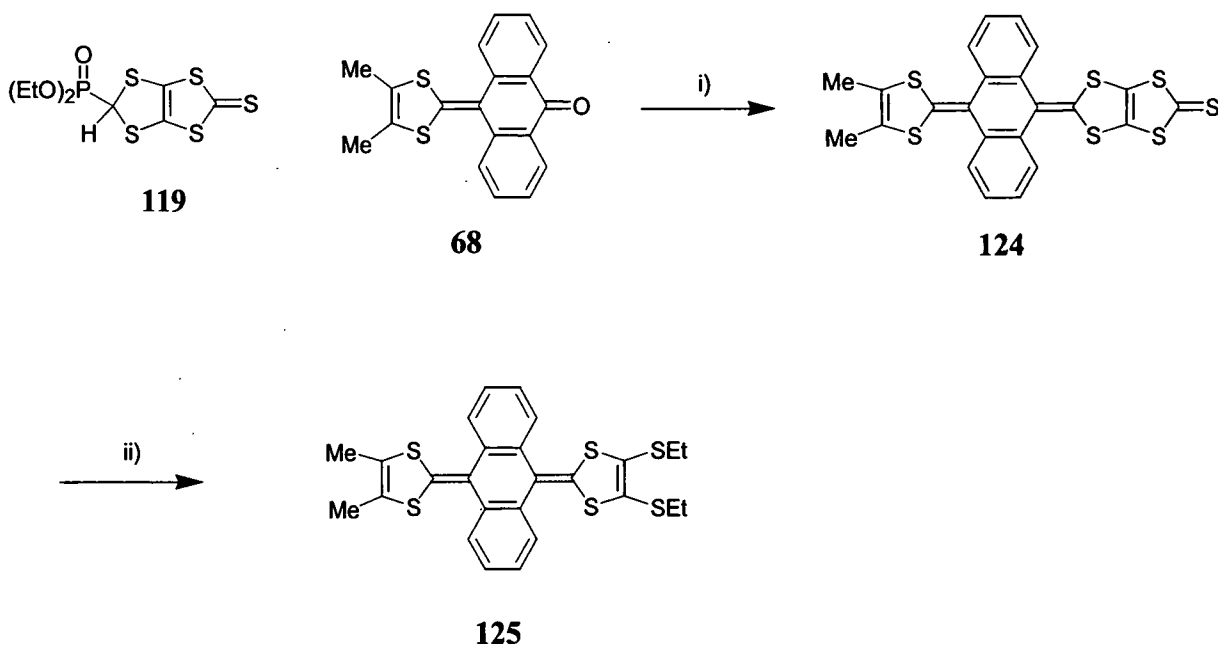


Scheme 5.3: Reagents and conditions i) LDA, THF, -78 °C, 3h.

With the aim of synthesising a cyclic derivative by intramolecular coupling, compound **123** was subjected to the standard phosphite-induced coupling reaction under high dilution, however, no coupled product was obtained. We believed the failure of the reaction might have been due to several factors. These factors may, include the failure of the phosphite to react with the thione present, the formation of multiple oligomers or the steric limitation imposed on intramolecular coupling. To further investigate the coupling reaction, compound **124** was prepared, as this compound could only undergo a single intermolecular coupling.

Reaction of compound **68** with the anion generated from phosphonate ester **119** gave the expected product **124** in 60% yield. Compound **124** was subjected to the

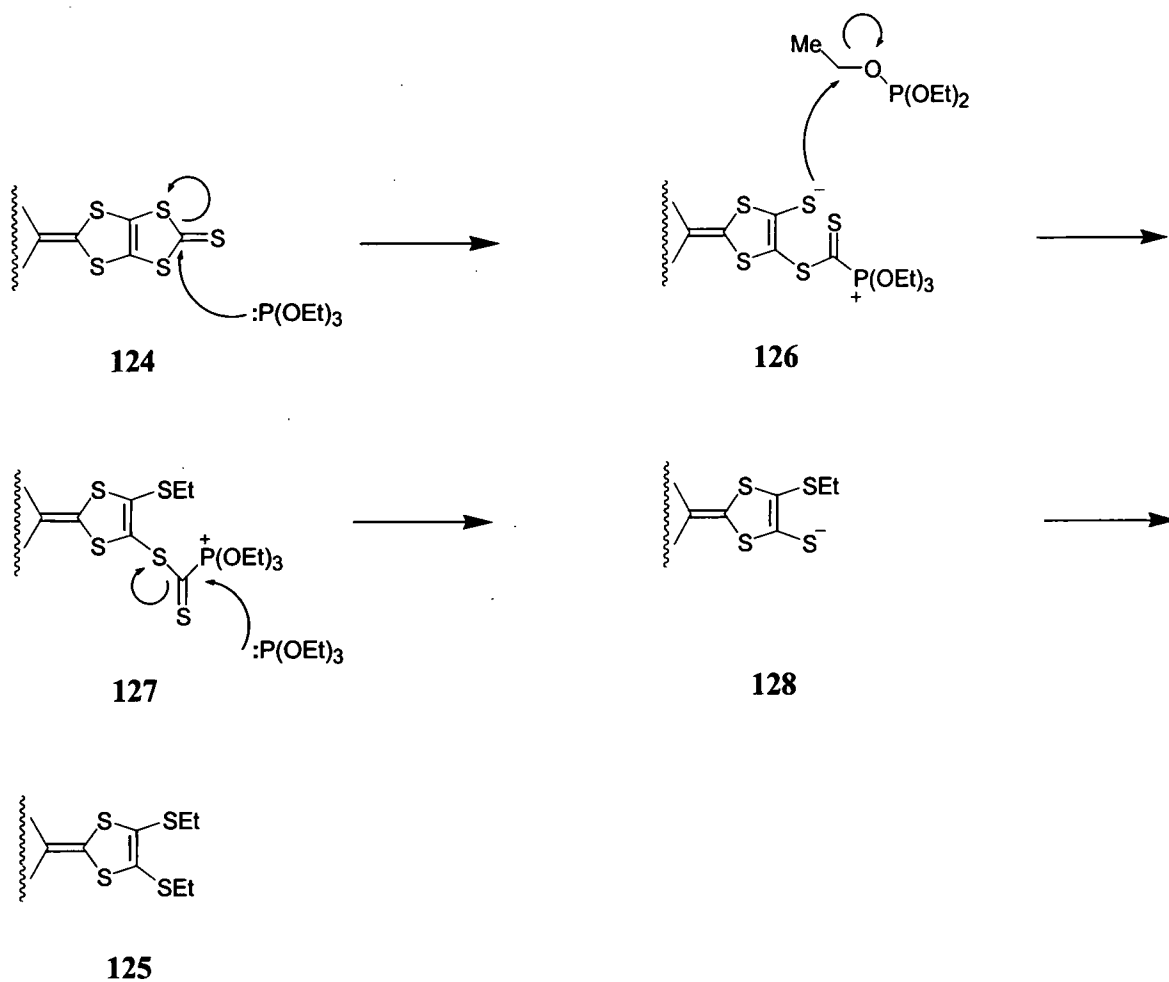
standard phosphite coupling conditions. No coupled product was obtained; the only isolated product was the unexpected compound **125** (50% yield) in which the 1,3-dithiole-2-thione ring has been transformed into two ethylsulfanyl substituents (Scheme 5.4).



Scheme 5.4 Reagents and conditions: i) LDA, THF, -78°C , 3 h. ii) $\text{P}(\text{OEt})_3$, reflux.

The structures of both compounds **124** and **125** were established unequivocally by single crystal X-ray analysis. The conversion of **124** into **125** under these conditions appears to proceed *via* an unprecedented reaction of the 1,3-dithiole-2-thione system. Reactions of trialkylphosphite reagents with cyclic trithiocarbonates are generally assumed to proceed *via* an initial thiophilic addition, although a carbophilic mechanism has been considered.⁸¹⁻⁸⁴ It is not readily apparent how a thiophilic addition can explain the formation of compound **125**; we propose initial opening of the 1,3-dithiole-2-thione ring of **124** induced by carbophilic addition of triethylphosphite, to form the zwitterionic intermediate **126**. Ethylation of **126** then occurs by a transfer of an ethyl group from triethyl phosphite to yield **127**.⁸⁵ This is more likely to be an intermolecular transfer than

an intramolecular process. Generation of a second thiolate anion, and ethylation then gives product **125** (Scheme 5.5).

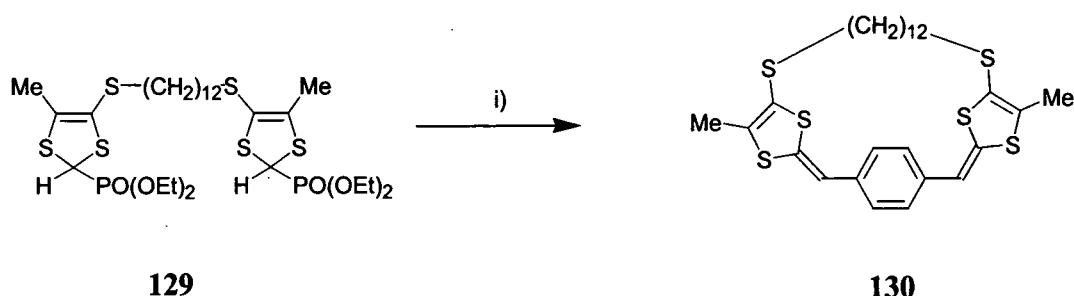


Scheme 5.5: The Proposed mechanism for the thioalkylation of **125**.

The ethylation of compound **125** prevented the formation of a cyclic system. It was now apparent that an alternative synthetic approach to bridged systems was required.

5.3 Synthesis of the First Anthracenediylidene Cyclophanes

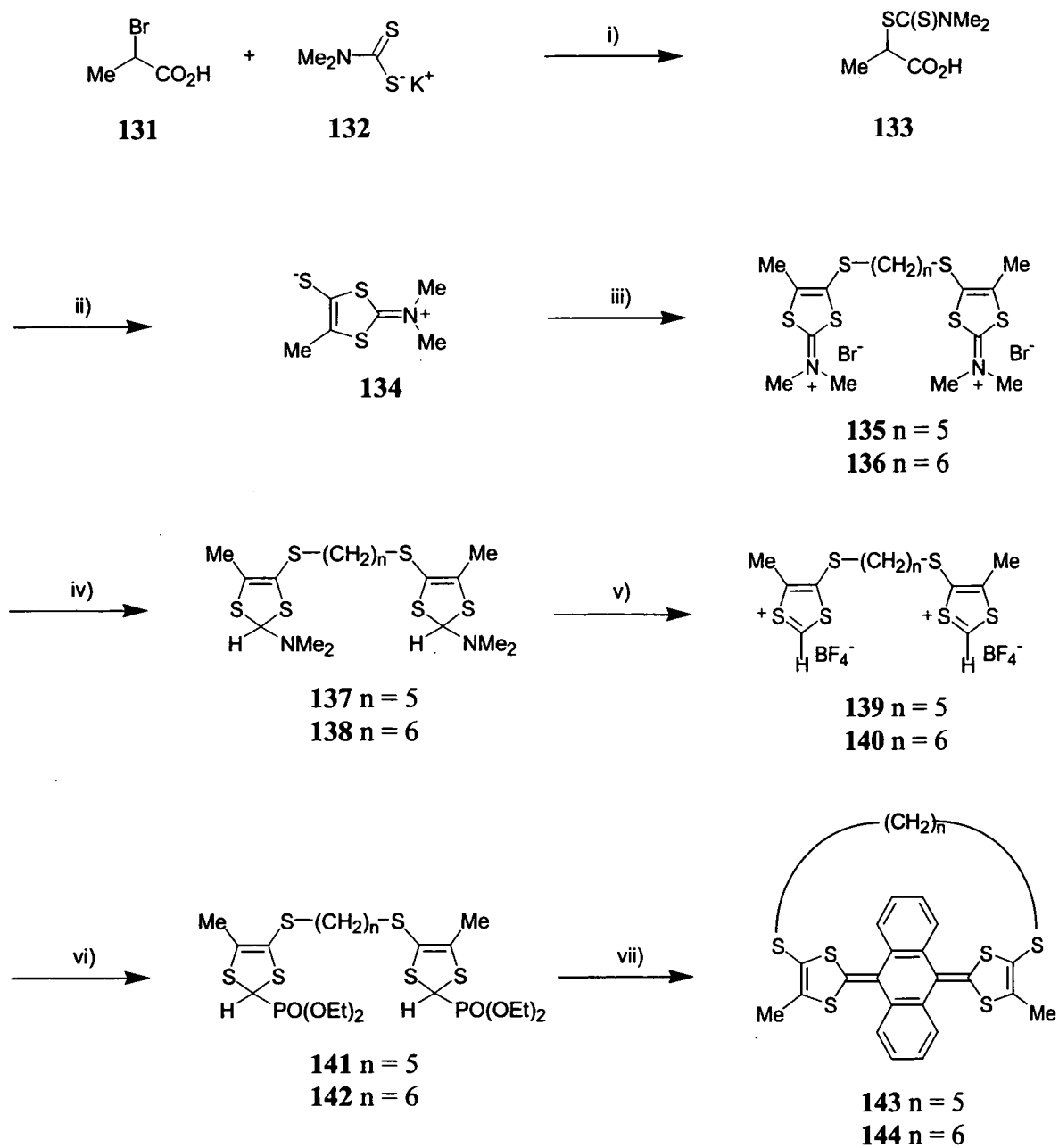
In 1995, Lorcy *et al.* reported the synthesis of a novel bis-Horner-Wadsworth-Emmons reagent **129** in the course of the preparation of tetrathiafulvalenophanes **130**.⁸⁶ This communication lacked experimental detail but clearly showed the capability of this new reagent to form cyclic systems by reaction with bis-ketones (Scheme 5.6).



Scheme 5.6 Reagents and conditions i) *n*-BuLi, THF, -78 °C, terephthalaldehyde (0.5 equiv.)

We sought to apply reagents analogous to **129** to the synthesis of a new class of anthracenediylidene cyclophane compounds.

The preparation of the bis-imminium salts **135** and **136** had been described previously en route to symmetrically substituted TTFs.⁸⁷⁻⁸⁸ Reduction of bis(dithiolium) salts **135** and **136** with sodium borohydride followed by reaction of the bis(aminodithiole) intermediates with tetrafluoroboric acid afforded **139** and **140**, which reacted with triethylphosphite in the presence of sodium iodide to give the corresponding bis(phosphonates), **141** and **142**, in moderate yields. The synthesis of anthracenediylidene cyclophanes, **143** and **144**, was achieved by a two-fold olefination reaction, under high dilution conditions, with anthraquinone and the anions generated from **141** and **142** respectively, [lithium diisopropylamide (LDA) at -78°C] following literature precedents for other 1,3-dithiole phosphonate ester reagents (Scheme 5.7).³⁷ Compounds **143** and **144** were isolated as single isomers, and the *cis* configuration was confirmed by X-ray structural analysis.



Scheme 5.7 Reagents and conditions i) H_2O ii) Et_3N , Ac_2O , CS_2 , Me_2CO . iii) dibromoalkane, Me_2CO . iv) $NaBH_4$, $EtOH$ $0^\circ C$. v) HBf_4 , DCM , $0^\circ C$. vi) NaI , $P(OEt)_3$, $MeCN$. vii) LDA , THF , $-78^\circ C$, anthraquinone.

5.4 Electrochemistry

The solution electrochemistry of compounds **143** and **144** was studied by cyclic voltammetry and differential pulse voltammetry. Both compounds displayed an irreversible two-electron oxidation wave at $E^{\text{ox}} +0.69$ V (compound **144**) and $E^{\text{ox}} +0.74$ V (compound **143**) [vs Ag/AgCl, electrolyte $\text{Bu}_4\text{N}^+\text{ClO}_4^-$ (0.1 M), acetonitrile, room temperature, scan rate 100 mVs^{-1}] *i.e.* The oxidation wave of the bridged system **144** and **143** showed a significant positive shift (ΔE^{ox} *ca.* 300 mV) compared to the non-bridged analogue. This is explained by the rigidity of **143** and **144** (imparted by the bridge) restricting the conformational change which is known to accompany oxidation of the 9,10-bis(1,3-dithiol-2-ylidene)-9,10-dihydroanthracene system.²⁶ The slightly higher oxidation potential of **143** compared to **144** (ΔE^{ox} 50 mV) is also consistent with oxidation becoming progressively harder as the strain in the system increases. A second oxidation wave is observed at $E^{\text{ox}} +1.0$ V. Simulation of the data suggest an *ECE* process where dication formation is followed by a chemical reaction to form a new electroactive species, which gives rise to the oxidation wave at a more positive potential.

5.5 Single Crystal X-ray Crystallography of Compounds 124, 125, 143 and 144.

The structure of compound **124** has been determined by single crystal X-ray analysis (Figure 5.1). The asymmetric unit **124** comprises two title molecules (A and B) and one severely disordered molecule of CDCl_3 . Both molecules A and B have essentially planar S(1)C(1)S(2)S(3)C(2)C(3) systems, which form dihedral angles of 90.4° (A) and 94.1° (B) with the S(6)C(6)C(7)S(7) moieties. Folding of the anthracene system along the C(10)...C(11) axis is unequal (35.9° in A, vs. 45.2° in B), while folding along the S(4)...S(5) vector is reversed (13.7° outward in A, vs. 7.6° in B). The crystal packing of **124** (Figure 5.2) is rather dissimilar from that of the other compounds studied herein. Molecules of A engulf each other's dimethyldithiole ends, as does molecule B. In each dimer, the dithiole rings overlap in an antiparallel fashion, with interplanar

separations of 3.64 Å (A-A) and 3.55 Å (B-B) with the shortest contact being C...S at 3.66 Å in either case. These two dimers are orientated in mutually perpendicular planes and give rise to an unusual three-dimensional network of intermolecular contacts comparable to (or shorter than) the standard van der Waals distances S...S 3.60 Å and C...S 3.61 Å.⁸⁹ Thus, dimethyldithiole rings of the A-A dimer are sandwiched between dithiolethione systems of two adjacent B molecules (interplanar angle 7°, shortest S...S contact 3.63 Å). This tetramer is additionally strengthened by interactions between molecules A and B: S(2A)...S(2B) 3.66 Å and S(2A)...S(4B) 3.49 Å. However, no continuous stacks exist in the structure, and the forementioned stack is 'underpinned' at either end by the thione C(1A)=S(1A) bond of another A molecule. This bond is aligned perpendicular to the stacked plane and points towards the midpoint of the C(1B)...S(3B) bond (S(A)...S(3B) 3.52 Å, S(1A)...C(1B) 3.45 Å). The dimethyldithiole rings of B dimer are contacted on the outside by dithiolethione moieties of adjacent A molecules, in an edge-to-face fashion. Thereby, S(3A) forms extremely short contacts with C(6B) and C(7B) 3.29 Å each, as well as rather close contact with S(6B) and S(7B) (3.61 Å and 3.62 Å respectively).

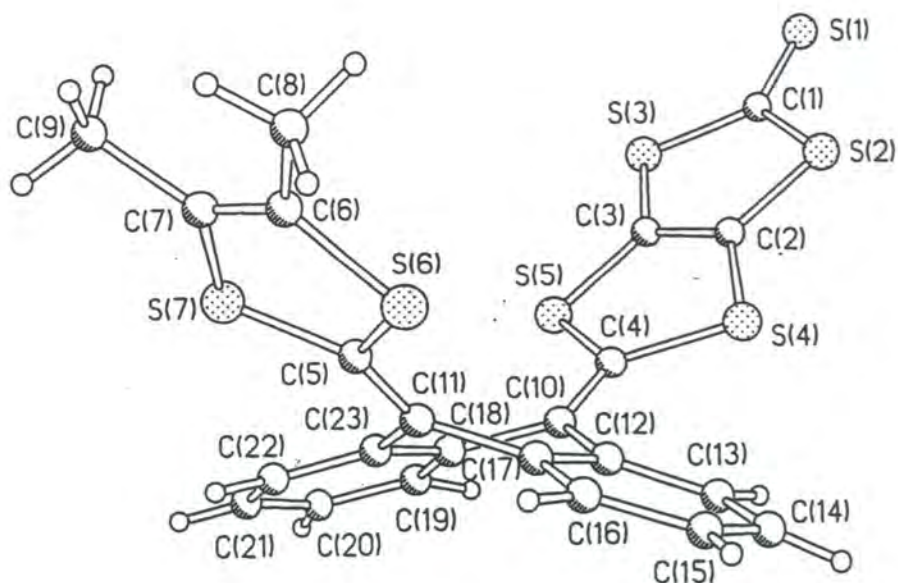


Figure 5.1: The single crystal X-ray structure of compound 124.

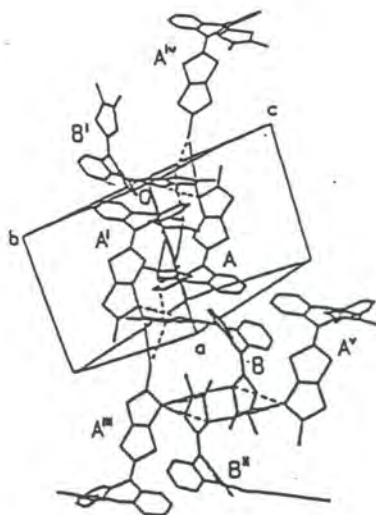


Figure 5.2: The crystal lattice packing of compound 124.

In compound 125 (Figure 5.3), one of the ethylthio substituents is disordered over two positions, S(6)C(19)C(20) and S(6')C(19')C(20'); their occupancies were refined to 61.2% and 38.8%, respectively. The conformation ($\phi = 40.6^\circ$, $\theta = 79.1^\circ$) is practically identical with that of 75, but here the ethylthio groups enter the intramolecular cavity of the opposing molecule (Figure 5.4).

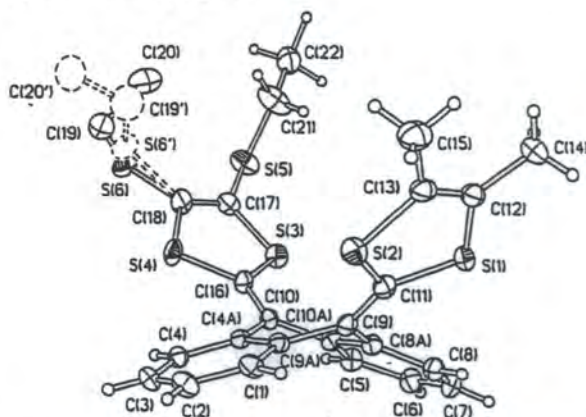


Figure 5.3: The single crystal X-ray structure of compound 125.

Compound 144 gave a mixture of amber block- and needle- like crystals, which were characterised as monoclinic (α) and orthorhombic (β) polymorphs, respectively, of *cis*-144. Two symmetrically independent molecules in the β -144 structure adopt very similar conformations (Figure 5.4), while that of α -144 is significantly different. In each case, the conformation of the hexamethylene bridge is rather strained and asymmetric: torsion angles around the C-C bonds range from 144° to 180° in β -144 and from 58° to

176° in α -144, where two methylene groups are disordered. The bridge aggravates the U-bend of the bis(dithiolene)benzoquinone system: the dihedral angle between the outer S(1)C(16)C(17)S(2) and S(3)C(19)C(20)S(4) moieties is reduced from 77° in non-bridge tetrathiomethyl molecule⁴³ to 54° in β -144 and to only 46° in α -144, mostly through increased folding of both dithiole rings along the S(1)...S(2) and S(3)...S(4) vectors (24° and 13° respectively in α -144, 24° and 20° in β -144).

The structure of **143** contains two independent molecules, one of which shows disorder that can be rationalised as either a varying degree of molecular bending or a rocking of the molecule as a whole. In the other (ordered) molecule (Figure 5.5) the pentamethylene bridge adopts a nearly all *trans* conformation (C-C-C-C torsion angle 164°-177°) and enhances the folding of the anthracene moiety by 43.4° and both dithiole rings (by 29.4° and 22.6°), thus narrowing the dihedral angle between the S(1)C(16)C(17)S(2) and S(3)C(19)C(20)S(4) planes to 34.7°.

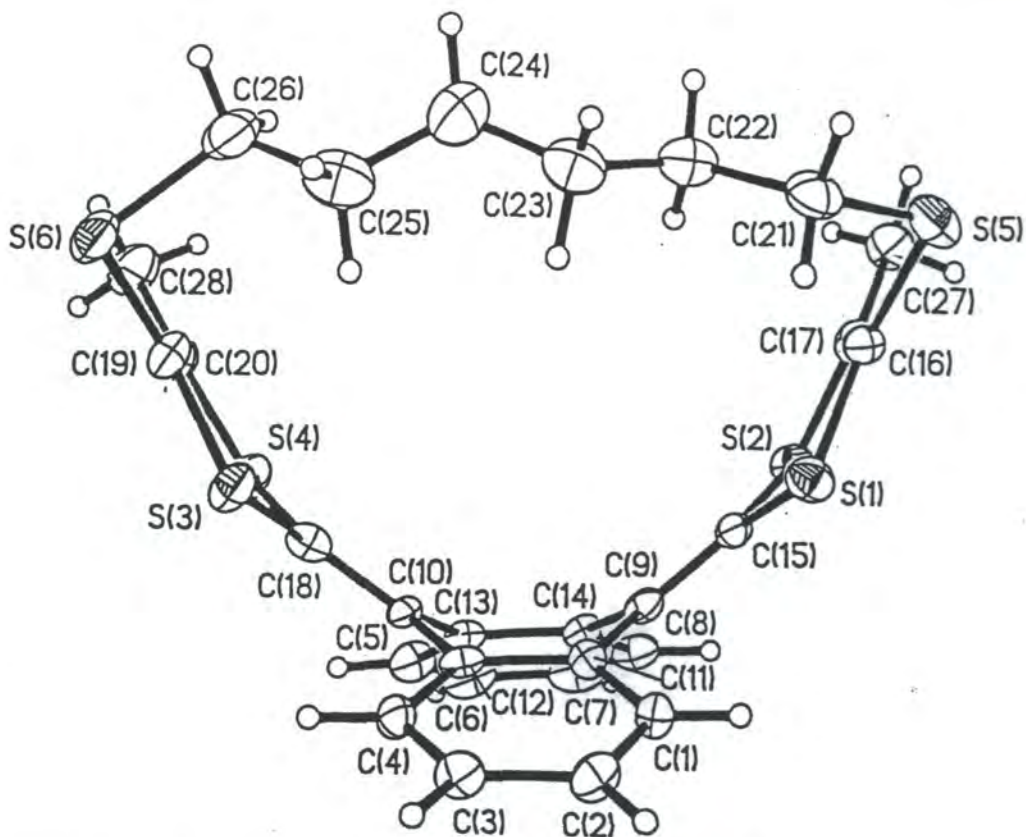


Figure 5.4: The single crystal X-ray structure of compound β -144.

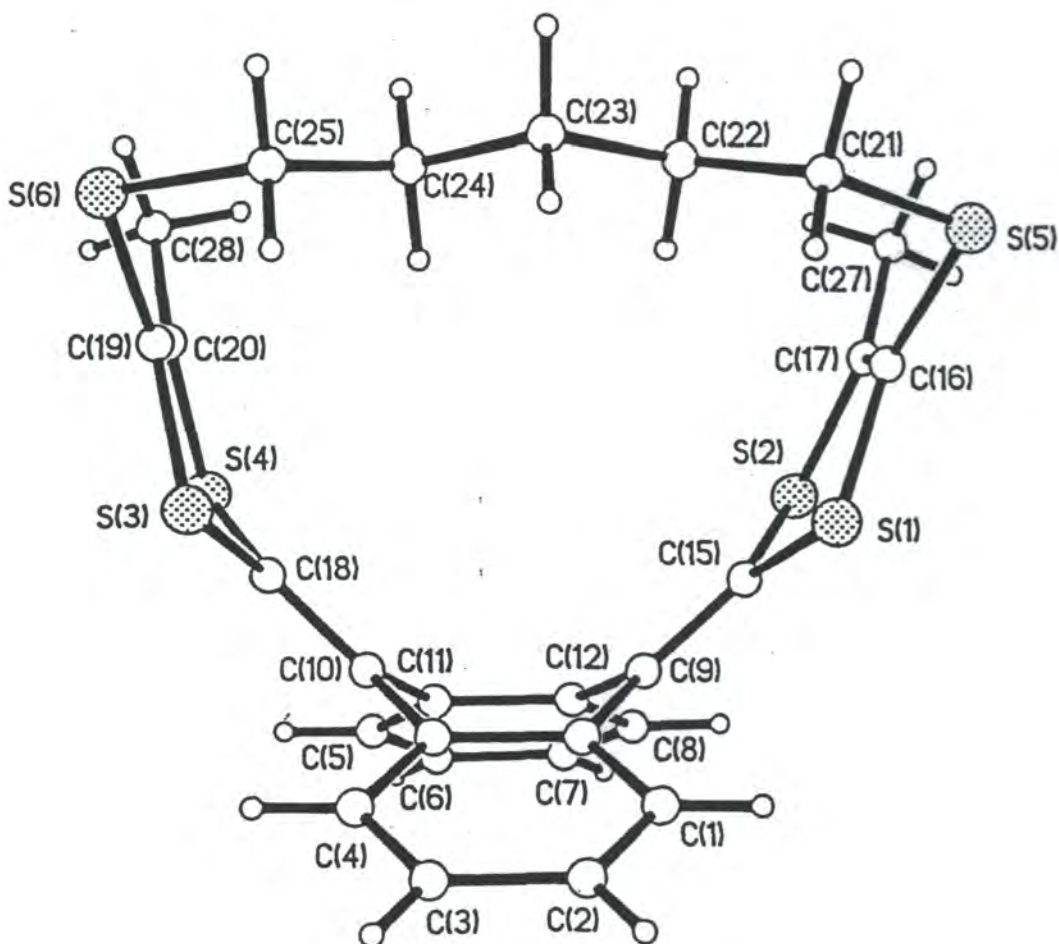


Figure 5.5: The single crystal X-ray structure of compound 143.

5.6 Conclusion

In summary, double olefination reactions of anthraquinone have afforded novel bridged 9,10-bis(methylene)-9,10-dihydroanthracenes, paving the way for studies on a new family of cyclophane molecules with interesting electrochemical and structural properties.

6.1 General Methods

Reactions were carried out under an inert atmosphere of argon, which was dried by passage through a column of phosphorus pentoxide. Diethyl ether, toluene and tetrahydrofuran were dried and distilled over sodium metal. Dichloromethane, acetone and acetonitrile were dried and distilled over calcium chloride. Ethanol and methanol were dried and distilled over magnesium. Anhydrous dimethyl formamide was obtained from Aldrich. All reagents were of commercial quality.

^1H and ^{13}C Spectra were obtained on a Varian Unity 300, Oxford 200, Varian VXR 400s. Mass spectra were recorded on a Micromass Autospec spectrometer operating at 70eV. Infra-red spectra were recorded using a Golden Gate on a paragon 1000 FTIR spectrometer operated from a Grams Analyst 1600. Electronic absorption spectra were obtained using a Perkin-Elmer II UV-vis spectrometer operating with 1cm quartz cells. Melting points were obtained on a Philip Harris melting point apparatus and are uncorrected. Cyclic voltammetric data were measured with iR compensation using a BAS CV50 electrochemical analyser. The experiments were carried out with 5mL of *ca.* 10^{-4} M solution of the compound in acetonitrile containing 0.1M tetrabutylammonium hexafluorophosphate (Fluka, Puriss, electrochemical grade) as the supporting electrolyte, at a scan rate of 100 mV s^{-1} . The potentials were measured *versus* decamethylferrocene/decamethylferrocene⁺ by adding decamethylferrocene to the studied solution after the experiment, and referenced *versus* Ag/AgCl.

6.2 Experimental Procedures For Chapter 2

2,6-Dibutoxyanthraquinone Acid 52.

To a solution of anthraflavic acid **51** (0.487 g, 1.15 mmol) in dry dimethylformamide (100 ml), was added silver (I) oxide (981 mg, 4.23 mmol) and iodobutane (0.7 ml, 6.15 mmol). After the mixture was stirred at 20°C for 48 h under an argon atmosphere, the solvent was removed *in vacuo*. The residue was purified by column chromatography on silica gel with acetone/hexane (1:3, v/v) as the eluent to afford **52** as a yellow solid (205 mg, 56%). M.p. 109-111°C, MS (CI) 353 *m/z* [$M^+ + 1$]; (Found: C, 74.7; H, 6.9; C₂₂H₂₄O₄ requires C, 75.0; H, 6.9); ¹H NMR (CDCl₃) δ 1.00 (t, J = 7 Hz, 6H), 1.55 (m, 4H), 1.84 (m, 4H), 4.15 (t, J = 7 Hz, 4H), 7.26 (m, 2H), 7.69 (s, 2H), 8.19 (d, J = 9 Hz, 2H); ¹³C NMR (CDCl₃) δ 13.7, 19.1, 31.0, 68.4, 110.4, 120.8, 126.9, 129.5, 135.7, 163.9, 182.2 ppm. IR ν_{\max} (Golden Gate): 2359, 2340, 1661, 1578, 1330, 1292, 1260, 1229 cm⁻¹.

2,6-Dihexoxyanthraquinone Acid 53.

To a solution of anthraflavic acid **51** (2.45 g, 10.2 mmol) in dry dimethylformamide (250 ml), was added silver (I) oxide (9.69 g, 40.7 mmol) and iodohexane (6 ml, 41.0 mmol). After the mixture was stirred for 48 h under an argon atmosphere, the solvent was removed *in vacuo*. The residue was purified by column chromatography on silica gel with dichloromethane/hexane (1:3, v/v) as the eluent to afford **53** a yellow solid (2.31 g, 57%); M.p. 90-92°C; MS (CI) 409 *m/z* [$M^+ + 1$]; (Found: C, 76.0; H, 7.9; C₂₆H₃₂O₄ requires C, 76.4; H, 7.9); ¹H NMR (CDCl₃) δ 0.91 (t, J = 7.2 Hz, 6H), 1.36 (m, 8H), 1.49 (m, 4H), 1.83 (p, J = 7.0 Hz, 4H), 4.12 (t, J = 7.2 Hz, 4H), 7.19 (dd, J_{ab} = 2.0 Hz, J_{bc} = 7.0 Hz, 2H), 7.67 (d, J_{bc} = 2.0 Hz, 2H), 8.20 (d, J_{ab} = 9.0 Hz, 2H); ¹³C NMR (CDCl₃) δ 14.0, 22.6, 25.6, 29.0, 31.5, 68.8, 110.5, 120.8, 126.9,

129.6, 135.8, 164.0, 182.2 ppm; IR ν_{\max} (Golden Gate) 956, 2936, 2919, 2855, 1662, 1586, 1492, 1469, 1425, 1387, 1310, 1259, 1236, 1149, 1078 cm^{-1} .

2,6-Dibutoxy-9,10-bis(1,3-dithiol-2-ylidene)-9,10-dihydroanthracene 44.

Into a solution of 2-dimethoxyphosphinyl-1,3-dithiole **50** (1.0 g, 4.71 mmol) in dry tetrahydrofuran (50 ml) at -78°C under argon, was added lithium diisopropylamide (3.6 ml of 1.5 M solution in cyclohexane, 5.4 mmol) over a period of 15 min. The reaction mixture was left for 3 h until a pale cloudy solution formed. Then a solution of 2,6-dibutoxyanthraquinone **52** (508 mg, 1.44 mmol) in dry tetrahydrofuran (10 ml) was added over 15 min. The reaction was stirred overnight under an argon atmosphere. The reaction mixture was evaporated *in vacuo*. The residue was purified by column chromatography on silica gel with hexane/dichloromethane (2:1 v/v) as the eluent to afford **44** as yellow solid (260 mg, 51%). A single crystal X-ray sample was recrystallized from anhydrous acetonitrile. M.p. $129\text{--}133^{\circ}\text{C}$, (Found: C, 63.7; H, 5.3; $\text{C}_{28}\text{H}_{28}\text{O}_2\text{S}_4$ requires C, 64.0; H, 5.3); MS (EI) 524 m/z [M^+]; ^1H NMR (CDCl_3) δ 0.98 (t, $J = 7$ Hz, 6H), 1.50 (m, 4H), 1.80 (m, 4H), 4.03 (t, $J = 7$ Hz, 4H), 6.23 (s, 4H), 6.80 (dd, $J_{ab} = 3$ Hz, $J_{bc} = 9$ Hz, 2H), 7.26 (d, $J_{bc} = 3$ Hz, 2H), 7.50 (d, $J_{ab} = 9$ Hz, 2H). ^{13}C NMR (CDCl_3) δ 13.8, 19.4, 31.2, 31.0, 31.3, 67.9, 68.5, 110.5, 110.9, 111.9, 117.1, 120.9, 122.2, 126.0, 126.9, 128.2, 129.6, 133.4, 125.8, 136.9, 157.1, 164.0, 182.3 ppm.

A charge transfer complex of compound **44** and TCNQ **2** was prepared by the mixing of 20 mg of both compounds in refluxing acetonitrile; yielding a black solid (21.7 mg) IR ν_{\max} (Golden Gate): 2360, 2344, 2172, 2155, 1559, 1496 cm^{-1} .

2,6-Dihexoxy-9,10-bis(1,3-dithiol-2-ylidene-4,5-dimethyl)-9,10-dihydroanthracene 55.

Into a solution of 2-dimethoxyphosphinyl-4,5-methyl-1,3-dithiole **54** (129 mg, 0.538 mmol) in dry tetrahydrofuran (50 ml) at -78°C under argon, was added lithium

diisopropylamide (0.4 ml of 1.5 M solution in cyclohexane, 0.59 mmol). The reaction mixture was left for 3 h until a cloudy white solution formed. Then a solution of 2,6-dihydroxyanthraquinone **53** (97 mg, 0.24 mmol) was added. The reaction was stirred overnight under an argon atmosphere. The reaction mixture was evaporated *in vacuo*. The residue was purified by column chromatography on silica gel with hexane/dichloromethane (2:1 v/v) as the eluent to afford **55** as a yellow oil which solidified on standing (92 mg, 59%). M.p. 123-125°C; (Found: C, 67.6; H, 7.0; C₃₆H₄₄O₂S₄ requires C, 67.9; H, 7.0); MS (EI) 636 *m/z* [M⁺]; ¹H NMR (CDCl₃) δ 0.92 (m, 6H) 1.37 (m, 12H) 1.82 (m, 4H) 1.92 (s, 12H) 4.03 (t, J = 6.6 Hz, 4H) 6.78 (dd, J = 2.6 Hz, J = 8.6 Hz, 2H) 7.14 (d, J = 2.4 Hz, 2H) 7.51 (d, J = 8.4 Hz, 2H); ¹³C NMR (CDCl₃) δ 13.1, 14.1, 22.6, 25.7, 29.2, 31.6, 68.2, 105.4, 111.3, 111.6, 120.7, 121.4, 126.3, 128.1, 130.9, 136.8, 156.9 ppm.

2,6-Dibutoxy-9,10-bis(4,5-dibromo-1,3-dithiol-2-ylidene)-9,10-dihydroanthracene **64**

Into a solution of 2,6-dibutoxy-9,10-bis(1,3-dithiol-2-ylidene)-9,10-dihydroanthracene **44** (243 mg, 0.69 mmol) in dry tetrahydrofuran (50 ml) at -78°C under argon, was added lithium diisopropylamide (0.4 ml of 1.5 M solution in cyclohexane, 0.60 mmol) over a period of 15 min. The reaction mixture was left for 3 h until an orange solution formed. Then a solution of tosyl bromide (698 mg, 2.97 mmol) in dry tetrahydrofuran (20 ml) was added over 15 min. The reaction was stirred overnight under an argon atmosphere. The reaction mixture was evaporated *in vacuo*. The residue was purified by column chromatography on silica gel with hexane/dichloromethane (2:1 v/v) as the eluent to afford **64** as a red solid (45 mg, 12%). M.p. 85-87°C; MS (EI) *m/z* 524 [M⁺]; ¹H NMR (CDCl₃) δ 0.99 (t, J = 7 Hz, 6H), 1.52 (m, 4H), 1.80 (m, 4H), 4.02 (t, J = 7 Hz, 4H), 6.23 (s, 4H), 6.80 (dd, J_{ab} = 3 Hz, J_{bc} = 9 Hz, 2H), 7.26 (d, J_{bc} = 3 Hz, 2H), 7.50 (d, J_{ab} = 9 Hz, 2H); ¹³C NMR (CDCl₃) δ 13.9, 19.3, 31.2, 68.0, 100.0, 111.7, 112.3, 124.7, 126.5, 128.7, 135.5, 157.9 ppm.

6.3 Experimental Procedures For Chapter 3

2-Piperidino-2-methyl-1,3-dithiole 72.

To a stirred suspension of salt 71 (75.0 g, 217 mmol) in dry tetrahydrofuran/isopropanol (1:1 v/v, 1.0 l) at 0°C, finely-ground sodium borohydride (37.8 g, 1.0 mol) was added in portions over *ca.* 6 h. The reaction was then maintained at 0°C for a further 2 h, whereupon it was allowed to warm to room temperature and stirred for a further 40 h. After concentrating to *ca.* 150 ml, water (500 ml) was added cautiously and the mixture extracted with diethyl ether (4 x 125 ml). The combined extracts were washed with water (3 x 125 ml), dried (MgSO₄) and evaporated *in vacuo* to afford compound 72 (40.6 g, 93%) as a yellow oil of high purity (¹H NMR analysis) suitable for use in the next step without further purification. ¹H NMR (CDCl₃): δ 1.41 (m, 2H), 1.53 (m, 4H), 2.02 (s, 3 H), 2.49 (t, *J* = 5.2 Hz, 4H), 5.72 (s, 1H), 6.18 (s, 1H).

4-Methyl-1,3-dithiolium Iodide 74.

To an ice-cooled, stirred solution of acetic anhydride (260 ml) was cautiously added hexafluorophosphoric acid (60 wt % in water, 115.0 g, 0.788 mol) over *ca.* 2 h. (CAUTION: vigorous exothermic reaction!). To the ice-cooled solution of anhydrous hexafluorophosphoric acid thus formed, was added dropwise over *ca.* 0.5 h a solution of compound 72 (38.0 g, 189 mmol) in dry diethyl ether (250 ml), precipitating immediately the salt 73. The mixture was diluted with dry diethyl ether (250 ml), stirred for a further 0.5 h, and the product was collected by filtration and washed with diethyl ether (125 ml) affording hexafluorophosphate salt 73 as an off-white solid. Purification was achieved by anion exchange to the iodide salt. To a stirred solution of the hexafluorophosphate salt in anhydrous acetone (125 ml) at 20°C was added a solution of sodium iodide (28.3 g, 189 mmol) in anhydrous acetone (50 ml) to precipitate iodide salt 74 as a bright yellow solid, which was collected by filtration and washed initially with cold anhydrous acetone (25 ml) and then anhydrous diethyl ether (100 ml) to afford 40.6 g (88%) of compound 74.

M.p. 98-101°C. ^1H NMR ($\text{CD}_3)_2\text{SO}$: δ 2.91 (s, 3H), 9.09 (s, 1H), 11.47 (s, 1H). This salt can be stored under argon for 1 month or in a sealed ampule for several months without any observable decomposition.

4-Methyl-1,3-dithiole-2-dimethoxyphosphonate 75

To a stirred suspension of salt **74** (500 mg, 2.05 mmol) in dry acetonitrile (100 ml) at 20°C, was added trimethylphosphite (0.28 ml, 2.37 mmol) and the mixture was stirred for 1 h. The solvent was evaporated *in vacuo* to afford compound **75** (460 mg, 99%) as a light brown oil of high purity (^1H NMR analysis) suitable for use in the next step without further purification. ^1H NMR (CDCl_3): δ 1.95 (s, 3H), 3.89 (d, $J = 10.5$ Hz, 6H), 4.97 (d, $J = 4.2$ Hz, 1H), 5.53 (s, 1H).

9-(4,5-Dimethyl-1,3-dithiol-2-ylidene)-10-(4-methyl-1,3-dithiol-2-ylidene)-9,10-dihydroanthracene 65.

Into a solution of reagent **75** (465 mg, 2.05 mmol) in dry tetrahydrofuran (150 ml) at -78°C, was added lithium diisopropylamide (1.5 ml of 1.5 M solution in cyclohexane, 2.25 mmol) over a period of 15 min. The reaction was stirred for 3 h at -78°C until a pale cloudy solution formed. Then compound **68** (725 mg, 2.25 mmol) was added portionwise over 15 min. The reaction was stirred overnight at 20°C. The reaction mixture was evaporated *in vacuo* and the residue was purified by column chromatography on silica gel with hexane/dichloromethane (2:1 v/v) as the eluent to afford **65** as a yellow solid (474 mg, 55%). M.p. 288-290°C (from hexane/dichloromethane). ^1H NMR (CDCl_3): δ 2.02 (s, 6H), 2.14 (s, 3H), 5.93 (s, 1H), 7.36 (m, 4H), 7.75 (m, 4H); ^{13}C NMR (CDCl_3): δ 13.8, 15.9, 111.0, 120.8, 121.2, 122.1, 125.1, 125.3, 125.7, 129.3, 133.0, 135.1, 135.2, 136.0; UV (MeCN): λ_{max} ($\log \epsilon$) = 360 nm (4.18), 430 (4.43); CV (E^{ox}) 0.320 V; MS (EI); m/z (%) = 422 (37) [M^+], 149 (50), 84 (100); HRMS: $\text{C}_{23}\text{H}_{18}\text{S}_4$ (422.6): calcd. 422.0359; found 422.0359.

9-(4-Formyl-5-methyl-1,3-dithiol-2-ylidene)-10-(4,5-dimethyl-1,3-dithiol-2-ylidene)-9,10-dihydroanthracene 78.

Into a solution of **65** (159 mg, 0.376 mmol) in dry tetrahydrofuran (50 ml) at -78°C , was added lithium diisopropylamide (0.26 ml of 1.5 M solution in cyclohexane, 0.39 mmol). The reaction was stirred for 3 h at -78°C to give a yellow solution containing anion **77**. *N,N*-Dimethylformamide (0.055 ml, 0.71 mmol) was then added and the reaction was stirred overnight at 20°C . The reaction mixture was acidified with HCl (1M), and then extracted into dichloromethane (3 x 100 ml). The organic layer was separated and dried (MgSO_4) and evaporated *in vacuo* and the residue was purified by column chromatography on silica gel with hexane/dichloromethane (2:1 v/v) as the eluent to afford **78** as an orange solid (22 mg, 13%). M.p. 160°C (dec.); ^1H NMR (CDCl_3): $\delta = 1.93$ (s, 6H), 2.40 (s, 3H), 7.26 (m, 4H), 7.64 (m, 4H), 9.67 (s, 1H); IR ν_{max} (Golden Gate): 1635 (C=O) cm^{-1} ; UV (MeCN): λ_{max} ($\log \epsilon$) = 358 nm (3.90), 422 (4.08); CV (E^{ox}) 0.450 V; MS (EI) m/z (%) = 450 (100) [M^+], 306 (63), 252 (31) HRMS: $\text{C}_{24}\text{H}_{18}\text{OS}_4$ (450.6): calcd. 450.0308; found 450.0308.

9-(4-Methylthiocarbamoyl)-5-methyl-1,3-dithiol-2-ylidene)-10-(4,5-dimethyl-1,3-dithiol-2-ylidene)-9,10-dihydroanthracene 79.

Into a solution of **65** (102 mg, 0.241 mmol) in dry tetrahydrofuran (50 ml) at -78°C was added lithium diisopropylamide (0.17 ml of 1.5 M solution in cyclohexane, 2.55 mmol). The reaction was stirred for 3 h, then methyl isothiocyanate (0.10 ml, 1.46 mmol) was added and the reaction was stirred overnight at 20°C . Workup and purification as described for **78**, gave **79** as an orange solid (20 mg, 17%). M.p. 197 - 200°C ; ^1H NMR (CDCl_3): $\delta = 1.92$ (s, 6H), 2.03 (s, 3H), 2.99 (d, $J = 4.8$ Hz, 3H), 7.30 (m, 4H), 7.52 (m, 2H), 7.66 (m, 2H), (NH not observed); ^{13}C NMR (CDCl_3): $\delta = 13.1$, 15.0, 32.6, 120.9, 125.3, 125.3, 125.5, 125.6, 125.8, 125.9, 126.2, 127.3, 129.3, 131.1, 134.0, 134.3, 134.4, 135.1 ppm; UV (MeCN): λ_{max} ($\log \epsilon$) = 362 nm (4.11), 430 (4.32);

CV (E^{ox}) 0.365 V; MS (EI) m/z (%) = 495 (100) [M^+], 447 (36), 350 (40); HRMS: $C_{25}H_{21}NS_5$ (495.8): calcd. 495.0362; found 495.0362.

9-(4-Iodo-5-methyl-1,3-dithiol-2-ylidene)-10-(4,5-dimethyl-1,3-dithiol-2-ylidene)-9,10-dihydroanthracene 80.

Into a solution of **65** (200 mg, 0.47 mmol) in dry tetrahydrofuran (150 ml) at -78°C was added lithium diisopropylamide (1.0 ml of 1.5 M solution in cyclohexane, 1.50 mmol) over a period of 15 min. The reaction was stirred for 3 h, then perfluorohexyl iodide (0.511 ml, 2.37 mmol) was added over 15 min and the reaction was stirred overnight at 20°C . Workup and purification as described for **78**, with hexane/dichloromethane (3:1 v/v) as the eluent to afford **80** as a brown solid (141 mg, 55%). ^1H NMR (CDCl_3): δ = 1.92 (s, 6H) 2.03 (s, 3H) 7.26 (m, 4H) 7.52 (m, 2H) 7.63 (m, 2H); ^{13}C NMR (CDCl_3): δ = 13.3, 14.4, 19.1, 22.9, 27.2, 31.8, 62.0, 121.1, 123.5, 125.3, 125.6, 125.7, 125.9, 126.1, 126.4, 130.4, 134.2, 134.6, 134.8, 135.0, 135.4, 135.5 ppm; MS (EI) m/z (%) = 548 (100) [M^+]; $C_{23}H_{17}IS_4$ (548): calcd. C 50.36, H 3.12; found C 50.20, H 3.30.

9-(4-Methoxycarbonyl-5-methyl-1,3-dithiol-2-ylidene)-10-(4,5-dimethyl-1,3-dithiol-2-ylidene)-9,10-dihydroanthracene 81.

Into a solution of **65** (504 mg, 1.19 mmol) in dry tetrahydrofuran (150 ml) at -78°C was added lithium diisopropylamide (0.87 ml of 1.5 M solution in cyclohexane, 1.30 mmol) over a period of 15 min. The reaction was stirred for 3 h, then methyl chloroformate (0.27 ml, 3.54 mmol) was added over 15 min and the reaction was stirred overnight at 20°C . Workup and purification as described for **78**, with hexane/dichloromethane (3:1 v/v) as the eluent afforded **81** as a yellow solid (475 mg, 83%). M.p. $218\text{--}220^{\circ}\text{C}$; ^1H NMR (CDCl_3): δ = 1.83 (s, 6H), 2.28 (s, 3H), 3.69 (s, 3H), 7.20 (m, 4H), 7.51 (m, 2H), 7.57 (m, 2H); ^{13}C NMR (CDCl_3): δ = 13.4, 15.7, 52.4, 117.2, 121.0, 121.2, 123.7, 125.4, 125.5, 125.7, 125.9, 126.1, 126.4, 129.5, 134.2, 134.8,

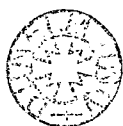
135.5, 145.8, 160.9 ppm; IR (powder) ν_{\max} 1714 (C=O) cm^{-1} ; UV (MeCN): λ_{\max} (log ϵ) = 358 nm (4.18), 426 (4.40); CV (E^{ox}) 0.425 V; MS (EI) m/z (%) = 480 (100) [M^+], 306 (37), 175 (35); $\text{C}_{25}\text{H}_{20}\text{O}_2\text{S}_4$ (480.0): calcd. C 62.47, H 4.19; found C 62.40, H 4.12; Crystals for X-ray analysis were grown from CDCl_3 .

9-(4-Benzoylsulfanyl-5-methyl-1,3-dithiol-2-ylidene)-10-(4,5-dimethyl-1,3-dithiol-2-ylidene)-9,10-dihydroanthracene 83.

Into a solution of compound **68** (199 mg, 0.471 mmol) in dry tetrahydrofuran (50 ml) at -78°C was added lithium diisopropylamide (0.38 ml of 1.5 M solution in cyclohexane, 0.57 mmol) over a period of 15 min. The reaction was stirred for 3 h at -78°C . Finely powdered, elemental sulfur (78 mg, 2.37 mmol) was added and the reaction was stirred for a further 2 h at -78°C before benzoyl chloride (0.275 ml, 2.37 mmol) was added. The colour of the solution turned a darker yellow, and the reaction was stirred overnight at 20°C . Workup and purification as described for **78**, gave **83** as a yellow solid (138 mg, 53%). M.p. 160°C (dec.); ^1H NMR (CDCl_3): δ = 1.84 (s, 6H), 1.97 (s, 3H), 7.19 (m, 4H), 7.39 (t, J = 7.5 Hz, 2H), 7.53 (m, 5H), 7.86 (d, J = 7.9 Hz, 2H); ^{13}C NMR (CDCl_3): δ = 13.1, 14.9, 108.1, 120.8, 120.9, 121.0, 123.0, 125.1, 125.2, 125.4, 125.5, 125.7, 125.8, 126.0, 126.1, 126.8, 126.9, 131.3, 133.9, 134.2, 134.7, 134.9, 135.3, 135.4, 135.7, 139.3, 187.7; IR (powder) ν_{\max} 1737 (C=O) cm^{-1} ; UV (MeCN): λ_{\max} (log ϵ) = 364 nm (4.16), 430 (4.38); CV (E^{ox}) 0.420 V; MS (EI) m/z (%) = 558 (5) [M^+], 84 (100), 64 (71); $\text{C}_{30}\text{H}_{22}\text{OS}_5$ (558.0): calcd. C 64.48, H 3.97; found C 64.29, H 4.25.

9-(4-Methylsulfanyl-5-methyl-1,3-dithiol-2-ylidene)-10-(4,5-dimethyl-1,3-dithiol-2-ylidene)-9,10-dihydroanthracene 84.

Into a solution of compound **65** (97 mg, 0.174 mmol) in dry tetrahydrofuran (35 ml) at 20°C was added sodium methoxide (0.39 ml of 0.5 M solution in methanol, 0.195 mmol). The reaction was stirred for 1 h until a dark red solution formed. Then



iodomethane was added (0.10 ml, 1.61 mmol) and the reaction was stirred overnight at 20°C. The reaction mixture was evaporated *in vacuo* and the residue was purified by column chromatography on silica gel with hexane/dichloromethane (2:1 v/v) as eluent to afford **84** as a yellow solid (65 mg, 80%). M.p. 220°C (dec.); ¹H NMR (CDCl₃): δ = 1.86 (s, 6H), 2.03 (s, 3H), 2.20 (s, 3 H), 7.20 (m, 4H), 7.51 (m, 2H), 7.59 (m, 2H); ¹³C NMR (CDCl₃): δ = 13.1, 14.5, 19.3, 118.3, 120.8, 125.2, 125.3, 125.4, 125.6, 125.8, 125.9, 132.0, 134.8, 135.0, 135.2, 197.9; UV (MeCN): λ_{max} (log ε) = 360 nm (3.89), 432 (4.38); CV (*E*^{ox}) 0.355 V; MS (EI) *m/z* (%) = 468 (100) [M⁺], 350 (50), 57 (60); C₂₄H₂₀S₅ (468.0): calcd. C 61.50, H 4.30; found C 61.30, H 4.26; Crystals for X-ray analysis were grown from CS₂/CH₂Cl₂.

9-[4-(6-Hydroxyhexylsulfanyl)-5-methyl-1,3-dithiol-2-ylidene]-10-(4,5-dimethyl-1,3-dithiol-2-ylidene)-9,10-dihydroanthracene 85.

Into a solution of compound **65** (100 mg, 0.179 mmol) in dry tetrahydrofuran (50 ml) at 20°C was added sodium methoxide (0.39 ml of 0.5 M solution in methanol, 0.195 mmol). The reaction was left for 1 h before 6-bromohexan-1-ol was added (0.07 ml, 0.535 mmol), and the reaction was stirred overnight at 20°C. The reaction mixture was evaporated *in vacuo* and excess 6-bromohexan-1-ol was removed by Kügelrohr distillation at 140°C at *ca.* 0.1 mm Hg, and the distillate was discarded. The residue was purified by column chromatography on silica gel with ethyl acetate/dichloromethane (1:4 v/v) as the eluent to afford **85** as a red oil (93 mg, 93%). ¹H NMR (CDCl₃): δ = 1.37 (m, 4H), 1.55 (m, 4H), 1.92 (s, 6H), 2.09 (s, 3H), 2.66 (m, 2H), 3.60 (t, *J* = 6.6 Hz, 2H), 7.26 (m, 4H), 7.58 (m, 2H), 7.64 (m, 2H), (OH not observed); ¹³C NMR (CDCl₃): δ = 13.1, 14.7, 25.2, 28.1, 28.9, 29.6, 32.5, 35.9, 62.8, 117.1, 120.8, 122.3, 125.2, 125.3, 125.6, 125.8, 125.8, 125.9, 131.3, 133.0, 133.1, 134.8, 135.0, 135.2 ppm; UV (MeCN): λ_{max} (log ε) = 366 nm (4.14), 432 (4.39); CV (*E*^{ox}) 0.380 V; MS (EI) *m/z* (%) = 554 (100) [M⁺], 350 (76), 220 (31); HRMS: C₂₉H₃₀OS₅ (554.9) calcd. 554.0985; found 554.0985.

2-Methylsulfanyl-4-(2-cyanoethylsulfanyl)-5-methylthio-1,3-dithiolium trifluoromethylsulfonate 92.

Into a solution of thione **91** (1.029 g, 4.10 mmol) in dry dichloromethane (100 ml) at 20°C, was added methyl trifluoromethylsulfonate (0.90 ml, 7.97 mmol). The reaction was left for 1 h until a dark yellow solution formed. The reaction mixture was concentrated *in vacuo* to ca. 10 ml and the resulting suspension washed with dry diethyl ether (50 ml), which was then decanted off and discarded. The reaction mixture was then evaporated *in vacuo* affording **92**, as an unstable red oil which was quickly used without further purification; ¹H NMR (CDCl₃): δ = 2.85 (s, 3H), 2.92 (t, *J* = 6.6 Hz, 2H), 3.22 (s, 3H), 3.33 (t, *J* = 6.4 Hz, 2H).

10-[4-(2-Cyanoethylsulfanyl)]-5-methylsulfanyl-1,3-dithiol-2-ylidene)-anthracene-9-(10H)-one 95.

Into a solution of anthrone **93** (773 mg, 3.98 mmol) in dry isopropanol (50 ml) at 20°C was added lithium diisopropylamide (2.65 ml, of 1.5 M solution in cyclohexane, 3.98 mmol). The reaction was stirred for 15 min until a bright yellow solution formed. Then salt **92** (1.653 g, 3.98 mmol) in dry tetrahydrofuran (50 ml) was added and the reaction mixture was stirred overnight. The mixture was evaporated *in vacuo* and the residue was purified by column chromatography on silica gel with hexane/dichloromethane (1:1 v/v) as the eluent to afford crude compound **94** as a red solid. ¹H NMR (CDCl₃): δ = 2.00 (s, 3H), 2.26 (s, 3H), 2.47 (m, 2H), 2.73 (m, 2H), 4.91 (s, 1H), 7.51 (m, 4H), 7.69 (m, 2H), 8.15 (m, 2H). This solid (398 mg, 0.889 mmol) was dissolved in dry toluene (100 ml) at 20°C and *p*-toluene sulfonic acid (100 mg, 0.526 mmol) was added. The reaction mixture was refluxed for 16 h to give a dark red solution. The mixture was evaporated *in vacuo* and the residue purified by column chromatography on silica gel with dichloromethane as eluent to afford **95** as a red solid (293 mg, 18% based on **91**). M.p. 142-145°C; ¹H NMR (CDCl₃): δ = 2.04 (s, 3H), 2.24 (t, *J* = 6.8 Hz, 2H), 2.58 (t, *J* = 6.8 Hz, 2H), 7.04 (t, *J* = 7.8 Hz, 2H), 7.26 (m, 4H), 7.85

(d, $J = 7.4$ Hz, 2H); ^{13}C NMR (CDCl_3): $\delta = 18.7, 18.1, 31.3, 117.4, 119.6, 120.3, 126.1, 127.2, 127.3, 130.7, 131.9, 134.1, 138.2, 138.4, 183.4$ ppm; IR (powder) ν_{max} 1635 ($\text{C}=\text{O}$) cm^{-1} ; MS (EI) m/z (%) = 425 (61) [M^+], 236 (100), 91 (66); $\text{C}_{21}\text{H}_{15}\text{NOS}_4$ (425.6) calcd. C 59.27, H 3.55, N 3.29; found C 59.51, H 3.70, N 3.28.

10-[4-(6-Hydroxyhexylsulfanyl)-5-methylsulfanyl-1,3-dithiol-2-ylidene]-anthracene-9-(10H)-one 96.

Into a solution of **95** (200 mg, 0.471 mmol) in dry tetrahydrofuran (50 ml) at 20°C was added cesium hydroxide monohydrate (94 mg, 0.528 mmol). The reaction was stirred for 1 h until a dark red solution formed. 6-Bromohexan-1-ol (0.2 ml, 1.53 mmol) was added and the reaction was stirred overnight at 20°C then evaporated *in vacuo* and excess 6-bromohexan-1-ol was removed by Kugelrohr distillation at 140°C at *ca.* 0.1 mm Hg, and the distillate was discarded. The residue was purified by column chromatography on silica gel with hexane/dichloromethane (1:1 v/v) as eluent to afford **96** as a red oil (198 mg, 89 %); ^1H NMR (CDCl_3): $\delta = 1.47$ (m, 8H), 2.41 (s, 3H), 2.79 (t, $J = 7.2$ Hz, 2H), 3.60 (t, $J = 7.2$ Hz, 2H), 7.44 (t, $J = 7.8$ Hz, 2H), 7.65 (t, $J = 7.8$ Hz, 2H), 7.77 (d, $J = 7.8$ Hz, 2H), 8.26 (d, $J = 7.8$ Hz, 2H); ^{13}C NMR (CDCl_3): $\delta = 19.2, 25.1, 28.0, 29.4, 32.4, 36.2, 62.6, 119.0, 125.1, 126.1, 127.1, 127.6, 129.0, 130.5, 131.8, 138.5, 140.3, 183.4$; IR (Powder) ν_{max} 1649 ($\text{C}=\text{O}$) cm^{-1} ; MS (EI) m/z (%) = 472 (100) [M^+], 236 (58), 55 (79); HRMS: $\text{C}_{24}\text{H}_{24}\text{O}_2\text{S}_4$ (472.7): calcd. 472.0659; found 472.0644.

10-[4-(6-tert-Butyldiphenylsilyloxyhexylsulfanyl)-5-methylsulfanyl-1,3-dithiol-2-ylidene]-anthracene-9-(10H)-one 97.

Into a solution of compound **96** (305 mg, 0.646 mmol) in dry dimethylformamide (50 ml) was added *tert*-butylchlorodiphenylsilane (0.18 ml, 0.692 mmol) and imidazole (345 mg, 5.07 mmol). The reaction was stirred overnight at 20°C and then evaporated *in vacuo* and the residue was purified by column chromatography on silica gel with hexane/dichloromethane (1:1 v/v) as eluent to afford **97** as a red oil (413 mg, 90%); ^1H

NMR (CDCl₃): δ = 1.06 (s, 9H), 1.37 (m, 4H), 1.55 (m, 4H), 2.40 (s, 3H), 2.79 (t, J = 7.6 Hz, 2H) 3.65 (t, J = 6.4 Hz, 2H), 7.42 (m, 8H), 7.67 (m, 6H), 7.79 (m, 2H), 8.29 (d, J = 7.6 Hz, 2H); ¹³C NMR (CDCl₃): δ = 19.5, 25.6, 27.2, 28.4, 29.8, 32.6, 36.7, 64.0, 119.3, 125.6, 126.5, 127.5, 127.9, 129.3, 129.8, 130.9, 130.9, 132.1, 134.3, 135.8, 138.9, 140.7, 183.7. IR (Powder) ν_{\max} 1653 (C=O) cm⁻¹; MS (EI) m/z (%) = 710, (100) [M⁺], 653 (99), 135 (79); HRMS: C₄₀H₄₂O₂S₄Si (711.1) calcd. 710.1904; found 710.1902.

9-[4-(6-tert-Butyldiphenylsilyloxyhexylsulfanyl)-5-methylsulfanyl-1,3-dithiol-2-ylidene]-10-(4,5-dimethyl-1,3-dithiol-2-ylidene)-9,10-dihydroanthracene 98.

Into a solution of **54** (117 mg, 0.488 mmol) in dry tetrahydrofuran (150 ml) at -78°C was added lithium diisopropylamide (0.34 ml of 1.5 M solution in cyclohexane, 0.506 mmol) over a period of 15 min. The reaction was stirred for 3 h until a pale cloudy solution formed. Then compound **97** (171 mg, 0.241 mmol) was added over 15 min and the reaction was stirred overnight at 20°C and then evaporated *in vacuo* and the residue purified by column chromatography on silica gel with hexane/dichloromethane (2:1 v/v) as eluent to afford **98** as a yellow oil (138 mg, 70%); ¹H NMR (CDCl₃) δ 1.05 (s, 9H), 1.36 (m, 4H), 1.56 (m, 4H), 1.93 (s, 6H), 2.36 (s, 3H), 2.76 (m, 2H), 3.65 (t, J = 6.6 Hz, 2H), 7.30 (m, 4H), 7.41 (m, 6H), 7.54 (m, 2H), 7.66 (m, 6H); ¹³C NMR (CDCl₃) δ 13.1, 19.2, 25.3, 26.9, 28.1, 29.6, 31.6, 32.3, 34.6, 36.2, 63.7, 120.8, 120.9, 123.7, 124.2, 125.8, 126.1, 127.6, 129.5, 130.4, 133.5, 134.0, 134.6, 135.2, 135.5; MS (EI) m/z (%) = 824 (100) [M⁺], 350 (89), 220 (66); HRMS: C₄₅H₄₈OS₆Si (825.3): calcd. 824.1900; found 824.1900.

9-[4-(6-Hydroxyhexylsulfanyl)-5-methylsulfanyl-1,3-dithiol-2-ylidene]-10-(4,5-dimethyl-1,3-dithiol-2-ylidene)-9,10-dihydroanthracene 99.

Into a solution of compound **98** (137 mg, 0.167 mmol) in dry tetrahydrofuran (50 ml) was added tetrabutylammonium fluoride (0.5 ml of 1.0 M solution in water, 0.5mmol). After stirring for 1 h at 20°C a dark red solution had formed. The reaction

mixture was stirred at 20°C overnight and then evaporated *in vacuo* and the residue was purified by column chromatography on silica gel with dichloromethane as eluent to afford **99** as a yellow oil (77 mg, 79%); ¹H NMR (CDCl₃): δ = 1.39 (m, 4H), 1.56 (m, 4H), 1.93 (s, 6 H), 2.37 (s, 3H), 2.77 (m, 2H), 3.61 (t, *J* = 6.5 Hz, 2H), 4.35 (t, *J* = 7.0 Hz, 1H), 7.28 (m, 4H), 7.52 (m, 2H), 7.66 (m, 2H); ¹³C NMR (CDCl₃): δ = 13.1, 19.1, 25.2, 28.1, 29.6, 32.5, 36.0, 60.4, 62.8, 120.9, 123.8, 124.0, 125.3, 125.7, 126.1, 127.7, 130.2, 133.5, 134.5, 135.2; MS (EI) *m/z* (%) = 586 (21) [M⁺], 350 (100), 220 (100); HRMS: C₂₉H₃₀O₆ (586.9) calcd. 586.0621; found 586.0634.

9-[4-(6-Carbobenzoxyhexylsulfanyl)-5-methylsulfanyl-1,3-dithiol-2-ylidene]-10-(4,5-dimethyl-1,3-dithiol-2-ylidene)-9,10-dihydroanthracene 100.

Into a solution of compound **99** (74 mg, 0.127 mmol) in dry dichloromethane (50 ml) was added triethylamine (1 ml, excess) and benzoyl chloride (0.20 ml, 1.72 mmol). The reaction was stirred overnight at 20°C and then evaporated *in vacuo* and the residue purified initially by column chromatography on silica gel with hexane/dichloromethane (1:1 v/v) as the eluent, and then further purified by column chromatography on silica gel with acetone/hexane (1:3 v/v) as eluent, to afford **100** as a yellow oil (44 mg, 50%); ¹H NMR (CDCl₃): δ = 1.38 (m, 4H), 1.56 (m, 2H), 1.67 (m, 2H), 1.84 (s, 6H), 2.28 (s, 3H), 2.70 (m, 2H), 4.21 (t, *J* = 6.5 Hz, 2H), 7.20 (m, 4H), 7.35 (t, *J* = 8.0 Hz, 2H), 7.45 (m, 3H), 7.59 (m, 2H), 7.95 (d, *J* = 8.0 Hz, 2H). ¹³C NMR (CDCl₃): δ = 13.1, 19.1, 25.6, 28.0, 28.5, 29.5, 36.0, 64.9, 120.8, 120.9, 123.8, 123.9, 125.3, 125.3, 125.8, 126.1, 127.9, 128.3, 129.5, 130.2, 130.4, 132.8, 133.5, 134.6, 135.2, 166.6; UV (MeCN): λ_{max} (log ε) = 366 nm (4.09), 434 (4.33); CV (*E*^{ox}) 0.375 V; MS (DCI) *m/z* (%) = 691 (49) [M⁺+1], 322 (100), 105 (63); HRMS: C₃₆H₃₄O₂S₆ (691.0) calcd. 690.0985; found 690.0988.

**10-[4,5-bis(2-Cyanoethylsulfanyl)-1,3-dithiol-2-ylidene]-anthracene-9-(10H)-one
101.**

Into a solution of anthrone **93** (1.41 g, 7.26 mmol) in dry isopropanol (50 ml) at 20°C was added lithium diisopropylamide (4.83 ml, of 1.5 M solution in cyclohexane, 7.24 mmol). The reaction was stirred for 15 min until a bright yellow solution formed. Then the triflate salt of **90** (3.08 g, 6.58 mmol) in dry tetrahydrofuran (50 ml) was added and the reaction mixture was stirred overnight. The mixture was evaporated *in vacuo* and the residue was purified by column chromatography on silica gel with hexane/dichloromethane (1:1 v/v) as the eluent to afford crude compound **101** as a red solid. This solid (1.51 g) was dissolved in dry toluene (100 ml) at 20°C and *p*-toluene sulfonic acid (100 mg, 0.526 mmol) was added. The reaction mixture was refluxed for 16 h to give a dark red solution. The mixture was evaporated *in vacuo* and the residue purified by column chromatography on silica gel with dichloromethane as eluent to afford **101** as a red solid (590 mg, 19% based on **90**). M.p. 138-141°C; ¹H NMR (CDCl₃): δ 2.69 (m, 4H) 3.06 (m, 4H) 7.48 (m, 2H) 7.66 (m, 4H) 8.25 (m, 2H); ¹³C NMR (CDCl₃): δ = 18.8, 19.0, 31.3, 31.6, 117.3, 121.2, 126.0, 127.1, 127.4, 130.7, 132.0, 136.9, 138.2, 183.4, 197.9 ppm; IR (powder) ν_{\max} 1635 (C=O) cm⁻¹; MS (EI) *m/z* (%) = 464 [M⁺]; C₂₃H₁₆N₂OS₄ (464.0) calcd. C 59.46, H 3.47, N 6.03; found C 59.18, H 3.35, N 6.19.

6.4 Experimental Procedures For Chapter 4

1,10-Dibromo pentaethylene 107.

Into a mechanically stirred solution of pentaethylene glycol (35.7 g, 0.15 mmol) in pyridine (4 ml) was added phosphorus tribromide (33.9 g, 0.13 mmol) at 0°C for 7 h to give a cloudy white solution. The reaction mixture was extracted into dry diethyl ether (6 x 100 ml). The organic layer was separated and dried (MgSO₄) and evaporated *in vacuo* and the residue was purified by column chromatography on silica gel with ethylacetate as the eluent to afford **107** as a colourless oil (28.2 g, 51%) of high purity (¹H NMR analysis) suitable for use in the next step without further purification; ¹H NMR (CDCl₃): δ = 3.81 (t, *J* = 6.3 Hz, 4H) 3.67 (s, 12H) 3.48 (t, *J* = 6.3 Hz, 4H).

1,3-Dithiole-2-thione Crown 110.

Into a solution of 4,5-bis(thiobenzoyl)-1,3-dithiole-2-thione **108** (2.00 g, 4.93 mmol) in dry ethanol (40 ml) was added sodium methoxide (20 ml of 0.5 M in methanol, 10.0 mmol) at 0°C for 30 min to give a dark red solution. After 30 min, the solution was poured into dry diethyl ether (1 l) and stirred for 1 h. The red solid was then collected by Schlenk filtration. The red solid was transferred to a flask containing dry tetrahydrofuran (150 ml) and compound **107** (1.81 g, 4.97 mmol) and stirred for 12 h. Then the solvent was evaporated *in vacuo* and the residue was purified by column chromatography on silica gel with ethylacetate as the eluent to afford **110** as a yellow oil, which solidified on standing (1.56 g, 79%). ¹H NMR (CDCl₃): δ = 3.07 (t, *J* = 6.0 Hz, 4H) 3.64 (s, 12H) 3.75 (t, *J* = 6 Hz, 4H); C₁₃H₂₀O₄S₅ (400.0): calcd. C 38.98, H 5.03; found C 38.82, H 5.19.

Triflate salt 111.

Into a solution of **110** (2.7 g, 6.8 mmol) in dry methylene chloride (50 ml) was added methyl triflate (1.2 g, 7.3 mmol) at 20°C for 5 h to give a dark brown solution. Then the solvent was partially evaporated *in vacuo* (5 ml) and dry diethyl ether added (100 ml) and stirred for 30 min. Next, the solvent was decanted off and the oil dried *in vacuo* to afford **111**, as a brown oil (3.2 g, 84%) of high purity suitable for use in the next step without further purification. C₁₃H₂₃F₃O₇S₆ (564.0): calcd. C 31.91, H 4.08; found C 31.64, H 4.27.

1,3-Dithiole crown 112.

Into an ice cooled solution of **111** (120 mg, 1.9 mmol) in dry ethanol (75 ml) was added sodium cyanoborohydride portionwise (1.0 g, 1.8 mmol) at 0°C for 1 h. Then the solvent was evaporated *in vacuo* and the residue was purified by column chromatography on silica gel with ethylacetate as the eluent to afford **112**, as a pale reddish oil (0.72 g, 98%). The oil was recrystallized from hot ethyl acetate with cooling in acetone/dry ice to yield an off-white solid. ¹H NMR (CDCl₃): δ = 5.77 (s, 1H) 3.71 (t, J = 2.6 Hz, 4H) 3.70 (s, 12H) 2.98-3.16 (m, 4H) 2.24 (s, 3H). C₁₄H₂₄O₄S₅ (416.0): calcd. C 40.38, H 5.76; found C 40.25, H 5.84.

Triflate salt 113.

Into a solution of **112** (0.5, 1.2 mmol) in dry acetonitrile (5 ml) was added triflic acid (1 ml, 10 mmol) at 20°C for 10 min to give a deep red-orange solution. Then the solvent was partially evaporated *in vacuo* (5 ml) and dry diethyl ether added (100 ml) and stirred for 30 min. Next the solvent was decanted off and the oil dried *in vacuo* to afford **113**, as a brown oil (3.2 g, 84%) of high purity (¹H NMR analysis) suitable for use in the next step without further purification. ¹H NMR (CD₃CN): δ = 3.38 (s, 12H) 3.55 (t, J = 4.5 Hz, 4H) 3.85 (t, J = 4.5 Hz, 4H) 9.22 (s, 1H).

Horner-Wadsworth-Emmons reagent 114.

To a stirred suspension of salt **113** (540 mg, 1.0 mmol) in dry acetonitrile (5 ml) at 20°C, was added triethylphosphite (0.17 ml, 1.0 mmol) and the mixture was stirred for 1 h. Then the solvent was evaporated *in vacuo* and extracted into ethylacetate (2x50 ml). The organic layer was separated and dried (MgSO₄) and evaporated *in vacuo* and the residue was purified by column chromatography on silica gel with ethylacetate as the eluent to afford **114** as a colourless oil (0.40 g, 75%) of high purity (¹H NMR analysis) suitable for use in the next step without further purification; ¹H NMR (CDCl₃): δ = 1.30 (t, *J* = 7.0 Hz, 6H) 2.86-2.96 (m, 2H) 2.99-3.12 (m, 2H) 3.62 (s, 4H) 3.64 (s, 8H) 3.74 (t, *J* = 6.2 Hz, 2H) 3.75 (t, *J* = 6.8 Hz, 2H) 4.18 (p, *J*_p = *J*_H = 7.0 Hz, 2H) 4.63 (s, 1H).

Bis-Crown 106 and Mono-crown 116.

Into a solution of **114** (558 mg, 1.10 mmol) in dry tetrahydrofuran (70 ml) at -78°C, was added lithium diisopropylamide (0.74 ml of 1.5 M solution in cyclohexane, 1.11 mmol). The reaction was stirred for 3h at -78°C until a cloudy solution formed. Then anthraquinone (115 mg, 0.552 mmol) was added, the reaction was allowed to warm overnight to 20°C. The reaction mixture was evaporated *in vacuo* and the residue was purified by column chromatography on silica gel with ethyl acetate as eluent. The first product to elute was **116** as a red oil which solidified on standing (178 mg, 29%). M.p. 123-124°C. C₂₇H₂₈O₅S₄ (560) calcd. C 56.9, H 5.1; found C 56.7, H 5.0; *m/z* (EI) 560 [M⁺]; ¹H NMR (CDCl₃): δ = 3.04 (t, *J* = 6.0 Hz, 4H) 3.58 (m, 16H) 7.46 (t, *J* = 7.2 Hz, 2H) 7.66 (m, 2H) 7.76 (d, *J* = 7.6 Hz, 2H) 8.27 (m, 2H). ¹³C NMR (CDCl₃): δ = 35.8, 69.6, 70.4, 70.6, 119.5, 126.3, 126.9, 127.2, 127.3, 130.6, 131.9, 138.6, 140.1, 197.9 ppm. *v*_{max} (Golden Gate): 2853, 1646, 1591, 1482, 1429, 1291, 1105, 1087, 770.

Ethyl acetate/acetone (3:1v/v) as the eluent followed by recrystallization from dichloromethane/hexane afforded **106** as a yellow solid (335 mg, 67%). M.p. 216-218°C; C₄₀H₄₈O₈S₈ (912) calcd. C 52.1, H, 5.3; found C 51.9, H 5.4; *m/z* (EI) 912 [M⁺]; ¹H

NMR (CDCl₃): δ = 3.05 (m, 8H) 3.66 (m, 32H) 7.33 (m, 4H) 7.56 (m, 4H). ¹³C NMR (CDCl₃): δ = 19.4, 26.5, 116.1, 116.4, 120.4, 120.9, 126.2, 127.8, 128.7, 129.8, 131.3, 132.9, 135.5, 135.7, 136.6, 153.2 ppm.

Mono Crown 115.

Into a solution of **114** (250 mg, 0.494 mmol) in dry tetrahydrofuran (50 ml) at -78°C , was added lithium diisopropylamide (0.33 ml of 1.5 M solution in cyclohexane, 0.495 mmol). The reaction was stirred for 3 h at -78°C until a cloudy solution formed. Then compound **68** (159 mg, 0.494 mmol) was added, then the reaction was allowed to warm overnight to 20°C . The reaction mixture was evaporated *in vacuo* and the residue was purified by column chromatography on silica gel with ethyl acetate then ethyl acetate/acetone (3:1 v/v) as the eluent followed by recrystallization from dichloromethane/hexane to afford **115** as a yellow/orange solid (178 mg, 53%) M.p. 223-225 $^{\circ}\text{C}$; C₃₂H₃₄O₄S₆ requires HRMS 674.0883; found 674.0883; *m/z* [EI] 674 *m/z*; ¹H NMR (CDCl₃): δ = 1.94 (s, 6H) 3.00 (m, 4H) 3.58 (m, 16H) 7.29 (m, 4H) 7.52 (m, 2H) 7.68 (m, 2H). ¹³C NMR (CDCl₃): 13.1, 35.4, 53.4, 69.8, 70.4, 70.5, 70.6, 76.7, 77.0, 77.3, 120.8, 123.8, 125.3, 125.8, 126.1, 129.9, 133.4, 134.4, 135.1 ppm.

6.5 Experimental Procedures For Chapter 5

2,6-Dibutoxy-9,10-bis[(methylene-4,5-dithio)-1,3-dithiol-2-thione]-9,10-dihydroanthracene 123.

Into a solution of **119** (559 mg, 1.76 mmol) in dry tetrahydrofuran (50 ml) at -78°C , was added lithium diisopropylamide (1.0 ml of 1.5 M solution in cyclohexane, 1.5 mmol) over a period of 15 min. The mixture was stirred at -78°C for 3 h until a dark red solution formed. Then compound **52** (248 mg, 0.70 mmol) was added over 15 min and the mixture was stirred overnight at 20°C . The reaction mixture was evaporated *in vacuo* and the residue purified by column chromatography on silica gel with hexane/dichloromethane (2:1 v/v) as eluent to afford **123** as a red solid (220 mg, 43%). M.p. $106\text{--}108^{\circ}\text{C}$; ^1H NMR (CDCl_3): $\delta = 1.00$ (t, $J = 7$ Hz, 6H) 1.51 (m, 4H), 1.80 (m, 4H), 4.04 (t, $J = 7.6$ Hz, 4H), 6.87 (dd, $J_{ab} = 3$ Hz, $J_{bc} = 9$ Hz, 2H) 7.00 (d, $J = 3$ Hz, 2H) 7.39 (d, $J = 9$ Hz, 2H); ^{13}C NMR (CDCl_3): $\delta = 13.9, 19.3, 31.3, 68.2, 112.2, 122.1, 126.5, 126.7, 127.2, 131.5, 135.5; 158.2, 211.5$ ppm; MS (CI) 738 m/z [M^+]; $\text{C}_{30}\text{H}_{24}\text{O}_2\text{S}_{10}$ calcd. C 48.9, H 3.3; found C 49.5, H 3.6;

9-[(4-5-Methylenedisulfanyl)-1,3-dithiol-2-thione]-10-(4,5-dimethyl-1,3-dithiol-2-ylidene)-9,10-dihydroanthracene 124.

Into a solution of **119** (216 mg, 0.63 mmol) in dry tetrahydrofuran (50 ml) at -78°C , was added lithium diisopropylamide (0.46 ml of 1.5 M solution in cyclohexane, 0.69 mmol) over a period of 15 min. The mixture was stirred at -78°C for 3 h until a dark red solution formed. Then compound **68** (198 mg, 0.61 mmol) was added over 15 min and the mixture was stirred overnight at 20°C . The reaction mixture was evaporated *in vacuo* and the residue purified by column chromatography on silica gel with hexane/dichloromethane (2:1 v/v) as eluent to afford **124** as a red solid (189 mg, 60%). M.p. $246\text{--}249^{\circ}\text{C}$; ^1H NMR (CDCl_3): $\delta = 1.93$ (s, 6H) 7.27 (t, $J = 7.6$ Hz, 2H), 7.35 (t, $J = 7.6$ Hz, 2H), 7.42 (d, $J = 7.6$ Hz, 2H), 7.71 (d, $J = 7.6$ Hz, 2H); ^{13}C NMR (CDCl_3): $\delta =$

13.1, 29.7, 119.8, 121.0, 122.3, 125.2, 125.5, 125.8, 127.1, 128.8, 130.8, 133.7, 135.2, 135.9, 211.7; CV (E^{ox}) 0.430 V; MS (EI) m/z (%) = 514 (82) (M^+), 350 (100), 220 (82); $C_{23}H_{14}S_7$ (514.8) calcd. C 53.66, H 2.74; found C 53.80, H 3.19. Crystals for X-ray analysis were grown from $CDCl_3$.

9-(4,5-Diethylsulfanyl-1,3-dithiol-2-ylidene)-10-(4,5-dimethyl-1,3-dithiol-2-ylidene)-9,10-dihydroanthracene 125.

A solution of **124** (102 mg, 0.20 mmol) in triethylphosphite (10 ml) was heated at reflux for 3 h to give a pale orange solution. The reaction mixture was evaporated *in vacuo* and the residue was purified by column chromatography on silica gel with hexane/dichloromethane (2:1 v/v) as eluent to afford **125** as a yellow solid (46 mg, 50%). M.p. 255-258°C; 1H NMR ($CDCl_3$): δ = 1.22 (t, J = 7.4 Hz, 6H), 1.87 (s, 6H), 2.75 (m, 4H), 7.21 (m, 4H), 7.47 (m, 2H), 7.60 (m, 2H); CV (E^{ox}) 0.345 V. MS (EI) m/z (%) = 528 (14) (M^+), 350 (45), 468 (38); HRMS $C_{26}H_{24}S_6$ (528.8) calcd. 528.0304; found 528.0304. Crystals for X-ray analysis were grown from $CDCl_3$.

2-(Dimethylamino)-4-(pentylthio)-1,3-ditholium Salt 135.

The mesoion **134** (3.00 g, 15.7 mmol) was mixed in dry acetone (250 ml) with 1,5-diiodopentane (1.59 ml, 7.9 mmol) and refluxed for 3 h until the solution turned pale yellow. After being cooled to room temperature, the salt was filtered and washed sequentially with acetone and ether to afford **135** as an off white solid (3.61 g, 65%). Compound **135** was used in the following reaction without further purification. M.p. 142-145°C (dec.); 1H NMR ($DMSO-d_6$): δ = 1.49 (m, 2H) 1.60 (m, 4H) 2.50 (s, 6H) 2.95 (t, J = 7.2 Hz, 4H) 3.36 (s, 12H).

Bis[2-(dimethylamino)-4-(hexylthio)-1,3-dithiolium] Salt 136.

The mesoion **134** (0.956 g, 5.00 mmol) was mixed in dry acetone (100 ml) with 1,6-dibromohexane (0.38 ml, 2.47 mmol) and refluxed for 3 h until the solution turned pale yellow. After being cooled to room temperature, the salt was filtered and washed with acetone and ether to afford **136** as a pale yellow solid (1.29 g, 83%). Compound **136** was used in the following reaction without further purification. M.p. 188-191°C (dec.); ¹H NMR (DMSO-d₆): δ = 1.38 (m, 4H) 1.57 (m, 4H) 2.50 (s, 6H) 2.93 (t, J = 7.6 Hz, 4H) 3.50 (s, 12H).

Bis[2-(dimethylamino)-4-(pentylthio)-1,3-dithiole] 137.

To a stirred solution of salt **135** (3.50 g, 4.96 mmol) in dry ethanol at 0°C under argon was portionwise added finely ground sodium borohydride (0.40 g, 10.6 mmol) over *ca.* 1 h and the reaction maintained at 0°C for a further 3 h, whereupon the reaction is allowed to come to 20°C and the mixture stirred for a further 15 h. The reaction mixture was evaporated *in vacuo* and the residue dissolved in ethyl acetate (100 ml). Brine (200 ml) was added and the mixture extracted with ethyl acetate (3x75 ml), the combined extracts washed with water (2x100 ml), dried (MgSO₄) and evaporated *in vacuo*. The residue was purified by column chromatography on silica gel with ethyl acetate/dichloromethane (1:4 v/v) as the eluent to afford **137** as a pale brown (2.14 g, 95%). MS (EI) 454 *m/z* [M⁺]; ¹H NMR (CDCl₃): δ = 1.59 (m, 6H) 2.12 (s, 6H) 2.27 (s, 12H) 2.71 (m, 4H) 5.94 (s, 2H). ¹³C NMR (CDCl₃): δ = 15.4, 27.5, 28.9, 29.3, 35.5, 38.2, 115.6, 131.8 ppm.

Bis[2-(dimethylamino)-4-(hexylthio)-1,3-dithiole] 138

To a stirred solution of salt **136** (1.02 g, 1.63 mmol) in dry ethanol at 0°C under argon is portionwise added finely ground sodium borohydride (0.16 g, 4.23 mmol) over *ca.* 1 h and the reaction maintained at 0°C for a further 3 h, whereupon the reaction is

allowed to come to 20°C and the mixture stirred for a further 15 h. The reaction mixture was evaporated *in vacuo* and the residue dissolved in ethyl acetate (100 ml). Brine (200 ml) was added and the mixture extracted with ethyl acetate (3x75 ml), the combined extracts washed with water (2x100 ml), dried (MgSO₄) and evaporated *in vacuo*. The residue was purified by column chromatography on silica gel with ethyl acetate/dichloromethane (1:4 v/v) as the eluent to afford **138**, as a pale yellow oil which solidified on standing (0.610 g, 82%). M.p. 75-78°C (dec.); HRMS C₁₈H₃₂N₂S₆ (468.8) calcd: 468.0991; found 468.0991; ¹H NMR (CDCl₃): δ = 1.40 (m, 4H) 1.59 (m, 4H) 2.12 (s, 6H) 2.27 (s, 12H) 2.69 (m, 2H) 2.78 (m, 2H) 5.93 (s, 2H); ¹³C NMR (CDCl₃): δ = 15.5, 28.1, 29.6, 35.7, 38.3, 115.8, 131.8 ppm.

Bis[2-(dimethylamino)-4-(pentylthio)-1,3-dithiolium tetrafluoroborate] 139.

To a stirred solution of **137** (1.77 g, 4.02 mmol) in dry dichloromethane (15 ml) at 0°C under argon was added dropwise 54% hydrofluoroboric acid in diethyl ether (2.20 ml, 16.1 mmol). After the reaction mixture was stirred for 1 h, dry diethyl ether was added (200 ml). The precipitate was collected by filtration, washed with dry diethyl ether to afford **139** as a grey powder. Due to instability of the tetrafluoroborate salt the product was reacted on without further purification.

Bis[2-(dimethylamino)-4-(hexathio)-1,3-dithiolium tetrafluoroborate] 140.

To a stirred solution of **138** (1.01 g, 2.16 mmol) in dry dichloromethane (15 ml) at 0°C under argon was added dropwise 54% hydrofluoroboric acid in diethyl ether (1.17 ml, 8.55 mmol). Reaction and workup as described for **139** afforded **140** as a grey powder. Due to instability of the tetrafluoroborate salt the product was reacted on without further purification.

Bis[2-(dimethoxyphosphinyl)-4-(pentylthio)-1,3-dithiole] 141.

To a stirred solution of crude **139** (2.91 g, 4.72 mmol) and sodium iodide (2.83 g, 18.9 mmol) in dry acetonitrile (10 ml) at 20°C under argon was added trimethyl phosphite (2.2 ml, 18.9 mmol). After the reaction was stirred for 15 h, the solvent was evaporated *in vacuo*, the residue was dissolved in ethyl acetate (150 ml). Brine (100 ml) was added and the mixture extracted with ethyl acetate (3x50 ml); the combined extracts were washed with water (2x100 ml), dried (MgSO₄) and evaporated *in vacuo*. The residue was purified by column chromatography on silica gel with ethyl acetate as the eluent to afford **141** as an unstable pale brown oil (1.48 g, 54%). ¹H NMR (CDCl₃): δ = 1.77 (m, 6H) 2.03 (s, 6H) 2.78 (m, 4H) 3.87 (m, 12H) 4.73 (d, J = 4.4 Hz, 2H).

Bis[2-(dimethoxyphosphinyl)-4-(hexathio)-1,3-dithiole] 142.

To a stirred solution of crude **140** (2.76 g, 4.72 mmol) and sodium iodide (1.28 g, 8.54 mmol) in dry acetonitrile (10 ml) at 20°C under argon was added trimethyl phosphite (1 ml, 8.48 mmol). Reaction and workup as described for **141** afforded **142** as a pale brown oil (681 mg, 53%). ¹H NMR (CDCl₃): δ = 1.42 (m, 4H) 1.64 (m, 4H) 2.02 (s, 6H) 2.71 (m, 4H) 3.88 (dd, J = 10.6 Hz, J = 2.6 Hz, 12H) 4.73 (d, J = 4.4 Hz, 2H).

9,10-Bis-(4-methyl-1,3-dithiol-2-ylidene)-9,10-dihydroanthracenocyclophane 143

Into a solution of **141** (1.33 g, 2.27 mmol) in dry tetrahydrofuran (100 ml) at -78°C, was added lithium diisopropylamide (3.0 ml of 1.5 M solution in cyclohexane, 4.50 mmol). The reaction was stirred for 3 h at -78°C to give a pale cloudy solution then, anthraquinone (0.473 g, 2.27 mmol) in dry tetrahydrofuran (100 ml) at -78°C was added. The mixture was then stirred for a further 1 h at -78°C and then allowed to slowly warm to 20°C over 6 h. The mixture was evaporated *in vacuo* and the residue was purified by column chromatography on silica gel with dichloromethane/hexane (1:2 v/v) as the eluent to afford **143** as a yellow solid (122 mg, 10%). Recrystallization was achieved by

dissolution in dichloromethane and addition of hexane. A single crystal was grown for X-ray crystallography from acetonitrile/dichloromethane. M.p. 270-273°C (dec > 160°C); (found: C, 59.8; H, 4.5; C₂₇H₂₄S₆ (540) requires C, 60.0 H, 4.5); *m/z* (EI) 540, 264, 220 [M⁺]; ¹H NMR (CDCl₃): δ = 0.85 (m, 4H) 1.12 (m, 4H) 1.97 (s, 6H) 2.17 (m, 4H) 2.61 (m, 4H) 7.30 (m, 6H) 7.36 (m, 2H). ¹³C NMR (CDCl₃): δ = ppm.

9,10-Bis-(4-methyl-1,3-dithiol-2-ylidene)-9,10-dihydroanthracenocyclophane 144.

Into a solution of **142** (681 mg, 1.14 mmol) in dry tetrahydrofuran (50 ml) at -78°C, was added lithium diisopropylamide (1.7 ml of 1.5 M solution in cyclohexane, 2.55 mmol). The reaction was stirred for 3 h at -78°C to give a pale cloudy solution then, anthraquinone (0.237 g, 1.14 mmol) in dry tetrahydrofuran (50 ml) at -78°C was added. Reaction and workup as described for **143** afforded **144** as a pale green/yellow solid (138mg, 22%). Recrystallisation, if required, may be achieved by dissolution in dichloromethane and addition of hexane. A single crystal was grown for X-ray crystallography from acetonitrile/dichloromethane. M.p. 286-288°C (dec.); (found: C, 60.33; H, 4.71; C₂₈H₂₆S₆ (554.9) requires C, 60.61 H, 4.72); *m/z* (EI) 554, 264, 220 [M⁺]; ¹H NMR (CDCl₃): δ = 1.11 (m, 4H) 1.32 (m, 4H) 2.10 (s, 6H) 2.23 (m, 2H) 2.68 (m, 2H) 7.35 (m, 6H) 7.49 (m, 2H). ¹³C NMR (CDCl₃): δ = 14.8, 29.0, 30.9, 35.2, 116.7, 125.7, 125.7, 126.0, 126.2, 126.3, 126.5, 132.1, 132.7, 134.3, 135.3, 148.8 ppm.

7.0 References

- [1] J. B. Torrance, *Acc. Chem. Res.* **1979**, *12*, 79.
- [2] M. R. Bryce and L. C. Murphy, *Nature (London)* **1984**, *309*, 119.
- [3] F. Wudl, G. M. Smith, E. J. Hufnagel, *J. Chem. Soc., Chem. Commun.* **1970**, 1453.
- [4] J. P. Ferraris, D. O. Cowan, V. Walatka, J. H. Perlstein, *J. Am. Chem. Soc.* **1973**, *95*, 948.
- [5] T. J. Kistenmacher, T. E. Philips, D. O. Cowan, *Acta Cryst.* **1974**, *B30*, 763.
- [6] J. S. Chappell, A. N. Bloch, W. A. Bryden, M. Maxfield, T. O. Poehler, D. O. Cowan, *J. Am. Chem. Soc.* **1981**, *103*, 2442.
- [7] Y. A. Jackson, C. L. White, M. V. Lakshmikantham, M. P. Cava, *Tetrahedron Lett.* **1987**, *28*, 5635.
- [8] M. D. Mays, R. D. McCullough, D. O. Cowan, T. O. Poehler, W. A. Bryden, T. J. Kistenmacher, *Solid State Commun.* **1988**, *65*, 1089.
- [9] J. P. Ferraris, T. O. Poehler, A. N. Bloch, D. O. Cowan, *Tetrahedron Lett.* **1973**, 2553.
- [10] K. Bechgaard, C. S. Jacobsen, K. Mortensen, H. J. Pedersen, N. Thorup, *Solid State Commun.* **1980**, *33*, 1119.
- [11] J. M. Williams, M. A. Beno, H. H. Wang, T. J. Emge, P. T. Copps, N. L. Hall, K. D. Carlson, G. W. Crabtree, *Philos. Trans. Of the Royal Society Of London* **1985**, *A1528*, *314*, 83.
- [12] Z. Yoshida, T. Kawase, H. Awaji, S. Yoneda, *Tetrahedron Lett.* **1982**, *24*, 3476.
- [13] T. T. Nguyen, Y. Gouriou, M. Salle, P. Frere, M. Jubault, A. Gorgues, L. Toupet, A. Riou, *Bull. Soc. Chim. Fr.* **1996**, *133*, 301.
- [14] G. Markl, A. Poll, G. Aschenbrenner, C. Schmaus, T. Troll, P. Kreitmeier, H. Noth, M. Schmidt, *Helv. Chim. Acta* **1996**, *79*, 1497.
- [15] A. Benahmed-Gasmi, P. Frere, B. Garrigues, A. Gorgues, M. Jubault, R. Carlier, F. Texier, *Tetrahedron Lett.* **1992**, *33*, 6457.
- [16] T. K. Hansen, M. V. Lakshmikantham, M. P. Cava, R. E. Niziurskimann, F. Jensen, J. Becher, *J. Am. Chem. Soc.* **1992**, *114*, 5035.

- [17] K. Takahashi, T. Nihira, M. Yoshifuji, K. Tomitani, *Bull. Chem. Soc. Jpn.* **1993**, *66*, 2330.
- [18] A. Benahmed-Gasmi, P. Frere, M. Jubault, A. Gorgues, J. Cousseau, B. Garrigues, *Synth. Met.* **1993**, *55*, 1751.
- [19] J. Roncali, L. Rasmussen, C. Thobie-Gautier, P. Frere, H. Brisset, M. Salle, J. Becher, O. Simonsen, T. K. Hansen, A. Benahmed-Gasmi, J. Orduna, J. Garin, M. Jubault, A. Gorgues, *Adv. Mater.* **1994**, *6*, 841.
- [20] J. Roncali, M. Griffard, P. Frere, M. Jubault, A. Gorgues, *J. Chem. Soc., Chem. Commun.* **1993**, 689.
- [21] K. Takahashi, I. Toshihiro, *Heterocycles* **1997**, *45*, 1051.
- [22] M. G. Miles, J. D. Wilson, M. H. Cohen, U.S. Patent 3,779,814, **1973**.
- [23] M. Sato, M. V. Lakshmikantham, M. P. Cava, A. F. Garito, *J. Org. Chem.* **1978**, *43*, 2085.
- [24] Y. Yamashita, Y. Kobayashi, T. Miyashi, *Angew. Chem. Int. Ed. Engl.* **1989**, *101*, 1090.
- [25] K. Akiba, K. Ishikawa, N. Inamoto, *Bull. Chem. Soc. Jpn.* **1978**, *51*, 2674.
- [26] M. R. Bryce, A. J. Moore, M. Hasan, G. J. Ashwell, A. T. Fraser, W. Clegg, M. B. Hursthouse, A. I. Karaulov, *Angew. Chem. Int. Ed. Engl.* **1990**, *29*, 1450.
- [27] M. R. Bryce, M. A. Coffin, M. B. Hursthouse, A. I. Karaulov, K. Müllen, H. Scheich, *Tetrahedron Lett.* **1991**, *32*, 6029.
- [28] N. Martín, L. Sánchez, C. Seoane, C. Fernandez, *Synth. Met.* **1996**, *78*, 137.
- [29] M. R. Bryce, A. J. Moore, D. Lorcy, A. S. Dhindsa, A. Robert, *J. Chem. Soc., Chem. Commun.* **1990**, 470.
- [30] M. R. Bryce, G. J. Marshallsay, *J. Org. Chem.* **1994**, *59*, 6847.
- [31] E. Cerrada, M. R. Bryce, A. J. Moore, *J. Chem. Soc., Perkin Trans. 1* **1993**, 537.
- [32] N. Martín, I. Pérez, L. Sánchez, C. Seoane, *J. Org. Chem.* **1997**, *62*, 870.
- [33] N. Martín, I. Pérez, L. Sánchez, C. Seoane, *J. Org. Chem.* **1997**, *62*, 5690.
- [34] M. R. Bryce, A. J. Moore, *Synth. Met.* **1988**, *27*, B557.
- [35] Y. Yamashita, Y. Kabayashi, T. Miyashi, *Angew. Chem. Int. Ed. Engl.* **1988**, *28*, 1052.
- [36] A. J. Moore, M. R. Bryce, *Synthesis* **1997**, 407.

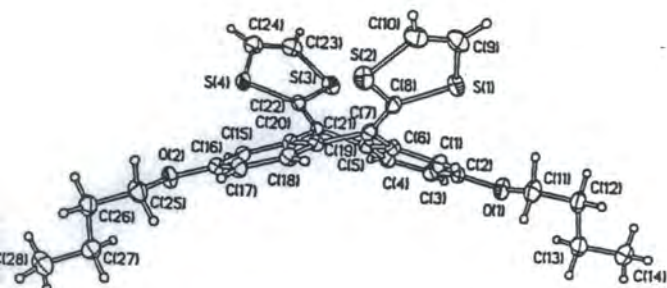
- [37] A. J. Moore, M. R. Bryce, *J. Chem. Soc., Perkin Trans. 1* **1991**, 157.
- [38] D. C. Green, *J. Org. Chem.* **1977**, *44*, 1476.
- [39] N. Martín, L. Sánchez, C. Seoane, E. Ortí, P. M. Viruela, R. Viruela, *J. Org. Chem.* **1998**, *66*, 1268.
- [40] N. Martín, L. Sánchez, C. Seoane, E. Ortí, P. M. Viruela, R. Viruela, *Eur. J. Org. Chem.* **1999**, 1239.
- [41] K. W. Stender, G. Klar, *Z. Naturforsch* **1985**, *40b*, 774.
- [42] O. Hammerich, V. D. Parker, *J. Am. Chem. Soc.* **1974**, *93*, 4289.
- [43] A. S. Batsanov, M. R. Bryce, M. A. Coffin, A. Green, R. E. Hester, J. A. K. Howard, I. K. Lednev, N. Martín, A. J. Moore, J. N. Moore, E. Ortí, L. Sánchez, M. Saviron, P. M. Viruela, R. Viruela, T. Q. Ye, *Chem. Eur. J.* **1998**, 2580.
- [44] S. Triki, L. Quahab, D. Lorcy, A. Robert, *Acta Cryst.* **1993**, *49*, 1189.
- [45] C. P. Brock, J. D. Dunitz, *Acta Cryst.* **1990**, *46*, 795.
- [46] R. P. Shibaeva, *Kristallografiya* **1984**, *29*, 480.
- [47] S. Flandrois, D. Chasseau, *Acta Cryst.* **1977**, Sect. B *33*, 2744.
- [48] R. Gompper, E. Kutter, *Chem. Ber.* **1965**, *98*, 2825.
- [49] A. J. Moore, M. R. Bryce, A. S. Batsanov, J. C. Cole, J. A. K. Howard, *Synthesis* **1995**, 675.
- [50] J. Garin, J. Orduna, S. Uriel, A. J. Moore, M. R. Bryce, S. Wegener, D. S. Yufit, J. A. K. Howard, *Synthesis* **1994**, 489.
- [51] S. Wawzonec, S. M. Heilmann, *J. Org. Chem.* **1974**, *39*, 511.
- [52] B. T. Fetkenhauser, H. Fetkenhauser, *Chem. Ber.* **1927**, *60B*, 2528.
- [53] H. Kolbe, *Justus Leibigs Ann. Chem.* **1868**, 140.
- [54] C. Wang, A. S. Batsanov, M. R. Bryce, J. A. K. Howard, *Synthesis* **1998**, 1615.
- [55] R. R. Schumaker, E. M. Engler, *J. Am. Chem. Soc.* **1977**, *99*, 5591.
- [56] T. K. Hansen, I. Hawkins, K. S. Varma, S. Edge, S. Larsen, J. Becher, A. E. Underhill, *J. Chem. Soc., Perkin Trans. II* **1991**, 1963.
- [57] C. Gemmell, J. D. Kilburn, H. Ueck, A. E. Underhill, *Tetrahedron Lett.* **1992**, *33*, 3923.
- [58] J. S. Zambounis, C. W. Mayer, *Tetrahedron Lett.* **1991**, *32*, 2737.
- [59] N. Svenstrup, K. M. Rasmussen, T. K. Hansen, J. Becher, *Synthesis* **1994**, 809.

- [60] T. K. Hansen, J. Becher, T. Jørgensen, K. S. Varma, R. Khedekar, M. P. Cava, *Org. Synth.* **1996**, *73*, 270.
- [61] J. Becher, J. Lau, P. Leriche, P. Mork, N. Svenstrup, *J. Chem. Soc., Chem. Commun.* **1994**, 2715.
- [62] K. B. Simonson, N. Svenstrup, J. Lau, O. Simonsen, P. Mork, G. Kristensen, J. Becher, *Synthesis* **1996**, 407.
- [63] N. Martín, L. Sánchez, C. Seoane, E. Ortí, P. M. Viruela, R. Viruela, *J. Org. Chem.* **1998**, *63*, 1268.
- [64] A. J. Moore, M. R. Bryce, A. S. Batsanov, J. N. Heaton, C. W. Lehmann, J. A. K. Howard, N. Robertson, A. E. Underhill, I. F. Perepichka, *J. Mater. Chem.* **1998**, *8*, 1541.
- [65] J. Rebek Jr., *Angew. Chem. Int. Ed. Engl.* **1990**, *29*, 245.
- [66] D. J. Cram, *Angew. Chem. Int. Ed. Engl.* **1988**, *27*, 1009.
- [67] J. M. Lehn, *Angew. Chem. Int. Ed. Engl.* **1988**, *27*, 89.
- [68] H. J. Schneider, T. Blatter, *Angew. Chem. Int. Ed. Engl.* **1988**, *27*, 1163.
- [69] C. J. Pedersen, *J. Am. Chem. Soc.* **1967**, *89*, 7017.
- [70] T. M. Swager, M. J. Marsella, *Adv. Mater.* **1994**, *6*, 595.
- [71] P. D. Beer, *Advances in Inorganic Chemistry, Academic Press, Inc.* **1992**, *39*, 79.
- [72] P. D. Beer, *Accts. Chem. Res.* **1998**, *31*, 71.
- [73] M. L. H. Green, W. B. Heuer, G. C. Daunders, *J. Chem. Soc., Dalton Trans.* **1990**, 3789.
- [74] F. Van Veggel, M. Bos, S. Harkema, H. van de Bovenkamp, H. Reedijk, D. Reinhoudt, *J. Org. Chem.* **1991**, *56*, 225.
- [75] T. Otsubo, F. Ogura, *Bull. Chem. Soc. Jpn.* **1985**, *58*, 1345.
- [76] B. Girmay, J. D. Kilburn, A. E. Underhill, K. S. Varma, M. B. Hursthouse, M. E. Harman, J. Becher, G. Bojesen, *J. Chem. Soc., Chem. Commun.* **1989**, 1406.
- [77] R. Dieing, V. Morrisson, A. Moore, L. M. Goldenberg, M. R. Bryce, M. Raoul, M. C. Petty, J. Garin, M. Savirón, I. K. Lednev, R. E. Hester, J. N. Moore, *J. Chem. Soc., Perkin Trans. 2* **1996**, 1587.
- [78] T. K. Hansen, T. Jørgensen, P. C. Stein, J. Becher, *J. Org. Chem.* **1992**, *57*, 6404.

- [79] Y. Misaki, H. Nishikawa, K. Kawakami, T. Uehara, T. Yamabe, *Tetrahedron Lett.* **1992**, 33, 4321.
- [80] E. Corey, F. Corey, R. Winters, *J. Am. Chem. Soc.* **1965**, 87, 934.
- [81] M. Narita, C. U. Pittman, *Synthesis* **1976**, 489.
- [82] A. Krief, *Tetrahedron* **1986**, 42, 1209.
- [83] G. Schukat, A. M. Richter, E. Fanghänel, *Sulfur Rep.* **1987**, 7, 155.
- [84] R. P. Parg, J. D. Kilburn, T. G. Ryan, *Synthesis* **1994**, 195.
- [85] S. Masson, *Main Group Chem. News* **1994**, 2, 18.
- [86] D. Lorcy, P. Hascoat, A. Robert, K. Boubekeur, P. Batail, R. Carlier, A. Tallec, *J. Chem. Soc., Chem. Commun.* **1995**, 1229.
- [87] A. Souzi, A. Robert, *Tetrahedron* **1984**, 40, 1817.
- [88] M. Jørgensen, K. A. Lerstrup, K. Bechgaard, *J. Org. Chem.* **1991**, 56, 5684.
- [89] R. S. Rowland, R. Taylor, *J. Phys. Chem.* **1996**, 100, 7384

Appendix
X-Ray Crystallographic Data

2,6-Dibutoxy-9,10-bis(1,3-dithiol-2-ylidene)-9,10-dihydroanthracene 44.



Crystal data and structure refinement

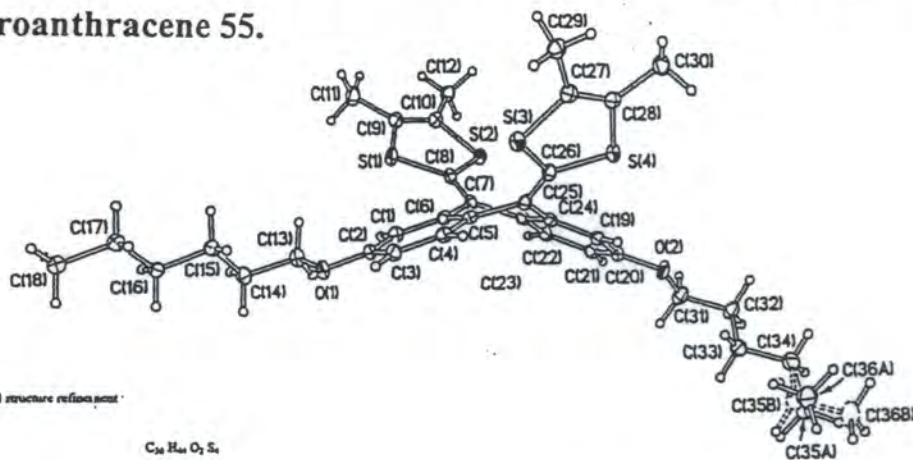
Empirical formula	C ₂₈ H ₃₈ O ₄ S ₄	
Formula weight	524.74	
Temperature	150(2) K	
Wavelength	1.54184 Å	
Crystal system	Monoclinic	
Space group	P2 ₁ /c (No. 14)	
Unit cell dimensions	a = 11.5057(12) Å	α = 90°
	b = 17.0266(13) Å	β = 103.283(7)°
	c = 13.2544(11) Å	γ = 90°
Volume	2527.1(4) Å ³	
Z	4	
Density (calculated)	1.379 g/cm ³	
Absorption coefficient	3.644 mm ⁻¹	
F(000)	1104	
Crystal size	0.40 × 0.30 × 0.15 mm ³	
θ range for data collection	3.93 to 75.00°	
Index ranges	-1 ≤ h ≤ 14, -1 ≤ k ≤ 21, -16 ≤ l ≤ 16	
Reflections collected	5801	
Independent reflections	4845 [R(int) = 0.0266]	
Reflections with I > 2σ(I)	4020	
Completeness to θ = 75.00°	93.0 %	
Absorption correction	ψ-scan	
Max. and min. transmission	1.0000 and 0.7577	
Refinement method	Full-matrix least-squares on F ²	
Data / restraints / parameters	4845 / 0 / 419	
Largest final shift/e.s.d. min	0.001	
Goodness-of-fit on F ²	1.057	
Final R indices [I > 2σ(I)]	R _w = 0.0433, wR ₂ = 0.1067	
R indices (all data)	R ₁ = 0.0545, wR ₂ = 0.1134	
Largest diff. peak and hole	0.443 and -0.355 e Å ⁻³	

Bond lengths (Å) and angles (°)

S(1)-C(9)	1.747(3)	C(12)-H(122)	1.04(3)
S(1)-C(8)	1.774(2)	C(13)-C(14)	1.512(4)
S(2)-C(10)	1.747(3)	C(13)-H(131)	1.06(3)
S(2)-C(9)	1.771(2)	C(13)-H(132)	1.01(3)
S(3)-C(23)	1.737(3)	C(14)-H(141)	0.96(4)
S(3)-C(22)	1.771(2)	C(14)-H(142)	0.94(3)
S(4)-C(24)	1.750(3)	C(14)-H(143)	1.00(3)
S(4)-C(25)	1.763(2)	C(15)-C(16)	1.396(3)
C(1)-C(2)	1.363(3)	C(15)-C(20)	1.396(3)
C(1)-C(11)	1.432(3)	C(15)-H(15)	0.97(3)
C(2)-C(16)	1.364(3)	C(16)-C(17)	1.391(3)
C(2)-C(25)	1.443(3)	C(17)-C(18)	1.377(3)
C(1)-C(2)	1.393(3)	C(17)-H(17)	0.90(3)
C(1)-C(6)	1.403(3)	C(18)-C(19)	1.395(3)
C(1)-H(1)	0.85(2)	C(18)-H(18)	0.91(3)
C(2)-C(3)	1.391(3)	C(19)-C(20)	1.421(3)
C(3)-C(4)	1.382(3)	C(20)-C(21)	1.470(3)
C(3)-H(3)	0.93(3)	C(21)-C(22)	1.367(3)
C(4)-C(5)	1.404(3)	C(22)-C(24)	1.322(4)
C(4)-H(4)	0.97(3)	C(23)-H(23)	0.94(3)
C(5)-C(6)	1.412(3)	C(24)-H(24)	0.91(4)
C(5)-C(21)	1.479(3)	C(25)-C(26)	1.511(4)
C(6)-C(7)	1.477(3)	C(25)-H(251)	1.07(4)

C(7)-C(8)	1.364(3)	C(25)-H(252)	1.03(3)
C(7)-C(19)	1.483(3)	C(26)-C(27)	1.518(3)
C(9)-C(10)	1.316(4)	C(26)-H(261)	0.99(3)
C(9)-H(9)	0.89(4)	C(26)-H(262)	1.06(4)
C(10)-H(10)	0.96(4)	C(27)-C(28)	1.514(4)
C(11)-C(12)	1.516(4)	C(27)-H(271)	1.01(3)
C(11)-H(111)	1.03(3)	C(27)-H(272)	1.04(4)
C(11)-H(112)	1.08(3)	C(28)-H(281)	1.04(3)
C(12)-C(13)	1.531(4)	C(28)-H(282)	1.01(4)
C(12)-H(121)	1.02(3)	C(28)-H(283)	0.96(3)
C(9)-S(1)-C(8)	96.26(12)	C(1)-C(11)-C(12)	107.3(2)
C(10)-S(1)-C(8)	96.32(12)	C(1)-C(11)-H(111)	110.1(16)
C(23)-S(3)-C(22)	96.46(12)	C(12)-C(11)-H(111)	110.3(16)
C(24)-S(4)-C(22)	96.19(12)	C(1)-C(11)-H(112)	110.6(17)
C(2)-C(1)-C(11)	117.70(19)	C(12)-C(11)-H(112)	108.1(17)
C(16)-C(2)-C(25)	117.69(19)	H(11)-C(11)-H(112)	110(2)
C(2)-C(1)-C(6)	120.7(2)	C(11)-C(12)-C(13)	114.0(2)
C(2)-C(1)-H(1)	119.5(16)	C(11)-C(12)-H(121)	107.2(16)
C(6)-C(1)-H(1)	119.8(16)	C(13)-C(12)-H(121)	107.1(16)
C(1)-C(2)-C(3)	114.8(2)	C(11)-C(12)-H(122)	108.0(19)
C(1)-C(2)-C(1)	125.2(2)	C(13)-C(12)-H(122)	109.4(19)
C(3)-C(2)-C(1)	120.0(2)	H(121)-C(12)-H(122)	111(2)
C(4)-C(3)-C(2)	119.6(2)	C(14)-C(13)-C(12)	112.2(2)
C(4)-C(3)-H(3)	122.2(16)	C(14)-C(13)-H(131)	108.5(16)
C(2)-C(3)-H(3)	118.2(16)	C(12)-C(13)-H(131)	109.8(16)
C(3)-C(4)-C(5)	121.8(2)	C(14)-C(13)-H(132)	110(2)
C(3)-C(4)-H(4)	118.4(15)	C(12)-C(13)-H(132)	105(2)
C(5)-C(4)-H(4)	119.8(15)	H(131)-C(13)-H(132)	111(3)
C(4)-C(5)-C(6)	118.4(2)	C(13)-C(14)-H(141)	113(2)
C(4)-C(5)-C(21)	122.92(19)	C(13)-C(14)-H(142)	109(2)
C(6)-C(5)-C(21)	118.71(19)	H(141)-C(14)-H(142)	110(3)
C(1)-C(6)-C(5)	119.4(2)	C(13)-C(14)-H(143)	109.5(18)
C(1)-C(6)-C(7)	122.5(2)	H(141)-C(14)-H(143)	105(3)
C(5)-C(6)-C(7)	118.11(19)	H(142)-C(14)-H(143)	109(3)
C(8)-C(7)-C(6)	122.8(2)	C(16)-C(15)-C(20)	121.4(2)
C(8)-C(7)-C(19)	114.19(19)	C(16)-C(15)-H(15)	118.7(15)
C(7)-C(8)-S(2)	123.83(18)	C(20)-C(15)-H(15)	119.7(15)
C(7)-C(8)-S(1)	124.18(18)	C(2)-C(16)-C(17)	124.6(2)
S(2)-C(8)-S(1)	111.82(12)	C(2)-C(16)-C(15)	115.6(2)
C(10)-C(9)-S(1)	117.6(2)	C(17)-C(16)-C(15)	119.8(2)
C(10)-C(9)-H(9)	126(2)	C(18)-C(17)-C(16)	119.1(2)
S(1)-C(9)-H(9)	116(2)	C(18)-C(17)-H(17)	121.6(16)
C(9)-C(10)-S(2)	117.6(2)	C(16)-C(17)-H(17)	119.2(16)
C(9)-C(10)-H(10)	125(2)	C(17)-C(18)-C(19)	122.5(2)
S(2)-C(10)-H(10)	118(2)	C(17)-C(18)-H(18)	115.9(16)
C(18)-C(19)-C(20)	118.3(2)	C(19)-C(18)-H(18)	121.5(16)
C(18)-C(19)-C(7)	123.2(2)	C(2)-C(25)-H(252)	109.1(15)
C(20)-C(19)-C(7)	118.46(19)	C(26)-C(25)-H(252)	112.2(15)
C(15)-C(20)-C(19)	119.0(2)	H(251)-C(25)-H(252)	105(3)
C(15)-C(20)-C(21)	122.93(19)	C(25)-C(26)-C(27)	112.9(2)
C(19)-C(20)-C(21)	118.10(19)	C(25)-C(26)-H(261)	110.4(18)
C(22)-C(21)-C(20)	123.0(2)	C(27)-C(26)-H(261)	108.6(19)
C(22)-C(21)-C(5)	122.5(2)	C(25)-C(26)-H(262)	105.2(19)
C(20)-C(21)-C(5)	114.42(18)	C(27)-C(26)-H(262)	109.8(19)
C(21)-C(22)-S(4)	125.22(17)	H(261)-C(26)-H(262)	110(3)
C(21)-C(22)-S(3)	122.94(17)	C(28)-C(27)-C(26)	112.2(2)
S(4)-C(22)-S(3)	111.74(12)	C(28)-C(27)-H(271)	108.3(18)
C(24)-C(23)-S(3)	117.43(19)	C(28)-C(27)-H(272)	109(2)
C(24)-C(23)-H(23)	126(2)	C(26)-C(27)-H(272)	104(2)
S(3)-C(23)-H(23)	116(2)	H(271)-C(27)-H(272)	113(3)
C(23)-C(24)-S(4)	117.30(19)	C(27)-C(28)-H(281)	111.1(18)
C(23)-C(24)-H(24)	127(2)	C(27)-C(28)-H(282)	111(2)
S(4)-C(24)-H(24)	115(2)	H(281)-C(28)-H(283)	111(3)
C(2)-C(25)-C(26)	107.9(2)	C(27)-C(28)-H(283)	111(2)
C(2)-C(25)-H(251)	109(2)	H(281)-C(28)-H(283)	110(3)
C(26)-C(25)-H(251)	113(2)	H(282)-C(28)-H(283)	102(3)

2,6-Dihexoxy-9,10-bis(1,3-dithiol-2-ylidene-4,5-dimethyl)-9,10-dihydroanthracene 55.



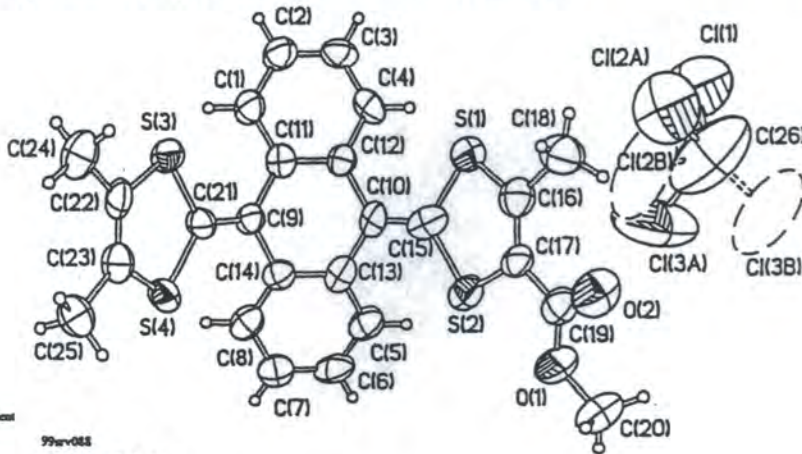
Crystal data and structure refinement

Identification code				C(5)-C(15)	1.443(3)	C(21)-C(31)	1.528(3)	
Empirical formula	C ₃₈ H ₄₄ O ₆ S ₄			C(6)-C(7)	1.483(3)	C(33)-C(34)	1.513(3)	
Formula weight	634.95			C(7)-C(8)	1.364(3)	C(34)-C(35A)	1.507(3)	
Temperature	120(2) K			C(7)-C(23)	1.487(3)	C(34)-C(35B)	1.620(4)	
Wavelength	0.71073 Å			C(9)-C(10)	1.350(3)	C(35A)-C(36A)	1.513(7)	
Crystal system	Triclinic			C(9)-C(11)	1.503(3)	C(35B)-C(36B)	1.515(6)	
Space group	P $\bar{1}$ (No. 2)			C(9)-S(1)-C(8)	97.32(10)	C(1)-C(2)-C(3)	119.63(19)	
Unit cell dimensions	<i>a</i> = 10.414(1) Å	<i>b</i> = 11.447(1) Å	<i>c</i> = 15.159(5) Å	α = 92.09(1)°	β = 103.87(1)°	γ = 112.43(1)°	C(4)-C(5)-C(2)	119.7(2)
Volume	1605.1(6) Å ³			C(10)-S(2)-C(8)	97.18(10)	C(4)-C(5)-C(6)	121.79(19)	
Z	2			C(26)-S(3)-C(27)	96.95(10)	C(3)-C(4)-C(5)	122.82(18)	
Density (calculated)	1.318 g/cm ³			C(28)-S(4)-C(26)	97.06(10)	C(4)-C(5)-C(25)	117.91(18)	
Absorption coefficient	0.328 mm ⁻¹			C(23)-C(1)-C(13)	116.41(16)	C(1)-C(6)-C(5)	119.55(19)	
F(000)	680			C(20)-C(2)-C(31)	118.56(16)	C(1)-C(6)-C(7)	122.20(18)	
Crystal size	0.30 × 0.15 × 0.07 mm ³			C(2)-C(1)-C(6)	121.21(19)	C(3)-C(6)-C(7)	118.19(18)	
θ range for data collection	1.9 to 27.5°			C(8)-C(7)-C(23)	124.00(18)	C(24)-C(23)-C(7)	118.14(18)	
Index ranges	-13 ≤ <i>h</i> ≤ 13, -14 ≤ <i>k</i> ≤ 14, -19 ≤ <i>l</i> ≤ 18			C(6)-C(7)-C(23)	113.48(17)	C(19)-C(24)-C(25)	117.58(17)	
Reflections collected	12690			C(7)-C(8)-S(2)	124.20(15)	C(25)-C(26)-S(3)	124.34(16)	
Independent reflections	7261 [R(int) = 0.0416]			C(7)-C(8)-S(1)	124.21(16)	C(25)-C(26)-S(4)	124.20(16)	
Reflections with I > 2 σ (I)	5008			S(2)-C(8)-S(1)	111.50(11)	S(3)-C(26)-S(4)	111.33(13)	
Completeness to $\theta = 27.5^\circ$	98.3 %			C(10)-C(9)-C(11)	128.16(19)	C(26)-C(25)-C(3)	122.39(18)	
Absorption correction	Integration			C(10)-C(9)-S(1)	116.84(16)	C(6)-C(25)-C(3)	123.90(18)	
Max. and min. transmission	0.9787 and 0.9172			C(11)-C(9)-S(1)	114.97(15)	C(24)-C(25)-C(5)	113.67(17)	
Refinement method	Full-matrix least-squares on F ²			C(9)-C(10)-C(12)	127.61(19)	C(25)-C(27)-C(20)	127.6(2)	
Data / restraints / parameters	7261 / 0 / 498			C(9)-C(10)-S(2)	116.84(16)	C(28)-C(27)-S(3)	116.51(17)	
Largest shift/e.s.d. ratio	0.003			C(12)-C(10)-S(2)	115.53(13)	C(29)-C(27)-S(3)	115.87(16)	
Goodness-of-fit on F ²	1.001			O(1)-C(13)-C(14)	108.22(17)	C(27)-C(28)-C(30)	128.0(2)	
Final R indices [I > 2 σ (I)]	R ₁ = 0.0420, wR ₂ = 0.0859			C(14)-C(15)-C(16)	111.87(19)	C(27)-C(28)-S(4)	116.82(17)	
R indices (all data)	R ₁ = 0.0771, wR ₂ = 0.0968			C(17)-C(16)-C(15)	115.24(19)	C(30)-C(28)-S(4)	115.19(15)	
Largest diff. peak and hole	0.345 and -0.308 e.Å ⁻³			C(16)-C(17)-C(18)	112.09(19)	C(2)-C(31)-C(32)	106.89(19)	
Comment: C(35) and C(36) with their hydrogens are disordered over 2 positions, A and B, with equal occupancies.				C(34)-C(19)-C(20)	121.35(19)	C(31)-C(32)-C(33)	114.0(2)	
				O(2)-C(20)-C(21)	125.11(19)	C(34)-C(33)-C(32)	113.2(2)	
				O(2)-C(20)-C(19)	115.15(18)	C(35A)-C(34)-C(33)	120.1(3)	
				C(21)-C(20)-C(19)	119.74(19)	C(35A)-C(34)-C(35B)	23.8(2)	
				C(20)-C(21)-C(22)	119.2(2)	C(33)-C(34)-C(35B)	107.5(3)	
				C(21)-C(22)-C(23)	122.4(2)	C(34)-C(35A)-C(36A)	106.8(4)	
				C(22)-C(23)-C(24)	117.98(18)	C(36B)-C(35B)-C(34)	111.0(4)	
				C(23)-C(23)-C(7)	123.80(18)			

Bond lengths [Å] and angles [°]

S(1)-C(9)	1.766(2)	C(10)-C(12)	1.508(3)
S(1)-C(8)	1.770(2)	C(13)-C(14)	1.520(3)
S(2)-C(10)	1.769(2)	C(14)-C(15)	1.520(3)
S(2)-C(8)	1.769(2)	C(15)-C(16)	1.531(3)
S(3)-C(26)	1.767(2)	C(16)-C(17)	1.519(3)
S(3)-C(27)	1.770(2)	C(17)-C(18)	1.532(3)
S(4)-C(28)	1.761(2)	C(19)-C(24)	1.394(3)
S(4)-C(26)	1.770(2)	C(19)-C(20)	1.395(3)
O(1)-C(2)	1.376(2)	C(20)-C(21)	1.391(3)
O(1)-C(13)	1.446(2)	C(21)-C(22)	1.392(3)
O(2)-C(20)	1.372(2)	C(22)-C(23)	1.395(3)
O(2)-C(31)	1.438(3)	C(23)-C(24)	1.425(3)
C(1)-C(2)	1.392(3)	C(24)-C(25)	1.480(3)
C(1)-C(6)	1.396(3)	C(26)-C(25)	1.365(3)
C(2)-C(3)	1.393(3)	C(27)-C(28)	1.335(3)
C(3)-C(4)	1.388(3)	C(27)-C(29)	1.503(3)
C(4)-C(5)	1.404(3)	C(28)-C(30)	1.507(3)
C(5)-C(6)	1.417(3)	C(31)-C(32)	1.517(3)

9-(4-Methoxycarbonyl-5-methyl-1,3-dithiol-2-ylidene)-10-(4,5-dimethyl-1,3-dithiol-2-ylidene)-9,10-dihydroanthracene 81.



Crystal data and structure refinement

Identification code	99wv088
Empirical formula	C ₂₆ H ₂₀ O ₄ S ₄
Formula weight	401.02
Temperature	293 K
Wavelength	0.71073 Å
Crystal system	Triclinic
Space group	P-1
Unit cell dimensions	a = 9.656(1) Å b = 11.290(1) Å c = 13.238(1) Å
Volume	1368.1(2) Å ³
Z	2
Density (calculated)	1.459 g/cm ³
Absorption coefficient	0.664 mm ⁻¹
F(000)	616
Crystal size	0.48 × 0.26 × 0.02 mm ³
Theta range for data collection	1.61 to 25.00°
Index ranges	-11 ≤ h ≤ 11, -13 ≤ k ≤ 13, -15 ≤ l ≤ 13
Reflections collected	8191
Independent reflections	4809 [R(int) = 0.1656]
Observed reflections, D>2σ(I)	1835
Completeness to theta = 25.00°	99.6 %
Absorption correction	None
Max. and min. transmission	0.9827 and 0.7571
Refinement method	Full-matrix least-squares on F ²
Data / restraints / parameters	4809 / 0 / 339
Goodness-of-fit on F ²	0.997
Final R indices [I>2σ(I)]	R1 = 0.1018, wR2 = 0.2436
R indices (all data)	R1 = 0.2053, wR2 = 0.3471
Largest final shift/e.s.d. ratio	0.05
Largest diff. peak and hole	0.854 and -0.586 e.Å ⁻³

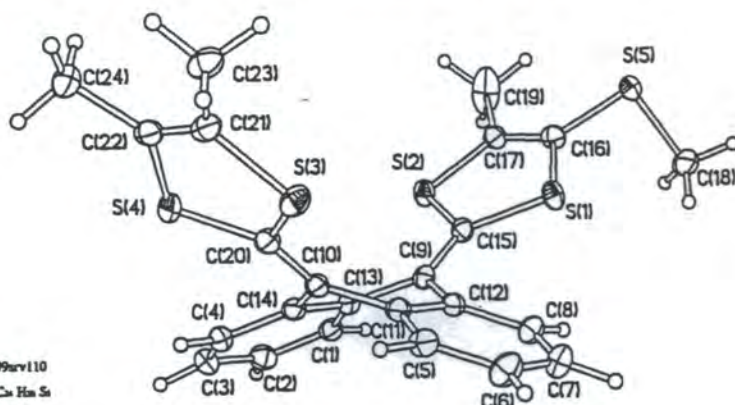
α = 94.37(1)°
β = 106.21(1)°
γ = 96.56(1)°

C(17)-S(1)-C(15)	95.4(5)	C(21)-C(9)-C(11)	124.2(8)
C(17)-S(2)-C(15)	95.8(5)	C(21)-C(9)-C(14)	122.8(8)
C(22)-S(3)-C(21)	97.1(5)	C(11)-C(9)-C(14)	113.0(7)
C(23)-S(4)-C(21)	96.7(5)	C(15)-C(10)-C(13)	123.7(8)
C(19)-C(1)-C(20)	116.2(8)	C(15)-C(10)-C(12)	123.1(9)
C(11)-C(1)-C(2)	120.1(9)	C(13)-C(10)-C(12)	113.2(8)
C(3)-C(2)-C(1)	120.4(10)	C(12)-C(11)-C(1)	119.5(9)
C(2)-C(2)-C(4)	119.3(9)	C(12)-C(11)-C(9)	118.5(8)
C(3)-C(4)-C(12)	121.6(9)	C(1)-C(11)-C(9)	121.9(8)
C(6)-C(5)-C(13)	120.8(10)	C(11)-C(12)-C(4)	119.0(9)
C(7)-C(6)-C(5)	121.7(9)	C(11)-C(12)-C(10)	117.7(8)
C(6)-C(7)-C(8)	118.5(9)	C(4)-C(12)-C(10)	123.3(8)
C(14)-C(8)-C(7)	120.2(10)	C(5)-C(13)-C(14)	118.8(9)
C(5)-C(13)-C(10)	123.6(9)	C(1)-C(13)-C(17)	108.7(9)
C(14)-C(13)-C(10)	117.6(8)	C(9)-C(21)-S(3)	123.8(7)
C(8)-C(14)-C(13)	120.0(9)	C(9)-C(21)-S(4)	124.8(7)
C(8)-C(14)-C(9)	122.3(8)	S(3)-C(21)-S(4)	111.0(4)
C(13)-C(14)-C(9)	117.6(8)	C(23)-C(22)-C(24)	128.2(9)
C(10)-C(15)-S(2)	124.4(8)	C(23)-C(22)-S(3)	116.9(7)
C(10)-C(15)-S(1)	123.6(7)	C(24)-C(22)-S(3)	114.9(8)
S(2)-C(15)-S(1)	111.7(6)	C(22)-C(23)-C(25)	128.2(9)
C(17)-C(16)-C(18)	127.2(11)	C(22)-C(23)-S(4)	117.5(7)
C(17)-C(16)-S(1)	117.6(8)	C(25)-C(23)-S(4)	114.3(8)
C(18)-C(16)-S(1)	115.0(8)	C(3B)-C(26)-C(28)	120.9(17)
C(16)-C(17)-C(19)	124.0(9)	C(3A)-C(26)-C(28)	107.8(14)
C(16)-C(17)-S(2)	117.2(8)	C(3B)-C(26)-C(1)	116.4(13)
C(19)-C(17)-S(2)	118.8(8)	C(2B)-C(26)-C(1)	119.8(13)
C(2)-C(19)-C(1)	124.4(10)	C(3A)-C(26)-C(1)	102.2(12)
C(2)-C(19)-C(17)	127.0(11)	C(2A)-C(26)-C(1)	101.4(10)

Bond lengths [Å] and angles [°]

S(1)-C(16)	1.743(11)	C(8)-C(14)	1.389(12)
S(1)-C(15)	1.785(11)	C(9)-C(21)	1.353(11)
S(2)-C(17)	1.756(10)	C(9)-C(11)	1.482(12)
S(2)-C(15)	1.757(10)	C(9)-C(14)	1.497(12)
S(3)-C(22)	1.748(10)	C(10)-C(15)	1.344(13)
S(3)-C(21)	1.766(9)	C(10)-C(13)	1.482(13)
S(4)-C(23)	1.750(9)	C(10)-C(12)	1.500(13)
S(4)-C(21)	1.768(9)	C(11)-C(12)	1.383(12)
O(1)-C(19)	1.365(12)	C(13)-C(14)	1.407(12)
O(1)-C(20)	1.442(12)	C(16)-C(17)	1.319(13)
O(2)-C(19)	1.303(12)	C(16)-C(18)	1.539(14)
C(1)-C(11)	1.399(13)	C(17)-C(19)	1.478(13)
C(1)-C(2)	1.412(13)	C(22)-C(23)	1.315(13)
C(2)-C(2)	1.365(13)	C(22)-C(24)	1.522(13)
C(3)-C(4)	1.382(13)	C(23)-C(25)	1.533(13)
C(4)-C(12)	1.410(12)	C(1)-C(26)	1.82(2)
C(5)-C(6)	1.379(14)	C(2A)-C(26)	1.81(2)
C(5)-C(13)	1.394(12)	C(3A)-C(26)	1.68(3)
C(6)-C(7)	1.366(14)	C(2B)-C(26)	1.66(3)
C(7)-C(8)	1.427(13)	C(3B)-C(26)	1.52(2)

9-(4-Methylsulfanyl-5-methyl-1,3-dithiol-2-ylidene)-10-(4,5-dimethyl-1,3-dithiol-2-ylidene)-9,10-dihydroanthracene 84.



Crystal data and structure refinement

Identification code	99arv110
Empirical formula	C ₂₄ H ₂₆ S ₅
Formula weight	468.70
Temperature	120(2) K
Wavelength	0.71073 Å
Crystal system	Triclinic
Space group	$P\bar{1}$ (No. 2)
Unit cell dimensions	$a = 9.077(1)$ Å $\alpha = 84.79(1)^\circ$ $b = 10.287(1)$ Å $\beta = 87.52(1)^\circ$ $c = 12.014(1)$ Å $\gamma = 76.02(1)^\circ$
Volume	1084.0(2) Å ³
Z	2
Density (calculated)	1.436 g/cm ³
Absorption coefficient	0.544 mm ⁻¹
F(000)	488
Crystal size	0.30 × 0.10 × 0.08 mm ³
θ range for data collection	1.7 to 27.5°
Index ranges	-11 ≤ h ≤ 10, -13 ≤ k ≤ 11, -11 ≤ l ≤ 15
Reflections collected	7879
Independent reflections	4910 [R(int) = 0.0281]
Reflections with I > 2σ(I)	3887
Completeness to $\theta = 27.5^\circ$	98.4 %
Absorption correction	Integration
Max. and min. transmission	0.9663 and 0.8850
Refinement method	Full-matrix least-squares on F ²
Data / restraints / parameters	4910 / 0 / 306
Largest final shift/e.s.d. ratio	0.001
Goodness-of-fit on F ²	1.027
Final R indices [I > 2σ(I)]	R _w = 0.0420, wR ₂ = 0.0931
R indices (all data)	R ₁ = 0.0610, wR ₂ = 0.1008
Largest diff. peak and hole	0.421 and -0.206 e Å ⁻³

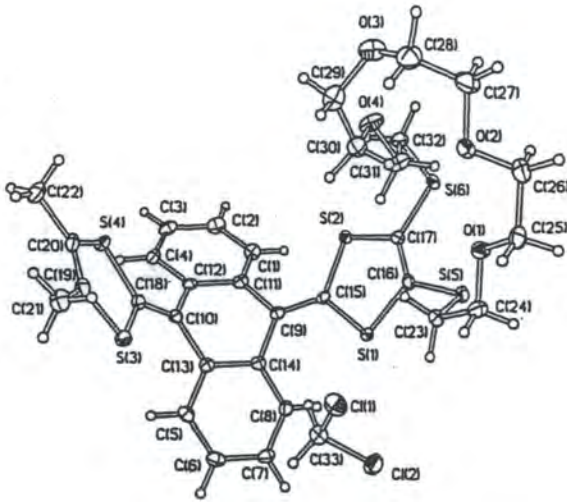
C(15)-S(1)-C(16)	96.69(11)	C(20)-C(10)-C(14)	123.0(2)
C(17)-S(2)-C(15)	97.25(11)	C(11)-C(10)-C(14)	113.56(19)
C(21)-S(3)-C(20)	96.85(12)	C(5)-C(11)-C(12)	118.5(2)
C(20)-S(4)-C(22)	97.17(12)	C(5)-C(11)-C(10)	123.2(2)
C(2)-C(1)-C(13)	121.2(2)	C(12)-C(11)-C(10)	117.9(2)
C(1)-C(2)-C(3)	119.9(2)	C(8)-C(12)-C(11)	119.0(2)
C(2)-C(3)-C(4)	119.8(2)	C(8)-C(12)-C(9)	123.5(2)
C(3)-C(4)-C(14)	121.1(2)	C(11)-C(12)-C(9)	117.4(2)
C(6)-C(5)-C(11)	121.2(2)	C(11)-C(12)-C(14)	119.3(2)
C(5)-C(6)-C(7)	119.8(2)	C(1)-C(13)-C(9)	123.1(2)
C(8)-C(7)-C(6)	119.9(2)	C(14)-C(13)-C(9)	117.5(2)
C(7)-C(8)-C(12)	121.2(2)	C(4)-C(14)-C(13)	118.7(2)
C(15)-C(9)-C(12)	123.6(2)	C(4)-C(14)-C(10)	123.5(2)
C(15)-C(9)-C(13)	122.6(2)	C(13)-C(14)-C(10)	117.7(2)
C(12)-C(9)-C(13)	113.81(19)	C(9)-C(15)-S(1)	124.68(18)
C(20)-C(10)-C(11)	123.4(2)	C(9)-C(15)-S(2)	123.05(18)
S(1)-C(15)-S(2)	112.09(12)	S(4)-C(20)-S(3)	111.64(12)
C(17)-C(16)-S(2)	124.79(18)	C(22)-C(21)-C(23)	127.7(2)
S(5)-C(16)-S(1)	117.80(14)	C(22)-C(21)-S(3)	116.80(19)
C(16)-C(17)-C(19)	125.0(2)	C(23)-C(21)-S(3)	115.46(19)
C(16)-C(17)-S(2)	116.55(18)	S(5)-C(21)-S(3)	134.3(8)
C(19)-C(17)-S(2)	118.41(16)	C(21)-C(22)-C(24)	128.0(2)
C(16)-S(5)-C(18)	100.03(13)	C(21)-C(22)-S(4)	116.66(19)
C(10)-C(20)-S(4)	123.53(18)	C(24)-C(22)-S(4)	115.33(19)
C(10)-C(20)-S(3)	124.73(19)		

Disorder: S(5) and C(19) refined as a single atom (80% S, 20% C), S(3) and C(19) refined as a single atom (15% S, 85% C), C(18) and C(18') with the occupancies of 80 and 15% respectively; C(23) and S(3') is separate positions with occupancies of 95 and 5%. All above mentioned (methyl) carbons have 'riding' H atoms with the same occupancies.

Bond lengths [Å] and angles [°]

S(1)-C(15)	1.763(2)	C(8)-C(12)	1.401(2)
S(1)-C(16)	1.769(2)	C(9)-C(13)	1.345(2)
S(2)-C(17)	1.755(2)	C(9)-C(12)	1.483(2)
S(2)-C(15)	1.777(2)	C(9)-C(13)	1.486(2)
S(3)-C(21)	1.768(2)	C(10)-C(20)	1.366(2)
S(3)-C(20)	1.769(2)	C(10)-C(11)	1.480(2)
S(4)-C(20)	1.763(2)	C(10)-C(14)	1.484(2)
S(4)-C(22)	1.765(2)	C(11)-C(12)	1.420(2)
C(1)-C(2)	1.388(3)	C(13)-C(14)	1.420(2)
C(1)-C(13)	1.394(3)	C(16)-C(17)	1.338(2)
C(2)-C(3)	1.392(3)	C(16)-S(5)	1.747(2)
C(3)-C(4)	1.393(4)	C(17)-C(19)	1.381(2)
C(4)-C(14)	1.401(3)	S(5)-C(18)	1.818(2)
C(5)-C(6)	1.392(4)	C(21)-C(22)	1.333(4)
C(5)-C(11)	1.401(3)	C(21)-C(23)	1.514(2)
C(6)-C(7)	1.393(4)	C(21)-S(3')	1.73(2)
C(7)-C(8)	1.387(2)	C(22)-C(24)	1.510(2)

Mono-crown 115.



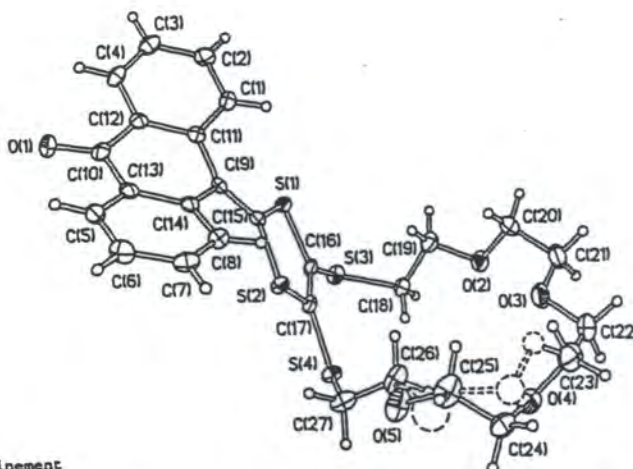
Crystal data and structure refinement

Identification code	99cr032
Empirical formula	C ₂₃ H ₂₄ O ₄ S
Formula weight	396.54
Temperature	120(2) K
Wavelength	0.71073 Å
Crystal system	Triclinic
Space group	P-1
Unit cell dimensions	a = 11.891(1) Å alpha = 104.928(4) deg. b = 12.548(1) Å beta = 97.021(5) deg. c = 12.691(1) Å gamma = 106.602(4) deg.
Volume	1713.5(2) Å ³
Z	2
Density (calculated)	1.473 g/cm ³
Absorption coefficient	0.593 mm ⁻¹
F(000)	792
Crystal size	0.46 x 0.20 x 0.15 mm
Theta range for data collection	1.70 to 27.48 deg.
Index ranges	-15 ≤ h ≤ 16, -11 ≤ k ≤ 16, -11 ≤ l ≤ 15
Reflections collected	9437
Independent reflections	7137 [R _{int} = 0.0251]
Observed reflections, I ≥ 3σ(I)	4209
Absorption correction	Empirical
Max. and min. transmission	0.9340 and 0.8714
Refinement method	Full-matrix least-squares on F ²
Data / restraints / parameters	7090 / 0 / 351
Goodness-of-fit on F ²	1.176
Final R indices [I ≥ 3σ(I)]	R ₁ = 0.0370, wR ₂ = 0.0717
R indices (all data)	R ₁ = 0.0476, wR ₂ = 0.0869
Extinction coefficient	0.0623(1)
Largest shift/e.s.d. ratio	0.001
Largest diff. peak and hole	0.128 and -0.293 e.Å ⁻³

Bond lengths [Å] and angles [deg]

S(1)-C(18)	1.764(2)	S(1)-C(15)	1.776(2)
S(2)-C(17)	1.760(2)	S(2)-C(18)	1.776(2)
S(3)-C(18)	1.767(2)	S(3)-C(18)	1.767(2)
S(4)-C(20)	1.761(2)	S(4)-C(16)	1.767(2)
S(5)-C(16)	1.753(2)	S(5)-C(23)	1.836(2)
S(6)-C(17)	1.750(2)	S(6)-C(23)	1.828(2)
O(1)-C(24)	1.422(3)	O(1)-C(25)	1.425(3)
O(2)-C(27)	1.425(3)	O(2)-C(26)	1.424(3)
O(3)-C(19)	1.425(3)	O(3)-C(28)	1.427(3)
O(4)-C(21)	1.423(3)	O(4)-C(20)	1.427(3)
C(1)-C(2)	1.397(3)	C(1)-C(3)	1.400(3)
C(2)-C(3)	0.95(3)	C(2)-C(1)	1.392(3)
C(3)-C(4)	0.94(3)	C(3)-C(5)	0.93(3)
C(4)-C(5)	0.96(3)	C(4)-C(6)	0.95(3)
C(5)-C(6)	1.402(3)	C(5)-C(7)	0.96(3)
C(6)-C(7)	1.397(3)	C(6)-C(8)	0.96(3)
C(7)-C(8)	1.406(3)	C(7)-C(9)	0.96(3)
C(8)-C(9)	1.360(3)	C(8)-C(10)	1.346(3)
C(9)-C(10)	1.482(3)	C(9)-C(11)	1.484(3)
C(10)-C(11)	1.480(3)	C(10)-C(12)	1.439(3)
C(11)-C(12)	1.420(3)	C(11)-C(13)	1.339(3)
C(12)-C(13)	1.346(3)	C(12)-C(14)	1.301(3)
C(13)-C(14)	1.300(3)	C(13)-C(15)	1.481(3)
C(14)-C(15)	0.94(3)	C(14)-C(16)	0.92(3)
C(15)-C(16)	0.93(3)	C(15)-C(17)	0.95(4)
C(16)-C(17)	1.517(3)	C(16)-C(18)	0.96(3)
C(17)-C(18)	0.94(3)	C(17)-C(19)	1.03(3)
C(18)-C(19)	0.97(3)	C(18)-C(20)	1.302(4)
C(19)-C(20)	0.96(3)	C(19)-C(21)	1.03(3)
C(20)-C(21)	1.06(3)	C(20)-C(22)	1.03(3)
C(21)-C(22)	1.515(4)	C(21)-C(23)	0.99(3)
C(22)-C(23)	0.96(3)	C(22)-C(24)	0.99(3)
C(23)-C(24)	1.360(3)	C(23)-C(25)	1.309(4)
C(24)-C(25)	0.98(3)	C(24)-C(26)	0.97(3)
C(25)-C(26)	0.96(3)	C(25)-C(27)	0.96(3)
C(26)-C(27)	1.311(4)	C(26)-C(28)	1.00(4)
C(27)-C(28)	1.02(3)	C(27)-C(29)	0.93(3)
C(28)-C(29)	0.94(3)	C(28)-C(30)	1.773(3)
C(29)-C(30)	1.379(3)	C(29)-C(31)	0.95(3)
C(30)-C(31)	0.96(3)	C(30)-C(32)	0.95(3)
C(31)-C(32)	0.95(4)	C(31)-C(33)	0.95(4)
C(32)-C(33)	1.517(3)	C(32)-C(34)	1.03(3)
C(33)-C(34)	0.96(3)	C(33)-C(35)	1.302(4)
C(34)-C(35)	0.94(3)	C(34)-C(36)	1.03(3)
C(35)-C(36)	1.06(3)	C(35)-C(37)	1.03(3)
C(36)-C(37)	1.360(3)	C(36)-C(38)	1.00(4)
C(37)-C(38)	0.98(3)	C(37)-C(39)	0.93(3)
C(38)-C(39)	0.96(3)	C(38)-C(40)	1.773(3)
C(39)-C(40)	1.379(3)	C(39)-C(41)	0.95(3)
C(40)-C(41)	0.96(3)	C(40)-C(42)	0.95(3)
C(41)-C(42)	1.379(3)	C(41)-C(43)	0.95(3)
C(42)-C(43)	0.96(3)	C(42)-C(44)	0.95(3)
C(43)-C(44)	1.379(3)	C(43)-C(45)	0.95(3)
C(44)-C(45)	0.96(3)	C(44)-C(46)	0.95(3)
C(45)-C(46)	1.379(3)	C(45)-C(47)	0.95(3)
C(46)-C(47)	0.96(3)	C(46)-C(48)	0.95(3)
C(47)-C(48)	1.379(3)	C(47)-C(49)	0.95(3)
C(48)-C(49)	0.96(3)	C(48)-C(50)	0.95(3)
C(49)-C(50)	1.379(3)	C(49)-C(51)	0.95(3)
C(50)-C(51)	0.96(3)	C(50)-C(52)	0.95(3)
C(51)-C(52)	1.379(3)	C(51)-C(53)	0.95(3)
C(52)-C(53)	0.96(3)	C(52)-C(54)	0.95(3)
C(53)-C(54)	1.379(3)	C(53)-C(55)	0.95(3)
C(54)-C(55)	0.96(3)	C(54)-C(56)	0.95(3)
C(55)-C(56)	1.379(3)	C(55)-C(57)	0.95(3)
C(56)-C(57)	0.96(3)	C(56)-C(58)	0.95(3)
C(57)-C(58)	1.379(3)	C(57)-C(59)	0.95(3)
C(58)-C(59)	0.96(3)	C(58)-C(60)	0.95(3)
C(59)-C(60)	1.379(3)	C(59)-C(61)	0.95(3)
C(60)-C(61)	0.96(3)	C(60)-C(62)	0.95(3)
C(61)-C(62)	1.379(3)	C(61)-C(63)	0.95(3)
C(62)-C(63)	0.96(3)	C(62)-C(64)	0.95(3)
C(63)-C(64)	1.379(3)	C(63)-C(65)	0.95(3)
C(64)-C(65)	0.96(3)	C(64)-C(66)	0.95(3)
C(65)-C(66)	1.379(3)	C(65)-C(67)	0.95(3)
C(66)-C(67)	0.96(3)	C(66)-C(68)	0.95(3)
C(67)-C(68)	1.379(3)	C(67)-C(69)	0.95(3)
C(68)-C(69)	0.96(3)	C(68)-C(70)	0.95(3)
C(69)-C(70)	1.379(3)	C(69)-C(71)	0.95(3)
C(70)-C(71)	0.96(3)	C(70)-C(72)	0.95(3)
C(71)-C(72)	1.379(3)	C(71)-C(73)	0.95(3)
C(72)-C(73)	0.96(3)	C(72)-C(74)	0.95(3)
C(73)-C(74)	1.379(3)	C(73)-C(75)	0.95(3)
C(74)-C(75)	0.96(3)	C(74)-C(76)	0.95(3)
C(75)-C(76)	1.379(3)	C(75)-C(77)	0.95(3)
C(76)-C(77)	0.96(3)	C(76)-C(78)	0.95(3)
C(77)-C(78)	1.379(3)	C(77)-C(79)	0.95(3)
C(78)-C(79)	0.96(3)	C(78)-C(80)	0.95(3)
C(79)-C(80)	1.379(3)	C(79)-C(81)	0.95(3)
C(80)-C(81)	0.96(3)	C(80)-C(82)	0.95(3)
C(81)-C(82)	1.379(3)	C(81)-C(83)	0.95(3)
C(82)-C(83)	0.96(3)	C(82)-C(84)	0.95(3)
C(83)-C(84)	1.379(3)	C(83)-C(85)	0.95(3)
C(84)-C(85)	0.96(3)	C(84)-C(86)	0.95(3)
C(85)-C(86)	1.379(3)	C(85)-C(87)	0.95(3)
C(86)-C(87)	0.96(3)	C(86)-C(88)	0.95(3)
C(87)-C(88)	1.379(3)	C(87)-C(89)	0.95(3)
C(88)-C(89)	0.96(3)	C(88)-C(90)	0.95(3)
C(89)-C(90)	1.379(3)	C(89)-C(91)	0.95(3)
C(90)-C(91)	0.96(3)	C(90)-C(92)	0.95(3)
C(91)-C(92)	1.379(3)	C(91)-C(93)	0.95(3)
C(92)-C(93)	0.96(3)	C(92)-C(94)	0.95(3)
C(93)-C(94)	1.379(3)	C(93)-C(95)	0.95(3)
C(94)-C(95)	0.96(3)	C(94)-C(96)	0.95(3)
C(95)-C(96)	1.379(3)	C(95)-C(97)	0.95(3)
C(96)-C(97)	0.96(3)	C(96)-C(98)	0.95(3)
C(97)-C(98)	1.379(3)	C(97)-C(99)	0.95(3)
C(98)-C(99)	0.96(3)	C(98)-C(100)	0.95(3)
C(99)-C(100)	1.379(3)	C(99)-C(101)	0.95(3)
C(100)-C(101)	0.96(3)	C(100)-C(102)	0.95(3)
C(101)-C(102)	1.379(3)	C(101)-C(103)	0.95(3)
C(102)-C(103)	0.96(3)	C(102)-C(104)	0.95(3)
C(103)-C(104)	1.379(3)	C(103)-C(105)	0.95(3)
C(104)-C(105)	0.96(3)	C(104)-C(106)	0.95(3)
C(105)-C(106)	1.379(3)	C(105)-C(107)	0.95(3)
C(106)-C(107)	0.96(3)	C(106)-C(108)	0.95(3)
C(107)-C(108)	1.379(3)	C(107)-C(109)	0.95(3)
C(108)-C(109)	0.96(3)	C(108)-C(110)	0.95(3)
C(109)-C(110)	1.379(3)	C(109)-C(111)	0.95(3)
C(110)-C(111)	0.96(3)	C(110)-C(112)	0.95(3)
C(111)-C(112)	1.379(3)	C(111)-C(113)	0.95(3)
C(112)-C(113)	0.96(3)	C(112)-C(114)	0.95(3)
C(113)-C(114)	1.379(3)	C(113)-C(115)	0.95(3)
C(114)-C(115)	0.96(3)	C(114)-C(116)	0.95(3)
C(115)-C(116)	1.379(3)	C(115)-C(117)	0.95(3)
C(116)-C(117)	0.96(3)	C(116)-C(118)	0.95(3)
C(117)-C(118)	1.379(3)	C(117)-C(119)	0.95(3)
C(118)-C(119)	0.96(3)	C(118)-C(120)	0.95(3)
C(119)-C(120)	1.379(3)	C(119)-C(121)	0.95(3)
C(120)-C(121)	0.96(3)	C(120)-C(122)	0.95(3)
C(121)-C(122)	1.379(3)	C(121)-C(123)	0.95(3)
C(122)-C(123)	0.96(3)	C(122)-C(124)	0.95(3)
C(123)-C(124)	1.379(3)	C(123)-C(125)	0.95(3)
C(124)-C(125)	0.96(3)	C(124)-C(126)	0.95(3)
C(125)-C(126)	1.379(3)	C(125)-C(127)	0.95(3)
C(126)-C(127)	0.96(3)	C(126)-C(128)	0.95(3)
C(127)-C(128)	1.379(3)	C(127)-C(129)	0.95(3)
C(128)-C(129)	0.96(3)	C(128)-C(130)	0.95(3)
C(129)-C(130)	1.379(3)	C(129)-C(131)	0.95(3)
C(130)-C(131)	0.96(3)	C(130)-C(132)	0.95(3)
C(131)-C(132)	1.379(3)	C(131)-C(133)	0.95(3)
C(132)-C(133)	0.96(3)	C(132)-C(134)	0.95(3)
C(133)-C(134)	1.379(3)	C(133)-C(135)	0.95(3)
C(134)-C(135)	0.96(3)	C(134)-C(136)	0.95(3)
C(135)-C(136)	1.379(3)	C(135)-C(137)	0.95(3)
C(136)-C(137)	0.96(3)	C(136)-C(138)	0.95(3)
C(137)-C(138)	1.379(3)	C(137)-C(139)	0.95(3)
C(138)-C(139)	0.96(3)	C(138)-C(140)	0.95(3)
C(139)-C(140)	1.379(3)	C(139)-C(141)	0.95(3)
C(140)-C(141)	0.96(3)	C(140)-C(142)	0.95(3)
C(141)-C(142)	1.379(3)	C(141)-C(143)	0.95(3)
C(142)-C(143)	0.96(3)	C(142)-C(144)	0.95(3)
C(143)-C(144)	1.379(3)	C(143)-C(145)	0.95(3)
C(144)-C(145)	0.96(3)	C(144)-C(146)	0.95(3)
C(145)-C(146)	1.379(3)	C(145)-C(147)	0.95(3)
C(146)-C(147)	0.96(3)	C(146)-C(148)	0.95(3)
C(147)-C(148)	1.379(3)	C(147)-C(149)	0.95(3)
C(148)-C(149)	0.96(3)	C(148)-C(150)	0.95(3)
C(149)-C(150)	1.379(3)	C(149)-C(151)	0.95(3)
C(150)-C(151)	0.96(3)	C(150)-C(152)	0.95(3)
C(151)-C(152)	1.379(3)	C(151)-C(153)	0.95(3)
C(152)-C(153)	0.96(3)	C(152)-C(154)	0.95(3)
C(153)-C(154)	1.379(3)	C(153)-C(155)	0.95(3)
C(154)-C(155)	0.96(3)	C(154)-C(156)	0.95(3)
C(155)-C(156)	1.379(3)	C(155)-C(157)	0.95(3)
C(156)-C(157)	0.96(3)	C(156)-C(158)	0.95(3)
C(157)-C(158)	1.379(3)	C(157)-C(159)	0.95(3)
C(158)-C(159)	0.96(3)	C(158)-C(160)	0.95(3)
C(159)-C(160)	1.379(3)	C(159)-C(161)	0.95(3)
C(160)-C(161)	0.96(3)	C(160)-C(162)	0.95(3)
C(161)-C(162)	1.379(3)	C(161)-C(163)	0.95(3)
C(162)-C(163)	0.96(3)	C(162)-C(164)	0.95(3)
C(163)-C(164)	1.379(3)	C(163)-C(165)	0.95(3)
C(164)-C(165)	0.96(3)	C(164)-C(166)	0.95(3)
C(165)-C(166)	1.379(3)	C(165)-C(167)	0.95(3)
C(166)-C(167)	0.96(3)	C(166)-C(168)	0.95(3)
C(167)-C(168)	1.379(3)	C(167)-C(169)	0.95(3)
C(168)-C(169)	0.96(3)	C(168)-C(170)	0.95(3)
C(169)-C(170)	1.379(3)	C(169)-C(171)	0.95(3)
C(170)-C(171)	0.96(3)	C(170)-C(172)	0.95(3)

Mono-crown 116.



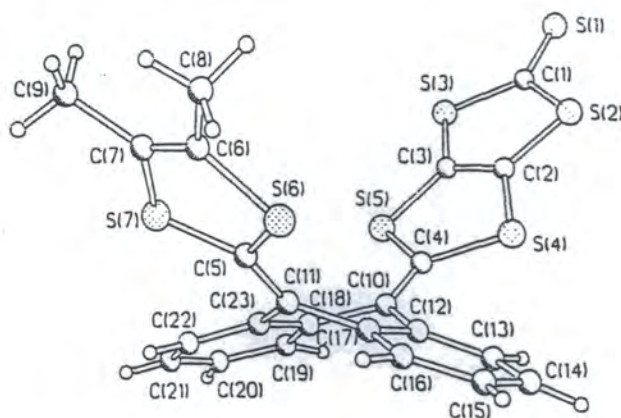
Crystal data and structure refinement

Identification code	99srv056	
Empirical formula	C ₂₇ H ₂₈ O ₅ S ₄	
Formula weight	560.73	
Temperature	150(2) K	
Wavelength	0.71073 Å	
Crystal system	Orthorhombic	
Space group	P2(1)2(1)2(1)	
Unit cell dimensions	a = 7.600(1) Å	alpha = 90 deg.
	b = 18.395(1) Å	beta = 90 deg.
	c = 18.566(1) Å	gamma = 90 deg.
Volume	2595.6(4) Å ³	
Z	4	
Density (calculated)	1.435 g/cm ³	
Absorption coefficient	0.404 mm ⁻¹	
F(000)	1176	
Crystal size	0.55 x 0.12 x 0.08 mm	
Theta range for data collection	1.56 to 26.37 deg.	
Index ranges	-9 < h < 9, -22 < k < 22, -21 < l < 17	
Reflections collected	10781	
Independent reflections	4235 [R(int) = 0.0373]	
Observed reflections, I > 2σ(I)	3920	
Absorption correction	Integration	
Max. and min. transmission	0.9808 and 0.9276	
Refinement method	Full-matrix least-squares on F ²	
Data / restraints / parameters	4219 / 5 / 418	
Goodness-of-fit on F ²	1.175	
Final R indices [I > 2σ(I)]	R1 = 0.0378, wR2 = 0.0743	
R indices (all data)	R1 = 0.0453, wR2 = 0.0827	
Absolute structure parameter	0.07(8)	
Largest shift/e.s.d. ratio	0.001	
Largest diff. peak and hole	0.276 and -0.213 e.Å ⁻³	

Bond lengths [Å] and angles [deg]

S(1)-C(15)	1.755(4)	S(1)-C(16)	1.761(3)
S(2)-C(17)	1.755(3)	S(2)-C(15)	1.771(3)
S(3)-C(16)	1.764(4)	S(3)-C(18)	1.826(3)
S(4)-C(17)	1.765(3)	S(4)-C(27)	1.805(5)
O(1)-C(10)	1.233(4)	O(2)-C(19)	1.433(4)
O(2)-C(20)	1.435(5)	O(3)-C(21)	1.419(5)
O(3)-C(22)	1.426(5)	O(4A)-C(23)	1.400(5)
O(4A)-C(24A)	1.427(5)	O(5A)-C(25)	1.411(6)
O(5A)-C(26)	1.413(5)	O(4B)-C(23)	1.30(2)
O(4B)-C(24B)	1.41(3)	O(5B)-C(25)	1.36(3)
O(5B)-C(26)	1.38(3)	C(1)-C(2)	1.385(5)
C(1)-C(11)	1.400(5)	C(2)-C(3)	1.391(5)
C(3)-C(4)	1.375(6)	C(4)-C(12)	1.400(5)
C(5)-C(6)	1.386(5)	C(5)-C(13)	1.393(5)
C(6)-C(7)	1.396(5)	C(7)-C(8)	1.384(5)
C(8)-C(14)	1.404(5)	C(9)-C(15)	1.377(4)
C(9)-C(11)	1.472(4)	C(9)-C(14)	1.478(5)
C(10)-C(12)	1.474(5)	C(10)-C(13)	1.488(5)
C(11)-C(12)	1.417(4)	C(13)-C(14)	1.422(4)
C(16)-C(17)	1.333(5)	C(18)-C(19)	1.503(5)
C(20)-C(21)	1.500(6)	C(22)-C(23)	1.470(7)
C(24A)-C(25)	1.511(5)	C(24B)-C(25)	1.47(3)
C(26)-C(27)	1.504(6)		
C(15)-S(1)-C(16)	96.9(2)	C(17)-S(2)-C(15)	96.9(2)
C(16)-S(3)-C(18)	101.0(2)	C(17)-S(4)-C(27)	102.3(2)
C(19)-O(2)-C(20)	112.8(3)	C(21)-O(3)-C(22)	113.2(3)
C(23)-O(4A)-C(24A)	112.8(4)	C(25)-O(5A)-C(26)	115.8(4)
C(23)-O(4B)-C(24B)	120(2)	C(25)-O(5B)-C(26)	121(2)
C(2)-C(1)-C(11)	121.2(3)	C(1)-C(2)-C(3)	121.0(4)
C(4)-C(3)-C(2)	118.8(3)	C(3)-C(4)-C(12)	121.2(3)
C(6)-C(5)-C(13)	121.0(3)	C(5)-C(6)-C(7)	119.1(4)
C(8)-C(7)-C(6)	120.7(4)	C(7)-C(8)-C(14)	121.3(3)
C(15)-C(9)-C(11)	121.4(3)	C(15)-C(9)-C(14)	121.5(3)
C(11)-C(9)-C(14)	116.1(3)	O(1)-C(10)-C(12)	121.8(3)
C(1)-C(10)-C(12)	121.4(3)	C(12)-C(10)-C(13)	116.6(3)
C(1)-C(11)-C(9)	117.4(3)	C(1)-C(11)-C(2)	123.2(3)
C(12)-C(11)-C(9)	119.4(3)	C(4)-C(12)-C(11)	120.2(3)
C(4)-C(12)-C(10)	118.7(3)	C(11)-C(12)-C(10)	121.0(3)
C(5)-C(13)-C(14)	120.3(3)	C(5)-C(13)-C(10)	119.2(3)
C(14)-C(13)-C(10)	120.5(3)	C(8)-C(14)-C(13)	117.5(3)
C(8)-C(14)-C(9)	122.2(3)	C(13)-C(14)-C(9)	119.3(3)
C(9)-C(15)-S(1)	125.0(3)	C(9)-C(15)-S(2)	123.1(3)
S(1)-C(15)-S(2)	111.8(2)	C(17)-C(16)-S(1)	116.9(2)
C(17)-C(16)-S(3)	127.2(2)	S(1)-C(16)-S(3)	115.9(2)
C(16)-C(17)-S(4)	116.7(2)	C(16)-C(17)-S(4)	123.7(2)
S(2)-C(17)-S(4)	119.5(2)	C(19)-C(18)-S(3)	113.4(2)
O(2)-C(19)-C(18)	105.3(3)	O(2)-C(19)-C(21)	108.7(3)
O(3)-C(21)-C(20)	108.8(3)	O(3)-C(21)-C(22)	109.7(3)
O(4B)-C(23)-C(22)	133.9(12)	O(4A)-C(23)-C(22)	112.5(4)
O(4A)-C(24A)-C(25)	114.8(4)	O(4B)-C(24B)-C(25)	102(2)
O(5B)-C(25)-C(24B)	124(2)	O(5A)-C(25)-C(24A)	115.4(4)
O(5B)-C(26)-C(27)	125(2)	O(5A)-C(26)-C(27)	105.8(4)
C(26)-C(27)-S(4)	114.9(3)		

9-[(4-5-Methylenedisulfanyl)-1,3-dithiol-2-thione]-10-(4,5-dimethyl-1,3-dithiol-2-ylidene)-9,10-dihydroanthracene 124.

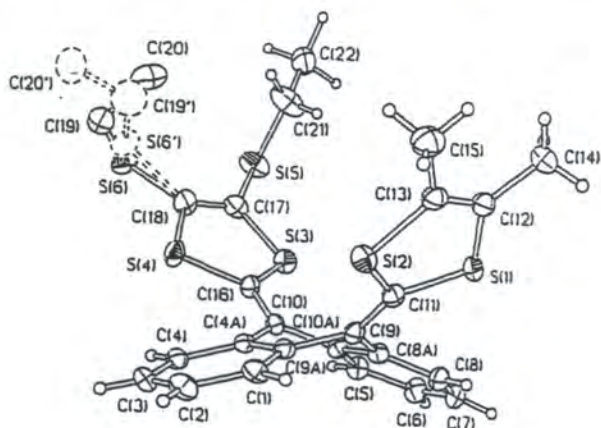


Bond lengths (Å) and angles (deg)

Identification code	98srv125
Empirical formula	C ₂₆ H ₂₄ S ₆
Formula weight	528.81
Temperature	150(2) K
Wavelength	0.71073 Å
Crystal system	Triclinic
Space group	P-1
Unit cell dimensions	a = 9.573(1) Å alpha = 98.34(1) deg. b = 9.793(1) Å beta = 90.36(1) deg. c = 13.159(1) Å gamma = 93.09(1) deg.
Volume	1231.4(2) Å ³
Z	2
Density (calculated)	1.426 g/cm ³
Absorption coefficient	0.569 mm ⁻¹
F(000)	552
Crystal size	0.48 x 0.24 x 0.04 mm
Theta range for data collection	1.56 to 27.48 deg.
Index ranges	-11 ≤ h ≤ 12, -12 ≤ k ≤ 13, -16 ≤ l ≤ 17
Reflections collected	8965
Independent reflections	5583 [R(int) = 0.0221]
Observed reflections, I > 2σ(I)	4751
Absorption correction	Integration
Max. and min. transmission	0.9787 and 0.9254
Refinement method	Full-matrix least-squares on F ²
Data / restraints / parameters	5532 / 3 / 177
Goodness-of-fit on F ²	1.173
Final R indices [I > 2σ(I)]	R1 = 0.0422, wR2 = 0.0915
R indices (all data)	R1 = 0.0549, wR2 = 0.1135
Largest shift/e.s.d. ratio	-0.025
Largest diff. peak and hole	0.397 and -0.345 e.Å ⁻³

S(1)-C(12)	1.761(3)	S(1)-C(11)	1.759(2)
S(2)-C(11)	1.758(2)	S(2)-C(13)	1.761(2)
S(3)-C(17)	1.755(3)	S(3)-C(16)	1.772(2)
S(4)-C(18)	1.761(3)	S(4)-C(15)	1.771(2)
S(5)-C(17)	1.764(2)	S(5)-C(12)	1.827(3)
S(6)-C(18)	1.732(3)	S(6)-C(19)	1.798(5)
S(6')-C(19')	1.815(12)	S(6')-C(18)	1.857(5)
C(1)-C(2)	1.399(3)	C(1)-C(9A)	1.401(3)
C(2)-C(3)	1.386(3)	C(3)-C(4)	1.394(3)
C(4)-C(4A)	1.399(3)	C(4A)-C(9A)	1.421(3)
C(4A)-C(10)	1.481(3)	C(5)-C(10A)	1.393(3)
C(5)-C(6)	1.397(3)	C(6)-C(7)	1.385(4)
C(7)-C(8)	1.393(4)	C(8)-C(8A)	1.402(3)
C(8A)-C(10A)	1.417(3)	C(8A)-C(9)	1.475(2)
C(9)-C(11)	1.365(3)	C(9)-C(9A)	1.475(2)
C(10)-C(16)	1.356(3)	C(10)-C(10A)	1.483(2)
C(12)-C(13)	1.335(4)	C(12)-C(14)	1.504(4)
C(13)-C(15)	1.503(4)	C(17)-C(18)	1.341(4)
C(19)-C(20)	1.478(8)	C(19')-C(20')	1.464(13)
C(21)-C(22)	1.489(5)		
C(12)-S(1)-C(11)	96.94(12)	C(11)-S(2)-C(13)	97.23(12)
C(17)-S(3)-C(16)	96.72(12)	C(13)-S(4)-C(15)	96.84(12)
C(17)-S(5)-C(12)	100.48(14)	C(13)-S(5)-C(19)	99.0(2)
C(19')-S(6')-C(18)	106.7(4)	C(2)-C(1)-C(9A)	120.7(2)
C(3)-C(2)-C(1)	120.1(2)	C(2)-C(3)-C(4)	120.0(2)
C(3)-C(4)-C(4A)	120.9(2)	C(4)-C(4A)-C(9A)	119.2(3)
C(4)-C(4A)-C(10)	123.1(2)	C(9A)-C(4A)-C(10)	117.8(2)
C(10A)-C(5)-C(5)	120.9(2)	C(7)-C(6)-C(5)	119.8(2)
C(6)-C(7)-C(8)	120.3(2)	C(7)-C(8)-C(8A)	120.6(2)
C(8)-C(8A)-C(10A)	119.0(2)	C(8)-C(8A)-C(9)	122.8(2)
C(10A)-C(8A)-C(9)	118.1(2)	C(11)-C(9)-C(8A)	122.6(2)
C(11)-C(9)-C(9A)	123.5(2)	C(8A)-C(9)-C(9A)	113.6(2)
C(1)-C(9A)-C(4A)	119.1(2)	C(1)-C(9A)-C(9)	123.2(2)
C(4A)-C(9A)-C(9)	117.7(2)	C(16)-C(10)-C(4A)	123.3(2)
C(16)-C(10)-C(10A)	122.5(2)	C(4A)-C(10)-C(10A)	114.0(2)
C(5)-C(10A)-C(8A)	119.4(2)	C(5)-C(10A)-C(10)	123.3(2)
C(8A)-C(10A)-C(10)	117.3(2)	C(9)-C(11)-S(2)	124.7(2)
C(9)-C(11)-S(1)	123.5(2)	S(2)-C(11)-S(1)	111.57(13)
C(13)-C(12)-C(11)	128.1(2)	C(13)-C(12)-S(1)	116.7(2)
C(14)-C(12)-S(1)	115.2(2)	C(12)-C(13)-C(15)	127.9(2)
C(12)-C(13)-S(2)	116.6(2)	C(15)-C(13)-S(2)	115.4(2)
C(10)-C(16)-S(4)	123.8(2)	C(10)-C(16)-S(3)	124.5(2)
S(4)-C(16)-S(3)	111.53(12)	C(18)-C(17)-S(3)	117.1(2)
C(18)-C(17)-S(5)	126.5(2)	S(3)-C(17)-S(5)	116.4(2)
C(17)-C(18)-S(6)	121.4(2)	C(17)-C(18)-S(4)	116.8(2)
S(6)-C(18)-S(4)	120.4(2)	C(17)-C(18)-S(6')	110.1(2)
S(4)-C(18)-S(6')	112.6(2)	C(20)-C(19)-S(6)	132.5(4)
C(20')-C(19')-S(6')	115.5(9)	C(22)-C(21)-S(5)	109.6(3)

9-(4,5-Diethylsulfanyl-1,3-dithiol-2-ylidene)-10-(4,5-dimethyl-1,3-dithiol-2-ylidene)-9,10-dihydroanthracene 125.



Bond lengths [Å] and angles [deg]

S(1A)-C(1A)	1.525(5)	S(2A)-C(2A)	1.735(4)
S(2A)-C(1A)	1.752(5)	S(3A)-C(1A)	1.723(5)
S(3A)-C(1A)	1.717(4)	S(4A)-C(2A)	1.745(4)
S(4A)-C(4A)	1.789(4)	S(5A)-C(3A)	1.748(4)
S(5A)-C(4A)	1.782(4)	S(6A)-C(5A)	1.755(4)
S(6A)-C(5A)	1.755(5)	S(7A)-C(7A)	1.754(5)
S(7A)-C(7A)	1.764(4)	C(2A)-C(1A)	1.343(6)
C(4A)-C(10A)	1.350(6)	C(5A)-C(11A)	1.354(6)
C(5A)-C(17A)	1.329(7)	C(6A)-C(18A)	1.302(5)
C(7A)-C(9A)	1.501(7)	C(10A)-C(18A)	1.474(6)
C(10A)-C(12A)	1.477(6)	C(11A)-C(23A)	1.485(5)
C(11A)-C(17A)	1.489(6)	C(12A)-C(13A)	1.391(6)
C(12A)-C(17A)	1.421(6)	C(13A)-C(14A)	1.386(7)
C(14A)-C(15A)	1.372(7)	C(15A)-C(16A)	1.393(7)
C(16A)-C(17A)	1.398(6)	C(18A)-C(19A)	1.400(6)
C(18A)-C(22A)	1.419(6)	C(19A)-C(20A)	1.382(7)
C(20A)-C(21A)	1.390(7)	C(21A)-C(22A)	1.397(7)
C(22A)-C(23A)	1.395(6)	S(1B)-C(1B)	1.535(5)
S(2B)-C(1B)	1.735(4)	S(3B)-C(1B)	1.752(5)
S(3B)-C(1B)	1.730(4)	S(4B)-C(2B)	1.749(5)
S(4B)-C(2B)	1.754(5)	S(4B)-C(4B)	1.745(4)
S(5B)-C(3B)	1.746(4)	S(5B)-C(4B)	1.778(4)
S(6B)-C(6B)	1.764(5)	S(6B)-C(8B)	1.775(4)
S(7B)-C(7B)	1.756(5)	S(7B)-C(5B)	1.755(4)
C(2B)-C(1B)	1.350(6)	C(4B)-C(10B)	1.357(6)
C(5B)-C(11B)	1.361(6)	C(6B)-C(7B)	1.345(6)
C(6B)-C(8B)	1.494(6)	C(7B)-C(9B)	1.505(6)
C(10B)-C(13B)	1.484(6)	C(10B)-C(13B)	1.484(6)
C(11B)-C(23B)	1.488(6)	C(11B)-C(17B)	1.490(6)
C(12B)-C(13B)	1.402(6)	C(12B)-C(17B)	1.412(5)
C(13B)-C(14B)	1.393(7)	C(14B)-C(15B)	1.378(7)
C(15B)-C(16B)	1.386(7)	C(16B)-C(17B)	1.396(6)
C(18B)-C(19B)	1.402(6)	C(18B)-C(23B)	1.415(6)
C(19B)-C(20B)	1.394(7)	C(20B)-C(21B)	1.374(7)
C(21B)-C(22B)	1.396(7)	C(22B)-C(23B)	1.409(6)
C(2A)-S(2A)-C(1A)	95.9(2)	C(1A)-S(3A)-C(3A)	96.4(2)
C(2A)-S(4A)-C(4A)	94.1(2)	C(3A)-S(5A)-C(4A)	93.9(2)
C(5A)-S(6A)-C(6A)	97.3(2)	C(7A)-S(7A)-C(5A)	97.5(2)
S(1A)-C(1A)-S(2A)	123.3(3)	S(1A)-C(1A)-S(3A)	122.9(3)
S(3A)-C(1A)-S(2A)	113.7(3)	C(3A)-C(2A)-S(2A)	117.1(3)
C(3A)-C(2A)-S(4A)	118.0(3)	S(2A)-C(2A)-S(4A)	124.7(3)
C(2A)-C(3A)-S(3A)	116.9(3)	C(2A)-C(3A)-S(5A)	118.4(3)
C(3A)-C(3A)-S(5A)	124.6(3)	C(10A)-C(14A)-S(5A)	123.1(3)
C(10A)-C(4A)-S(4A)	122.8(3)	S(5A)-C(4A)-S(6A)	114.0(2)
C(11A)-C(5A)-S(7A)	123.7(3)	C(11A)-C(5A)-S(6A)	124.7(3)
S(7A)-C(5A)-S(6A)	111.4(2)	C(7A)-C(6A)-C(8A)	127.7(5)
C(7A)-C(6A)-S(6A)	116.6(4)	C(8A)-C(6A)-S(6A)	115.7(4)
C(6A)-C(7A)-C(9A)	127.5(4)	C(5A)-C(7A)-S(7A)	117.0(4)
C(9A)-C(7A)-S(7A)	115.5(4)	C(4A)-C(10A)-C(18A)	122.3(4)
C(4A)-C(10A)-C(12A)	122.3(4)	C(18A)-C(10A)-C(12A)	114.5(4)
C(5A)-C(11A)-C(23A)	123.0(4)	C(5A)-C(11A)-C(17A)	122.7(4)
C(23A)-C(11A)-C(17A)	114.2(4)	C(13A)-C(12A)-C(10A)	119.8(4)
C(13A)-C(12A)-C(10A)	122.7(4)	C(17A)-C(12A)-C(10A)	117.5(4)
C(14A)-C(13A)-C(10A)	121.2(5)	C(15A)-C(14A)-C(13A)	121.5(5)
C(14A)-C(13A)-C(16A)	120.5(4)	C(15A)-C(14A)-C(17A)	121.2(5)
C(16A)-C(13A)-C(12A)	117.7(4)	C(16A)-C(17A)-C(11A)	124.3(4)
C(12A)-C(17A)-C(11A)	118.0(4)	C(19A)-C(18A)-C(23A)	120.2(4)
C(19A)-C(18A)-C(10A)	122.4(4)	C(23A)-C(18A)-C(10A)	117.4(4)
C(20A)-C(19A)-C(18A)	120.5(5)	C(19A)-C(20A)-C(21A)	119.9(5)
C(20A)-C(19A)-C(22A)	120.1(5)	C(22A)-C(20A)-C(21A)	121.1(5)
C(22A)-C(21A)-C(18A)	118.1(4)	C(22A)-C(21A)-C(11A)	123.5(4)
C(18A)-C(21A)-C(11A)	118.3(4)	C(2B)-S(2B)-C(1B)	96.4(2)
C(3B)-S(3B)-C(1B)	96.1(2)	C(2B)-S(4B)-C(4B)	94.6(2)
C(3B)-S(5B)-C(4B)	95.1(2)	C(6B)-S(6B)-C(5B)	97.0(2)
C(7B)-S(7B)-C(5B)	97.3(2)	S(1B)-C(1B)-S(3B)	123.5(3)
S(1B)-C(1B)-S(2B)	123.1(3)	S(3B)-C(1B)-S(2B)	113.3(3)
C(3B)-C(2B)-S(2B)	116.5(3)	C(3B)-C(2B)-S(4B)	118.0(3)
S(2B)-C(2B)-S(4B)	125.4(3)	C(2B)-C(3B)-S(3B)	117.6(3)
C(2B)-C(3B)-S(5B)	117.7(3)	S(3B)-C(3B)-S(5B)	124.5(3)
C(10B)-C(4B)-S(5B)	122.7(3)	C(10B)-C(4B)-S(4B)	123.4(3)
S(5B)-C(4B)-S(4B)	113.8(2)	C(11B)-C(5B)-S(6B)	125.1(3)
C(11B)-C(5B)-S(6B)	123.5(3)	S(7B)-C(5B)-S(6B)	111.4(2)
C(7B)-C(6B)-C(8B)	126.7(4)	C(7B)-C(6B)-S(6B)	116.3(4)
C(8B)-C(6B)-S(6B)	116.3(4)	C(6B)-C(7B)-C(9B)	125.7(4)
C(6B)-C(7B)-S(7B)	116.9(4)	C(9B)-C(7B)-S(7B)	117.1(4)
C(4B)-C(10B)-C(12B)	123.4(4)	C(4B)-C(10B)-C(18B)	122.8(4)
C(12B)-C(10B)-C(18B)	111.8(4)	C(5B)-C(11B)-C(23B)	123.8(4)
C(5B)-C(11B)-C(17B)	122.8(4)	C(23B)-C(11B)-C(17B)	113.4(4)
C(13B)-C(12B)-C(10B)	119.0(4)	C(13B)-C(12B)-C(10B)	123.2(4)
C(17B)-C(12B)-C(10B)	117.5(4)	C(14B)-C(13B)-C(12B)	120.6(5)
C(15B)-C(14B)-C(13B)	120.1(5)	C(14B)-C(13B)-C(16B)	120.1(4)
C(15B)-C(14B)-C(17B)	121.0(4)	C(16B)-C(17B)-C(12B)	119.2(4)
C(16B)-C(17B)-C(11B)	122.5(4)	C(12B)-C(17B)-C(11B)	113.0(4)
C(19B)-C(18B)-C(23B)	119.4(4)	C(19B)-C(18B)-C(10B)	122.9(4)
C(23B)-C(18B)-C(10B)	117.7(4)	C(20B)-C(19B)-C(18B)	122.3(5)
C(21B)-C(20B)-C(19B)	119.5(5)	C(20B)-C(19B)-C(22B)	120.7(5)
C(21B)-C(20B)-C(22B)	120.6(5)	C(22B)-C(20B)-C(18B)	120.5(4)
C(22B)-C(21B)-C(11B)	123.5(4)	C(18B)-C(21B)-C(11B)	117.3(4)

Crystal data and structure refinement

Identification code	98sr074
Empirical formula	C ₂₃ H ₁₄ S ₇ · 0.5(C ₆ OCl ₃)
Formula weight	575.44
Temperature	150(2) K
Wavelength	0.71073 Å
Crystal system	Triclinic
Space group	P-1
Unit cell dimensions	a = 11.6822(8) Å alpha = 79.481(4) deg. b = 13.4825(6) Å beta = 71.432(4) deg. c = 17.7155(9) Å gamma = 59.385(4) deg.
Volume	2475.3(2) Å ³
Z	4
Density (calculated)	1.541 g/cm ³
Absorption coefficient	0.311 mm ⁻¹
F(000)	1172
Crystal size	0.25 × 0.20 × 0.06 mm
Theta range for data collection	1.61 to 30.65 deg.
Index ranges	-16 < h < 16, -19 < k < 15, -24 < l < 24
Reflections collected	19705
Independent reflections	12897 [R(int) = 0.0308]
Observed reflections, I > 2σ(I)	8252
Absorption correction	Multi-scan (SADABS)
Max. and min. transmission	0.9077 and 0.7860
Refinement method	Full-matrix least-squares on F ²
Data / restraints / parameters	12778 / 0 / 653
Goodness-of-fit on F ²	1.125
Final R indices [I > 2σ(I)]	R1 = 0.0670, wR2 = 0.1259
R indices (all data)	R1 = 0.1195, wR2 = 0.1748
Largest shift/e.s.d. ratio	-0.010
Largest diff. peak and hole	1.142 and -0.950 e.Å ⁻³

9,10-Bis-(4-methyl-1,3-dithiol-2-ylidene)-9,10-dihydroanthracenocyclophane 143.

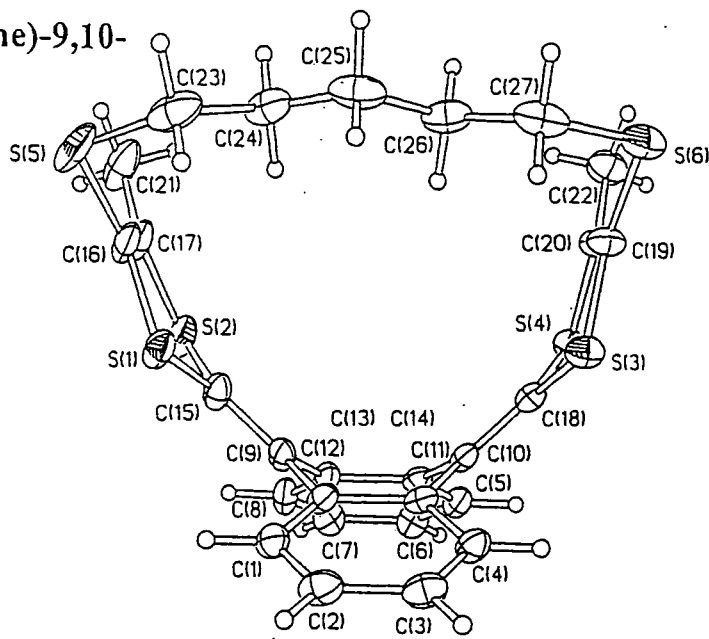


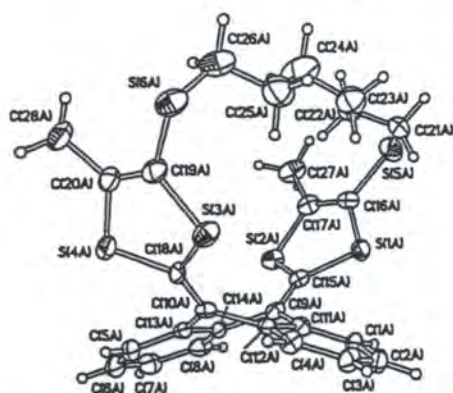
Table 1. Crystal data and structure refinement for 99sv191.

Identification code	99sv191
Chemical formula	C ₂₇ H ₂₄ S ₆
Molecular weight	540.32
Temperature	120(2) K
Wavelength	0.71073 Å
Crystal system	Triclinic
Space group	P $\bar{1}$ (No. 2)
Cell dimensions	a = 10.944(4) Å α = 71.13(1)° b = 13.391(5) Å β = 89.63(2)° c = 16.923(7) Å γ = 85.66(1)°
Volume	2530.2(17) Å ³
Z	4
D _c (calculated)	1.409 g/cm ³
Absorption coefficient	0.552 mm ⁻¹
F(000)	1128
Crystal size	0.40 × 0.12 × 0.04 mm ³
θ range for data collection	2.24 to 27.5°
θ ranges	-12 ≤ θ ≤ 14, -13 ≤ θ ≤ 17, -21 ≤ φ ≤ 21
Reflections collected	23433
Independent reflections	11538 [R(int) = 0.0340]
Reflections with I > 2σ(I)	7045
Completeness to θ = 27.5°	98.7 %
Empirical correction	none
and min. transmission	0.9732 and 0.3814
Refinement method	Full-matrix least-squares on F ²
Restraints / parameters	11538 / 0 / 678
Best fit shift/e.s.d. ratio	0.006
R indices (I > 2σ(I))	R ₁ = 0.0478, wR ₂ = 0.0889
R indices (all data)	R ₁ = 0.1023, wR ₂ = 0.1036
Extinction coefficient	0.460 and -0.521 a.u. ⁻¹

Table 2. Bond lengths [Å] and angles [°] for 99sv191.

C(1)-C(2)	1.768(3)	C(21)-C(22)	1.521(5)	C(19)-C(20)-S(4)	115.7(2)	C(48)-C(40)-C(41)	121.1(3)	S(2)-C(15)-S(1)	111.3(9)
C(1)-C(16)	1.771(2)	C(23)-C(22)	1.514(5)	C(28)-C(20)-S(4)	116.3(2)	C(44)-C(40)-C(41)	114.0(2)	C(17)-C(16)-S(1)	123.3(5)
C(1)-C(17)	1.759(2)	C(25)-C(24)	1.526(5)	C(23)-C(21)-S(5)	113.9(3)	C(35)-C(41)-C(42)	119.9(3)	C(17)-C(16)-S(1)	117.1(2)
C(1)-C(15)	1.771(3)	C(24)-C(25)	1.520(5)	C(23)-C(22)-C(21)	113.3(3)	C(35)-C(41)-C(40)	123.9(3)	S(5)-C(16)-S(1)	117.3(0)
C(1)-S(1)	1.750(2)	S(7A)-C(45A)	1.774(6)	C(25)-C(24)-C(23)	112.7(2)	C(42)-C(41)-C(40)	116.2(3)	C(16)-C(17)-C(27)	127.7(1)
C(1)-S(1)	1.753(3)	S(7A)-C(46A)	1.750(6)	C(25)-C(24)-S(6)	113.0(3)	C(41)-C(42)-C(38A)	109.3(4)	C(16)-C(17)-S(2)	116.4(1)
C(1)-S(1)	1.768(3)	S(8A)-C(47A)	1.774(7)	C(24)-C(25)-S(6)	114.7(2)	C(41)-C(42)-C(38B)	114.7(2)	C(17)-C(18)-S(2)	114.0(1)
C(1)-S(1)	1.768(2)	S(8A)-C(45A)	1.790(6)	C(45A)-S(7A)-C(46A)	95.0(2)	C(38A)-C(42)-C(38B)	124.4(2)	C(10)-C(18)-S(2)	124.5(1)
C(1)-S(1)	1.757(3)	S(7B)-C(45B)	1.772(6)	C(47A)-S(8A)-C(45A)	95.2(2)	C(41)-C(42)-C(39)	116.2(3)	C(10)-C(18)-S(4)	123.0(1)
C(1)-S(1)	1.831(4)	S(7B)-C(46B)	1.730(7)	C(45B)-S(7B)-C(46B)	93.7(3)	C(38A)-C(42)-C(39)	124.4(4)	S(2)-C(18)-S(4)	112.2(3)
C(1)-S(1)	1.757(2)	S(8B)-C(45B)	1.736(6)	C(47B)-S(8B)-C(47B)	95.0(3)	C(38B)-C(42)-C(39)	120.4(4)	C(20)-C(19)-S(6)	128.6(2)
C(1)-S(1)	1.822(4)	S(8B)-C(47B)	1.761(8)	C(49)-S(9)-C(48)	94.36(12)	C(31)-C(43)-C(44)	119.2(2)	C(20)-C(19)-S(2)	117.3(2)
C(1)-C(2)	1.792(4)	S(9)-C(49)	1.770(3)	C(50)-S(10)-C(48)	95.31(12)	C(31)-C(43)-C(39)	124.2(3)	S(6)-C(19)-S(3)	117.0(0)
C(1)-C(3)	1.752(4)	S(9)-C(48)	1.770(3)	C(46A)-S(11A)-C(53A)	102.4(2)	C(44)-C(43)-C(39)	116.6(4)	C(19)-C(20)-C(23)	127.0(5)
C(1)-C(13)	1.597(4)	S(10)-C(50)	1.750(3)	C(46B)-S(11B)-C(53B)	101.3(2)	C(34)-C(44)-C(43)	119.2(2)	C(19)-C(20)-S(4)	116.6(7)
C(1)-C(7)	1.735(4)	S(10)-C(48)	1.770(3)	C(49)-S(12)-C(57)	101.00(12)	C(34)-C(44)-C(40)	123.2(3)	C(23)-C(20)-S(4)	116.2(8)
C(1)-C(14)	1.592(4)	S(11A)-C(46A)	1.750(3)	C(32)-C(31)-C(43)	120.3(3)	C(43)-C(44)-C(40)	115.2(3)	C(23)-C(21)-S(5)	116.5(1)
C(1)-C(6)	1.583(4)	S(11A)-C(53A)	1.754(6)	C(33)-C(32)-C(31)	119.9(3)	C(39)-C(45A)-S(7A)	121.7(5)	C(23)-C(22)-C(21)	111.7(1)
C(1)-C(11)	1.592(4)	S(11B)-C(46B)	1.762(7)	C(32)-C(33)-C(34)	120.4(3)	C(39)-C(45A)-S(8A)	127.1(5)	C(23)-C(22)-C(24)	115.2(1)
C(1)-C(7)	1.594(4)	S(11B)-C(53B)	1.816(7)	C(33)-C(33)-C(44)	120.6(2)	S(7A)-C(45A)-S(8A)	110.2(4)	C(23A)-C(24)-C(23)	111.4(1)
C(1)-C(3)	1.592(4)	S(12)-C(49)	1.763(5)	C(36A)-C(35)-C(41)	131.5(4)	C(47A)-C(46A)-S(11A)	124.2(5)	C(23A)-C(24)-C(23B)	108.0(1)
C(1)-C(12)	1.587(4)	S(12)-C(57)	1.827(3)	C(41)-C(35)-C(56B)	109.6(4)	S(11A)-C(46A)-S(7A)	118.2(3)	C(24)-C(23A)-C(23B)	113.4(1)
C(1)-C(15)	1.557(4)	C(31)-C(32)	1.359(4)	C(35)-C(36A)-C(37A)	110.9(5)	C(46A)-C(47A)-C(51A)	123.2(6)	C(25A)-C(26A)-S(6)	114.3(1)
C(1)-C(12)	1.484(4)	C(31)-C(43)	1.393(4)	C(36A)-C(35)-C(36B)	22.7(4)	C(47A)-C(46A)-S(8A)	117.3(5)	C(24)-C(23A)-C(23B)	108.9(1)
C(1)-C(13)	1.484(4)	C(32)-C(33)	1.382(4)	C(41)-C(35)-C(56B)	109.6(4)	S(11A)-C(46A)-S(7A)	118.2(3)	C(25A)-C(26A)-S(6)	114.3(1)
C(1)-C(14)	1.484(4)	C(33)-C(34)	1.382(4)	C(35)-C(36A)-C(37A)	110.9(5)	C(46A)-C(47A)-C(51A)	123.2(6)	C(26B)-C(25B)-C(24)	108.3(1)
C(1)-C(17)	1.541(4)	C(34)-C(44)	1.401(4)	C(36A)-C(35)-C(36B)	22.7(4)	C(31A)-C(47A)-S(8A)	115.2(5)	C(25B)-C(26B)-S(6)	105.1(1)
C(1)-C(20)	1.538(4)	C(35)-C(36A)	1.328(6)	C(37B)-C(36B)-C(35)	127.3(5)	C(39)-C(45B)-S(8B)	121.0(4)		
C(1)-C(23)	1.503(4)	C(35)-C(41)	1.392(4)	C(38B)-C(37B)-C(36B)	121.0(6)	C(39)-C(45B)-S(7B)	127.0(4)		
		C(36A)-C(37A)	1.310(5)	C(37B)-C(38B)-C(42)	111.1(6)	S(8B)-C(45B)-S(7B)	111.9(4)		
		C(37A)-C(38A)	1.398(5)	C(45A)-C(39)-C(42)	115.2(4)	C(47B)-C(46B)-S(11B)	124.2(5)		
		C(38A)-C(43)	1.322(5)	C(45A)-C(39)-C(43)	127.1(4)	C(47B)-C(46B)-S(7B)	117.4(6)		
		C(38B)-C(37B)	1.402(5)	C(42)-C(39)-C(43)	115.6(2)	S(11B)-C(46B)-S(7B)	118.2(3)		
				C(43)-C(39)-C(45B)	116.4(3)	C(46B)-C(47B)-C(51B)	126.2(7)		
				C(48)-C(40)-C(41)	123.9(2)	C(46B)-C(47B)-S(3B)	116.3(6)		
						C(51B)-C(47B)-S(3B)	117.2(5)		
						C(40)-C(46)-S(10)	123.0(2)		

9,10-Bis-(4-methyl-1,3-dithiol-2-ylidene)-9,10-dihydroanthracenocyclophane 144.



Crystal data and structure refinement

Identification code	
Empirical formula	C ₂₄ H ₂₄ S ₄
Formula weight	354.85
Temperature	293(2) K
Wavelength	0.71073 Å
Crystal system	Orthorhombic
Space group	Pna2 ₁
Unit cell dimensions	$a = 19.231(2)$ Å $b = 9.520(1)$ Å $c = 30.089(3)$ Å
Volume	5509(1) Å ³
Z	8
Density (calculated)	1.338 g/cm ³
Absorption coefficient	0.513 mm ⁻¹
F(000)	2320
Crystal size	0.44 × 0.12 × 0.11 mm ³
θ range for data collection	2.12 to 25.00°
Index ranges	-22 ≤ h ≤ 19, -10 ≤ k ≤ 11, -35 ≤ l ≤ 35
Reflections collected	31379
Independent reflections	9683 [R(int) = 0.0617]
Reflections with I > 2σ(I)	5758
Completeness to $\theta = 25.00^\circ$	100.0 %
Absorption correction	Integration
Max. and min. transmission	0.9534 and 0.9081
Refinement method	Full-matrix least-squares on F ²
Data / restraints / parameters	9683 / 1 / 617
Largest final shift/e.s.d. ratio	0.011
Goodness-of-fit on F ²	1.000
Final R indices [I > 2σ(I)]	R ₁ = 0.0487, wR ₂ = 0.0816
R indices (all data)	R ₁ = 0.1106, wR ₂ = 0.0993
Absolute structure parameter	-0.15(9)
Largest diff. peak and hole	0.215 and -0.208 e.Å ⁻³

Bond lengths [Å] and angles [°]

S(1A)-C(16A)	1.758(7)	C(21A)-C(22A)	1.511(9)
S(1A)-C(15A)	1.766(6)	C(22A)-C(23A)	1.482(10)
S(2A)-C(17A)	1.757(7)	C(23A)-C(24A)	1.500(13)
S(2A)-C(15A)	1.768(5)	C(24A)-C(25A)	1.454(14)
S(3A)-C(18A)	1.745(11)	C(25A)-C(26A)	1.528(12)
S(3A)-C(19A)	1.778(6)	S(1B)-C(15B)	1.760(6)
S(4A)-C(20A)	1.763(7)	S(1B)-C(16B)	1.764(8)
S(4A)-C(18A)	1.827(11)	S(2B)-C(15B)	1.769(6)
S(5A)-C(16A)	1.775(7)	S(2B)-C(17B)	1.773(7)
S(5A)-C(21A)	1.814(7)	S(3B)-C(19B)	1.756(6)
S(6A)-C(19A)	1.758(6)	S(3B)-C(18B)	1.783(10)
S(6A)-C(26A)	1.803(8)	S(4B)-C(18B)	1.714(12)
C(1A)-C(2A)	1.359(12)	S(4B)-C(20B)	1.765(7)
C(1A)-C(11A)	1.376(12)	S(5B)-C(16B)	1.743(8)
C(2A)-C(3A)	1.389(13)	S(5B)-C(21B)	1.824(6)
C(3A)-C(4A)	1.377(8)	S(6B)-C(19B)	1.760(6)
C(4A)-C(12A)	1.402(11)	S(6B)-C(26B)	1.814(8)
C(13B)-C(14B)	1.426(13)	C(8A)-C(14A)-C(9A)	123.7(8)
C(16B)-C(17B)	1.346(10)	C(13A)-C(14A)-C(9A)	116.7(7)
C(17B)-C(27B)	1.489(12)	C(9A)-C(15A)-S(1A)	124.3(4)
C(19B)-C(20B)	1.345(8)	S(1A)-C(15A)-S(2A)	110.7(3)
C(20B)-C(28B)	1.496(8)	C(17A)-C(16A)-S(1A)	118.5(6)
C(16A)-S(1A)-C(15A)	94.4(3)	C(17A)-C(16A)-S(5A)	124.8(6)
C(17A)-S(2A)-C(15A)	95.9(3)	S(1A)-C(16A)-S(5A)	116.7(5)
C(18A)-S(3A)-C(19A)	97.0(4)	C(4A)-C(3A)-C(2A)	120.0(7)
C(20A)-S(4A)-C(18A)	96.0(4)	C(3A)-C(4A)-C(12A)	120.3(6)
C(16A)-S(5A)-C(21A)	100.3(3)	C(6A)-C(5A)-C(13A)	121.9(6)
C(19A)-S(6A)-C(26A)	100.0(3)	C(5A)-C(6A)-C(7A)	119.9(6)
C(2A)-C(1A)-C(11A)	122.0(9)	C(6A)-C(7A)-C(8A)	119.8(6)
C(1A)-C(2A)-C(3A)	119.5(10)	C(14A)-C(8A)-C(7A)	120.7(7)
C(4A)-C(3A)-C(2A)	120.0(7)	C(15A)-C(9A)-C(11A)	121.5(6)
C(3A)-C(4A)-C(12A)	120.3(6)	C(15A)-C(9A)-C(14A)	123.2(6)
C(6A)-C(5A)-C(13A)	121.9(6)	C(11A)-C(9A)-C(14A)	114.9(6)
C(5A)-C(6A)-C(7A)	119.9(6)	C(18A)-C(10A)-C(13A)	124.2(8)
C(6A)-C(7A)-C(8A)	119.8(6)	C(18A)-C(10A)-C(12A)	120.8(8)
C(14A)-C(8A)-C(7A)	120.7(7)	C(13A)-C(10A)-C(12A)	114.7(7)
C(15A)-C(9A)-C(11A)	121.5(6)	C(1A)-C(11A)-C(12A)	119.2(8)
C(15A)-C(9A)-C(14A)	123.2(6)	C(1A)-C(11A)-C(9A)	124.0(8)
C(11A)-C(9A)-C(14A)	114.9(6)	C(12A)-C(11A)-C(9A)	116.7(8)
C(18A)-C(10A)-C(13A)	124.2(8)	C(11A)-C(12A)-C(4A)	118.9(8)
C(18A)-C(10A)-C(12A)	120.8(8)	C(11A)-C(12A)-C(10A)	117.8(8)
C(13A)-C(10A)-C(12A)	114.7(7)	C(4A)-C(12A)-C(10A)	123.2(8)
C(1A)-C(11A)-C(12A)	119.2(8)	C(3A)-C(13A)-C(14A)	118.1(6)
C(1A)-C(11A)-C(9A)	124.0(8)	C(5A)-C(13A)-C(10A)	124.9(6)
C(12A)-C(11A)-C(9A)	116.7(8)	C(14A)-C(13A)-C(10A)	117.0(6)
C(11A)-C(12A)-C(4A)	118.9(8)	C(8A)-C(14A)-C(13A)	119.6(7)
C(11A)-C(12A)-C(10A)	117.8(8)	C(5A)-C(6A)	1.363(8)
C(4A)-C(12A)-C(10A)	123.2(8)	C(5A)-C(13A)	1.397(7)
C(3A)-C(13A)-C(14A)	118.1(6)	C(6A)-C(7A)	1.383(9)
C(5A)-C(13A)-C(10A)	124.9(6)	C(7A)-C(8A)	1.393(9)
C(14A)-C(13A)-C(10A)	117.0(6)	C(8A)-C(14A)	1.379(12)
C(8A)-C(14A)-C(13A)	119.6(7)	C(9A)-C(15A)	1.351(7)
C(5A)-C(6A)	1.363(8)	C(9A)-C(11A)	1.487(10)
C(5A)-C(13A)	1.397(7)	C(9A)-C(14A)	1.488(10)
C(6A)-C(7A)	1.383(9)	C(10A)-C(18A)	1.349(13)
C(7A)-C(8A)	1.393(9)	C(10A)-C(13A)	1.468(9)
C(8A)-C(14A)	1.379(12)	C(10A)-C(12A)	1.472(12)
C(9A)-C(15A)	1.351(7)	C(11A)-C(12A)	1.397(12)
C(9A)-C(11A)	1.487(10)	C(13A)-C(14A)	1.417(11)
C(9A)-C(14A)	1.488(10)	C(16A)-C(17A)	1.320(9)
C(10A)-C(18A)	1.349(13)	C(17A)-C(27A)	1.512(11)
C(10A)-C(13A)	1.468(9)	C(19A)-C(20A)	1.324(8)
C(10A)-C(12A)	1.472(12)	C(20A)-C(28A)	1.524(8)
C(11A)-C(12A)	1.397(12)	C(18B)-C(22B)	1.507(8)
C(13A)-C(14A)	1.417(11)	C(22B)-C(23B)	1.525(10)
C(16A)-C(17A)	1.320(9)	C(23B)-C(24B)	1.572(13)
C(17A)-C(27A)	1.512(11)	C(24B)-C(25B)	1.475(13)
C(19A)-C(20A)	1.324(8)	C(25B)-C(26B)	1.492(11)
C(20A)-C(28A)	1.524(8)	C(8A)-C(14A)-C(9A)	123.7(8)
C(18B)-C(22B)	1.507(8)	C(13A)-C(14A)-C(9A)	116.7(7)
C(22B)-C(23B)	1.525(10)	C(9A)-C(15A)-S(1A)	124.3(4)
C(23B)-C(24B)	1.572(13)	S(1A)-C(15A)-S(2A)	110.7(3)
C(24B)-C(25B)	1.475(13)	C(17A)-C(16A)-S(1A)	118.5(6)
C(25B)-C(26B)	1.492(11)	C(17A)-C(16A)-S(5A)	124.8(6)
C(8A)-C(14A)-C(9A)	123.7(8)	S(1A)-C(16A)-S(5A)	116.7(5)
C(13A)-C(14A)-C(9A)	116.7(7)	C(4A)-C(3A)-C(2A)	120.0(7)
C(9A)-C(15A)-S(1A)	124.3(4)	C(3A)-C(4A)-C(12A)	120.3(6)
C(15A)-C(9A)-S(2A)	110.7(3)	C(6A)-C(5A)-C(13A)	121.9(6)
S(1A)-C(16A)-S(5A)	116.7(5)	C(5A)-C(6A)-C(7A)	119.9(6)
C(17A)-C(16A)-S(1A)	118.5(6)	C(6A)-C(7A)-C(8A)	119.8(6)
C(17A)-C(16A)-S(5A)	124.8(6)	C(14A)-C(8A)-C(7A)	120.7(7)
S(1A)-C(16A)-S(5A)	116.7(5)	C(15A)-C(9A)-C(11A)	121.5(6)
C(4A)-C(3A)-C(2A)	120.0(7)	C(15A)-C(9A)-C(14A)	123.2(6)
C(3A)-C(4A)-C(12A)	120.3(6)	C(11A)-C(9A)-C(14A)	114.9(6)
C(6A)-C(5A)-C(13A)	121.9(6)	C(18A)-C(10A)-C(13A)	124.2(8)
C(5A)-C(6A)-C(7A)	119.9(6)	C(18A)-C(10A)-C(12A)	120.8(8)
C(6A)-C(7A)-C(8A)	119.8(6)	C(13A)-C(10A)-C(12A)	114.7(7)
C(14A)-C(8A)-C(7A)	120.7(7)	C(1A)-C(11A)-C(12A)	119.2(8)
C(15A)-C(9A)-C(11A)	121.5(6)	C(1A)-C(11A)-C(9A)	124.0(8)
C(15A)-C(9A)-C(14A)	123.2(6)	C(12A)-C(11A)-C(9A)	116.7(8)
C(11A)-C(9A)-C(14A)	114.9(6)	C(11A)-C(12A)-C(4A)	118.9(8)
C(18A)-C(10A)-C(13A)	124.2(8)	C(11A)-C(12A)-C(10A)	117.8(8)
C(18A)-C(10A)-C(12A)	120.8(8)	C(4A)-C(12A)-C(10A)	123.2(8)
C(13A)-C(10A)-C(12A)	114.7(7)	C(3A)-C(13A)-C(14A)	118.1(6)
C(1A)-C(11A)-C(12A)	119.2(8)	C(5A)-C(13A)-C(10A)	124.9(6)
C(1A)-C(11A)-C(9A)	124.0(8)	C(14A)-C(13A)-C(10A)	117.0(6)
C(12A)-C(11A)-C(9A)	116.7(8)	C(8A)-C(14A)-C(13A)	119.6(7)
C(11A)-C(12A)-C(4A)	118.9(8)	C(18B)-C(22B)	1.401(13)
C(11A)-C(12A)-C(10A)	117.8(8)	C(18B)-C(23B)	1.419(11)
C(4A)-C(12A)-C(10A)	123.2(8)	C(23B)-C(24B)	1.356(14)
C(3A)-C(13A)-C(14A)	118.1(6)	C(24B)-C(25B)	1.385(9)
C(5A)-C(13A)-C(10A)	124.9(6)	C(4B)-C(12B)	1.378(11)
C(14A)-C(13A)-C(10A)	117.0(6)	C(5B)-C(13B)	1.387(7)
C(8A)-C(14A)-C(13A)	119.6(7)	C(3B)-C(6B)	1.403(6)
C(5A)-C(6A)	1.363(8)	C(6B)-C(7B)	1.370(9)
C(5A)-C(13A)	1.397(7)	C(7B)-C(8B)	1.375(9)
C(6A)-C(7A)	1.383(9)	C(8B)-C(14B)	1.416(13)
C(7A)-C(8A)	1.393(9)	C(9B)-C(15B)	1.353(7)
C(8A)-C(14A)	1.379(12)	C(9B)-C(14B)	1.464(12)
C(9A)-C(15A)	1.351(7)	C(10B)-C(11B)	1.475(10)
C(9A)-C(11A)	1.487(10)	C(10B)-C(18B)	1.365(13)
C(9A)-C(14A)	1.488(10)	C(10B)-C(13B)	1.480(10)
C(10A)-C(18A)	1.349(13)	C(10B)-C(12B)	1.483(13)
C(10A)-C(13A)	1.468(9)	C(11B)-C(12B)	1.424(12)
C(10A)-C(12A)	1.472(12)	C(12B)-C(13B)	1.507(8)
C(11A)-C(12A)	1.397(12)	C(13B)-C(14B)	1.525(10)
C(13A)-C(14A)	1.417(11)	C(14B)-C(15B)	1.572(13)
C(16A)-C(17A)	1.320(9)	C(15B)-C(16B)	1.475(13)
C(17A)-C(27A)	1.512(11)	C(16B)-C(17B)	1.492(11)
C(19A)-C(20A)	1.324(8)	C(17B)-C(18B)	1.507(8)
C(20A)-C(28A)	1.524(8)	C(18B)-C(19B)	1.525(10)
C(18B)-C(22B)	1.507(8)	C(19B)-C(20B)	1.572(13)
C(22B)-C(23B)	1.525(10)	S(3B)-C(15B)-S(2B)	124.7(4)
C(23B)-C(24B)	1.572(13)	C(17B)-C(16B)-S(1B)	116.5(6)
C(24B)-C(25B)	1.475(13)	S(5B)-C(16B)-S(1B)	117.4(5)
C(25B)-C(26B)	1.492(11)	C(16B)-C(17B)-C(27B)	127.2(8)
C(8A)-C(14A)-C(9A)	123.7(8)	S(1B)-C(15B)-S(2B)	110.8(3)
C(13A)-C(14A)-C(9A)	116.7(7)	C(17B)-C(16B)-S(5B)	125.9(6)
C(9A)-C(15A)-S(1A)	124.3(4)	C(17B)-C(16B)-S(1B)	116.5(6)
S(1A)-C(15A)-S(2A)	110.7(3)	C(18B)-C(17B)-S(2B)	115.8(6)
C(17A)-C(16A)-S(1A)	118.5(6)	C(27B)-C(17B)-S(2B)	117.0(6)
C(17A)-C(16A)-S(5A)	124.8(6)	C(10B)-C(18B)-S(4B)	125.8(8)
S(1A)-C(16A)-S(5A)	116.7(5)	C(10B)-C(18B)-S(3B)	121.4(8)
C(4A)-C(3A)-C(2A)	120.0(7)	S(4B)-C(18B)-S(3B)	112.5(5)
C(3A)-C(4A)-C(12A)	120.3(6)	C(20B)-C(19B)-S(3B)	117.1(5)
C(6A)-C(5A)-C(13A)	121.9(6)	C(20B)-C(19B)-S(6B)	125.6(5)
C(5A)-C(6A)-C(7A)	119.9(6)	S(3B)-C(19B)-S(6B)	117.2(4)
C(6A)-C(7A)-C(8A)	119.8(6)	C(19B)-C(20B)-C(28B)	127.9(6)
C(14A)-C(8A)-C(7A)	120.7(7)	C(19B)-C(20B)-S(4B)	115.6(5)
C(15A)-C(9A)-C(11A)	121.5(6)	C(23B)-C(23B)-S(4B)	116.5(5)
C(15A)-C(9A)-C(14A)	123.2(6)	C(23B)-C(21B)-S(3B)	114.5(5)
C(11A)-C(9A)-C(14A)	114.9(6)	C(21B)-C(22B)-C(23B)	112.8(6)
C(18A)-C(10A)-C(13A)	124.2(8)	C(23B)-C(23B)-C(24B)	109.4(7)
C(18A)-C(10A)-C(12A)	120.8(8)	C(25B)-C(24B)-C(23B)	115.4(8)
C(13A)-C(10A)-C(12A)	114.7(7)	C(24B)-C(25B)-C(26B)	113.6(8)
C(1A)-C(11A)-C(12A)	119.2(8)	C(25B)-C(26B)-S(6B)	115.9(6)
C(1A)-C(11A)-C(9A)	124.0(8)		
C(12A)-C(11A)-C(9A)	116.7(8)		
C(11A)-C(12A)-C(4A)	118.9(8)		
C(11A)-C(12A)-C(10A)	117.8(8)		
C(4A)-C(12A)-C(10A)	123.2(8)		
C(3A)-C(13A)-C(14A)	118.1(6)		
C(5A)-C(13A)-C(10A)	124.9(6)		
C(14A)-C(13A)-C(10A)	117.0(6)		
C(8A)-C(14A)-C(13A)	119.6(7)		
C(5A)-C(6A)	1.363(8)		
C(5A)-C(13A)	1.397(7)		
C(6A)-C(7A)	1.383(9)		
C(7A)-C(8A			

Appendix Two
Publications

Publications

Part of the work presented in this thesis has been reported in the following publications.

1. T. Finn, M. R. Bryce, A. J. Moore, A. S. Batsanov and J. A. K. Howard, *Pure and Appl. Chem.*, In Press.
2. T. Finn, M. R. Bryce and A. J. Moore, *Tetrahedron lett.*, **1999**, 3271.
3. T. Finn, M. R. Bryce, A. J. Moore, A. S. Batsanov and J. A. K. Howard, *Eur. J. Org. Chem.*, **2000**, 51.
4. T. Finn, M. R. Bryce, A. S. Batsanov and J. A. K. Howard, *J. Chem. Soc., Chem. Commun.*, **1999**, 1835.
5. T. Finn, M. R. Bryce, R. Katakya, S. B. Lyubchik, A. S. Batsanov and J. A. K. Howard, *Eur. J. Org. Chem.*, In Press.

Appendix Three
Research Colloquia

RESEARCH COLLOQUIA

The author attended the following colloquia.

1996

- October 14 Professor A. R. Katritzky, University of Gainesville, University of Florida, USA
Recent Advances in Benzotriazole Mediated Synthetic Methodology
- October 22 Professor B. J. Tighe, Department of Molecular Sciences and Chemistry, University of Aston

Making Polymers for Biomedical Application - can we meet Nature's Challenge?
Joint lecture with the Institute of Materials
- October 23 Professor H. Ringsdorf (Perkin Centenary Lecture), Johannes Gutenberg-Universität, Mainz, Germany
Function Based on Organisation
- November 12 Professor R. J. Young, Manchester Materials Centre, UMIST
New Materials - Fact or Fantasy?
Joint Lecture with Zeneca & RSC
- November 18 Professor G. A. Olah, University of Southern California, USA
Crossing Conventional Lines in my Chemistry of the Elements
- November 19 Professor R. E. Grigg, University of Leeds
Assembly of Complex Molecules by Palladium-Catalysed Queuing Processes
- November 27 Dr Richard Templar, Imperial College, London
Molecular Tubes and Sponges
- December 11 Dr Chris Richards, Cardiff University
Stereochemical Games with Metallocenes

1997

- January 15 Dr V. K. Aggarwal, University of Sheffield
Sulfur Mediated Asymmetric Synthesis
- January 16 Dr Sally Brooker, University of Otago, NZ
Macrocycles: Exciting yet Controlled Thiolate Coordination Chemistry
- January 21 Mr D. Rudge, Zeneca Pharmaceuticals
High Speed Automation of Chemical Reactions

- February 4 Dr A. J. Banister, University of Durham
From Runways to Non-metallic Metals - A New Chemistry Based on Sulphur
- February 5 Dr A. Haynes, University of Sheffield
Mechanism in Homogeneous Catalytic Carbonylation
- February 19 Professor Brian Hayden, University of Southampton
The Dynamics of Dissociation at Surfaces and Fuel Cell Catalysts
- February 25 Professor A. G. Sykes, University of Newcastle
The Synthesis, Structures and Properties of Blue Copper Proteins
- February 26 Dr Tony Ryan, UMIST
Making Hairpins from Rings and Chains
- March 4 Professor C. W. Rees, Imperial College
Some Very Heterocyclic Chemistry
- October 23 Professor M R Bryce, University of Durham, Inaugural Lecture

New Tetrathiafulvalene Derivatives in Molecular, Supramolecular and Macromolecular
Chemistry: controlling the electronic properties of organic solids
- November 5 Dr M Hii, Oxford University
Studies of the Heck reaction
- November 26 Professor R W Richards, University of Durham, Inaugural Lecture
A random walk in polymer science
- December 2 Dr C J Ludman, University of Durham
Explosions
- December 3 Professor A P Davis, Department. of Chemistry, Trinity College
Dublin.
Steroid-based frameworks for supramolecular chemistry
- 1998
- January 28 Dr S Rannard, Courtaulds Coatings (Coventry)
The synthesis of dendrimers using highly selective chemical reactions
- February 3 Dr J Beacham, ICI Technology
The chemical industry in the 21st century
- February 4 Professor P Fowler, Department of Chemistry, Exeter University
Classical and non-classical fullerenes

- February 24 Professor R Ramage, University of Edinburgh
The synthesis and folding of proteins
- March 4 Professor T C B McLeish, IRC of Polymer Science Technology, Leeds University
The polymer physics of pyjama bottoms (or the novel rheological characterisation of long branching in entangled macromolecules)
- October 9 Professor M F Hawthorne, Department Chemistry & Biochemistry, UCLA, USA, RSC Endowed Lecture
- October 27 Professor A Unsworth, University of Durham
What's a joint like this doing in a nice girl like you?
In association with The North East Polymer Association
- October 28 Professor J P S Badyal, Department of Chemistry, University of Durham
Tailoring Solid Surfaces, Inaugural Lecture
- November 3 Dr C J Ludman, Chemistry Department, University of Durham
Bonfire night Lecture
- November 11 Dr M Wills, Department of Chemistry, University of Warwick
New Methodology for the Asymmetric Transfer Hydrogen of Ketones
- November 12 Professor S Loeb, University of Windsor, Ontario, Canada
From Macrocycles to Metallo-Supramolecular Chemistry
- November 17 Dr J McFarlane
Nothing but Sex and Sudden Death!
- December 1 Professor N Billingham, University of Sussex
Plastics in the Environment - Boon or Bane
In association with The North East Polymer Association.
- December 2 Dr M Jaspers, Department of Chemistry, University of Aberdeen
Bioactive Compounds Isolated from Marine Invertebrates and Cyanobacteria

1999

- January 19 Dr J Mann, University of Reading
The Elusive Magic Bullet and Attempts to find it?
- February 9 Professor D J Cole-Hamilton, St. Andrews University
Chemistry and the Future of life on Earth
- February 23 Dr C Viney, Heriot-Watt
Spiders, Slugs And Mutant Bugs

